PolyPublie
Polytechnique Montréal

POLYTECHNIQUE MONTRÉAL
UNIVERSITÉ D'INGÉNIERIE

Titre: Title:	Wireless hazardous fall detection and location tracking for medical urgency and residence care applications
Auteur: Author:	Pengyan Zhang
Date:	2008
Type:	Mémoire ou thèse / Dissertation or Thesis
Référence: Citation:	Zhang, P. (2008). Wireless hazardous fall detection and location tracking for medical urgency and residence care applications [Master's thesis, École Polytechnique de Montréal]. PolyPublie. https://publications.polymtl.ca/8311/

Document en libre accès dans PolyPublie
Open Access document in PolyPublie

URL de PolyPublie: PolyPublie URL:	https://publications.polymtl.ca/8311/
Directeurs de recherche: Advisors:	
Programme: Program:	Unspecified

Ce fichier a été téléchargé à partir de PolyPublie, le dépôt institutionnel de Polytechnique Montréal
This file has been downloaded from PolyPublie, the institutional repository of Polytechnique Montréal

https://publications.polymtl.ca

UNIVERSITÉ DE MONTRÉAL

WIRELESS HAZARDOUS FALL DETECTION AND LOCATION TRACKING FOR MEDICAL URGENCY AND RESIDENCE CARE APPLICATIONS

PENGYAN ZHANG
DÉPARTEMENT DE GÉNIE ÉLECTRIQUE
ÉCOLE POLYTECHNIQUE DE MONTRÉAL

MÉMOIRE PRÉSENTÉ EN VUE DE L'OBTENTION
DU DIPLÔME DE MAÎTRISE ÈS SCIENCES APPLIQUÉES
(GÉNIE ÉLECTRIQUE)
DÉCEMBRE 2008

© Pengyan Zhang, 2008.

Library and Archives Canada

Published Heritage Branch

395 Wellington Street
Ottawa ON K1A 0N4
Canada

Bibliothèque et Archives Canada

Direction du Patrimoine de l'édition

395, rue Wellington
Ottawa ON K1A 0N4
Canada

Your file Votre référence
ISBN: 978-0-494-49444-8
Our file Notre référence
ISBN: 978-0-494-49444-8

NOTICE:
The author has granted a non-exclusive license allowing Library and Archives Canada to reproduce, publish, archive, preserve, conserve, communicate to the public by telecommunication or on the Internet, loan, distribute and sell theses worldwide, for commercial or non-commercial purposes, in microform, paper, electronic and/or any other formats.

The author retains copyright ownership and moral rights in this thesis. Neither the thesis nor substantial extracts from it may be printed or otherwise reproduced without the author's permission.

AVIS:
L'auteur a accordé une licence non exclusive permettant à la Bibliothèque et Archives Canada de reproduire, publier, archiver, sauvegarder, conserver, transmettre au public par télécommunication ou par l'Internet, prêter, distribuer et vendre des thèses partout dans le monde, à des fins commerciales ou autres, sur support microforme, papier, électronique et/ou autres formats.

L'auteur conserve la propriété du droit d'auteur et des droits moraux qui protège cette thèse. Ni la thèse ni des extraits substantiels de celle-ci ne doivent être imprimés ou autrement reproduits sans son autorisation.

In compliance with the Canadian Privacy Act some supporting forms may have been removed from this thesis.

While these forms may be included in the document page count, their removal does not represent any loss of content from the thesis.

Conformément à la loi canadienne sur la protection de la vie privée, quelques formulaires secondaires ont été enlevés de cette thèse.

Bien que ces formulaires aient inclus dans la pagination, il n'y aura aucun contenu manquant.

Canada

UNIVERSITÉ DE MONTRÉAL

ÉCOLE POLYTECHNIQUE DE MONTRÉAL

Ce mémoire intitulé:

WIRELESS HAZARDOUS FALL DETECTION AND LOCATION TRACKING FOR MEDICAL URGENCY AND RESIDENCE CARE APPLICATIONS

présenté par: ZHANG Pengyan

en vue de l'obtention du diplôme de: Maîtrise ès sciences appliquées

a été dûment accepté par le jury d'examen constitué de:

M. AKYEL Cevdet, D.Sc.A, président

M. WU Ke, Ph.D., membre et directeur de recherche

M. BOUTAYEB Halim, Ph.D., membre

To my parents

ACKNOWLEDGMENTS

I would like to express my gratitude and appreciation to everyone that has helped me with this thesis. This thesis would not have been possible without their help.

First and foremost, I would like to give my sincerely thanks to my supervisor, Professor Ke Wu, for his guidance, support and encouragement throughout my studies, which is indispensable for me to finish this thesis. I am very grateful to have the opportunity to participate in this interesting project.

Also, I would like to thank my friends: Xiaoping Chen, Philip Kassey, Liang Han, Xingliang Li, Gupta Shulabh, Djerafi Tarek, Ning Yang and Zhenyu Zhang. Their valuable suggestions and advices have made great contributions to my work.

This thesis was also made possible by M. Steve Dubé, M. Jules Gauthier, Thibault Maxime, Antonescu Traian. They have helped me fabricate my prototypes. And their technical support helps me quite a lot.

Finally, I would like to acknowledge my uncle, who has supported me through these work. And I would like to give my deepest gratitude and sincerest love to my parents for their love and support

RÉSUMÉ

Cette thèse propose l'analyse et la conception d'un système sans fil pour la surveillance des personnes qui ont besoin du soin des autres, c'est-à-dire les personnes âgées et les patients des hôpitaux. En effect, les chutes sont très dangereuses pour ces derniers, pouvant causer de graves dommages physiques. Le système présenté dans cette thèse permet de détecter si une personne tombe en utilisant un capteur porté par le patient. De plus, quand la chute est détecté, un réseau sans fil, qui couvre l'ensemble du bâtiment peut donner la position précise de la personne et envoyer les informations nécessaires a un serveur centrale. Ainsi, les médecins ou infermières peuvent venir à l'aide du patient.

Le système de détection proposé emploie des accéléromètres triaxiaux. La détection se fait en calculant les dénergie. L'avantage de notre système est qu'il ne nécessite pas de traitement numérique compliqué. Un simple microcontrôleur peut être utilise pour le traitement des données. Les mesures démontrent que ce système fonctionne très bien.

Le réseau de capteurs sans fil que nous proposons dans ce travail permet d'effectuer le positionnement et la communication sans fil. Le positionnement est effectué en utilisant la puissance du signal reçu(RSS). Ce type de système de positionnement à l'intérieur des immeubles n'est généralement pas aussi précis que les système de positionnement basé sur la mesure du temps d'arrivée, mais il coûte moins cher et est en mesure de fournir une précision acceptable pour notre travail. Beaucoup de travaux en cours sur le positionnement en utilisant le RSS se concentrent sur les dispositifs utilisés dans les ré seaux locaux sans fil. comme exemple de réseau sans fil, il existe le réseau IEEE802.11, qui est néanmoins spécialement conçu pour la communication sans file et non pour le positionnement. De plus, ce type de réseau est assez cher. En conséquence, un réseau très bon marché de capteurs sans fil est spécialement cçu pour la détection de position à l'intérieure d'une pièce. Le système présenté est analysé et les facteurs qui influencent

les performances sont étudiés expérimentalement.

Ce travail se divise en quatre chapitres. Le premier chapitre donne le contexte actuel et les bases sur les méthodes de détection et les systèmes de positionnement à l'intérieure des immeubles. Le deuxième chapitre décrit le système de détection proposé ainsi que la conception du circuit et l'algorithme de détection de chute. Des résultats expéri mentaux sont présentés pour valider notre étude et pour compléter l'analyse. Dans le chapitre trois, l'architecture du réseau de capteurs sans fil est mis en place en tenant en compte les protocoles de communications. Le chapitre quatre se consacre à la méthode de positionnement et à l'étude des performances mesurés, montrant les paramètres qui peuvent influer sur les performances. La méthode de Monte-Carlo est utilisée pour analyser les résultats expérimentaux.

ABSTRACT

In this thesis, a wireless system for monitoring and identifying people who need special care and medical attention such as elders disabled persons and patents. Fall is one of the most dangerous accidents for these people, which may cause serious physical injury. The wireless system presented in this thesis can detect if a person needs help. A wearable fall detection sensor is presented and demonstrated in this work. When a serious fall is detected, the wireless network that covers the whole building can position that person and send this information to a central server.

A fall detection system employing triaxial accelerometers is analyzed, designed, fabricated and tested. This fall detection system makes use of a simple method mainly based on energy expenditure. This system does not require high performance DSP circuits. A simple microcontroller can be used for data processing. Measurements show this system works very well.

A wireless sensor network used for target positioning and wireless communication. The positioning may be performed based on received signal strength(RSS). This kind of indoor positioning systems usually are not as accurate as positioning systems based on time measurements. However, they are less expensive and are able to provide an acceptable accuracy for this work. Many works on positioning with RSS focus on current devices used in wireless local area networks. If there are no such wireless networks, people have to build such an IEEE802.11 network, which is specially designed for wireless communication other than for positioning. And those network cards are relatively expensive. As a result, for indoor environment where there is no need for such networks, an affordable wireless sensor network is specially designed for indoor positioning. Factors that affect the performance have been presented and analyzed. The performance of the whole system is analyzed based on measurements.

There are four chapters in this thesis. Chapter one gives the background of current fall detection methods and indoor positioning systems. Chapter two explains our fall detection system, including hardware design and the fall detection algorithm. Measurement results for this system are also presented. In chapter three, the architecture of our wireless sensor network will be introduced, including the protocols and the wireless unit. Chapter four talks about the positioning method and performance. Several parameters that can affect the positioning performance are analyzed. Results based on measurements and Monte-Carlo method are also shown there.

CONDENSÉ EN FRANÇAIS

1. Introduction

En Amérique du nord, derrière une économie développée, la proportion de personnes de plus de 65 ans est en augmentation, mais la façon auquel nous utilisons pour prendre soin de cette augmentation du nombre des 'aînés a été l'un des sujets critiques rencontrés par notre société. Heureusement, avec le développement rapide de la technologie sans fil et l'industrie électronique, il nous est possible de concevoir un système de contrôle automatisé pour les personnes âgées.

Les statistiques montrent que les chutes peuvent être très dangereuses pour les personnes âgées. La fréquence des chutes est plus élevée pour ceux qui vivent dans des bâtiments de soins infirmiers. En conséquence, l'invention d'un système de détection automatique automne peut être utilisé en vue de réduire le nombre d'infirmières.

Apparemment, un système de surveillance idéal doit être capable d'effectuer la détection des substances dangereuses des activités telles que les chutes. De plus, afin d'aider la personne qui tombe dans le plus bref délai possible, le système doit également être en mesure de fournir les informations de position. On pourrait imaginer ce que se passera lorsque de l'aide est venu afin de savoir le lieu exact de la personne blessé dans tout le bâtiment.

Prenant en considération que nous avons développé un système de surveillance efficace qui permet de détecter une chute et en même temps identifier l'endroit où la personne tombe. Le système présenté dans ce mémoire est basé sur une architecture ouverte, ce qui signifie que d'autres types de capteurs peuvent être intégrés dans ce système à l'avenir. Actuellement, seul le capteur de détection de chute est employé dans ce système de

surveillance, mais d'autres types de capteurs peuvent également être utilisés à l'avenir afin de fournir de plus information nécessaire sur la victime. Par exemple, un capteur de température peut être facilement intégré dans ce système afin de surveiller la température du corps de l'aîné.

2. Détection du chute

Beaucoup de recherches sur la détection de chute ont été faites récemment. Selon la façon dont la chute est détectée, toutes les méthodes de détection ont été proposées dans les précédents les activités de recherche peuvent être divisés principalement en deux types. L'un est basé sur les capteurs portables, c'est-à-dire une personne peut porter ou tenir des capteurs afin de détecter leurs mouvements de son corps. Et le deuxième est basé sur d'autres équipements déployés dans l'environnement. Donc, les gens n'ont pas besoin de porter ou de détenir des appareils de contrôle, car des dispositifs sont déployés dans l'environnement.

Pour la première méthode, les appareils avec des capteurs, tels que des accéléromètres, des capteurs d'inclinaison, ainsi que les capteurs de vibrations, ont déjà été employés par un être afin de détecter leur posture et/ou leurs mouvements. Puis les chutes peuvent être détectées par une analyse des informations à partir des capteurs utilisés. Le principal avantage de ces systèmes est qu'ils sont très faciles à utiliser et le coût des équipements est très minime. De plus, la vie privée des gens est généralement protégée. Mais, ce système a aussi son désavantage. Les gens doivent utiliser ces capteurs de façon correcte en tout le temps quand ils sont surveillés. En même temps, ces capteurs pourraient provoquer un certain inconfort pour les personnes qui les portent.

La recherche sur l'autre méthode est essentiellement axée sur les techniques de vision

par ordinateur: habituellement par des vidéo caméras, des capteurs d'infrarouges et le son des capteurs. Et parmi eux, les caméras vidéo ou capteurs vidéo sont les plus utilisées. Avec la technique de traitement vidéo, les activités de l'intérieur la couverture du système peuvent être suivies. Les avantages de ces systèmes sont qu'ils sont capables de détecter de nombreux événements en même temps. En général, ils peuvent aussi fournir plus d'informations que celles des capteurs standard. En outre, elles n'apportent pas de gêne pour les usagers et elles peuvent fournir des informations de position en même temps. Toutefois, ils coûtent généralement beaucoup plus que celles méthodes basées sur les capteurs portables et ils ont généralement besoin de faire recours à des techniques de traitement des données qui sont sujettes à des erreurs et pour les calculs sont complexes.

Afin de rendre le système de détection de chute plus facile d'être intégré à un système sans fil et à réduire le coût, un capteur portable basé sur des accéléromètres a été utilisé dans ce projet.

Bien que le mot 'chute' semble très simple dans le bon sens, il pourrait être difficile de le décrire précisément et d'en préciser les caractéristiques de détection pour une chute. Il a été largement admis que l'énergie les dépenses peuvent être utilisées pour classer les activités quotidiennes, y compris les chutes. Malheureusement, la dépense d'énergie est très utile pour la chute de détection et qu'il n'est pas pratique de mesurer directement. Toutefois, les dépenses d'énergie peuvent être mesurées indirectement.

Il a été démontré qu'il existe des liens étroits entre les dépenses d'énergie et la sortie des accéléromètres utilisés pour analyser la démarche et d'autres mouvements. La meilleure prédiction de l'énergie des dépenses a été considérée comme la somme de la valeur absolue des trois orthogonales forces. En conséquence, d'autres que de mesurer la force appliquée directement, il peut être mesuré par l'accélération, parce que les accéléromètres

sont très bon marché et faciles à acheter.

Toutefois, les dépenses d'énergie ne suffisent pas de détection de chute, car il y a beaucoup d'activités à forte intensité, comme le saut d'obstacles, qui peuvent avoir une dépense d'énergie de valeur similaire à celle pour de la chute. Avec l'orientation de détection, ce problème peut être résolu. Parce que, quand une chute arrive, l'orientation de l'organisme a un changement de 90 degrés alors que pour les activités habituelles, il n'y a pas de changement dans l'orientation de l'organisme.

En outre, après une chute d'une personne, il n'y aura pas d'activités à forte intensité d'après. Ainsi, après une dépense d'énergie de haute valeur est mesurée, si la sortie de l'accéléromètre est stable, sans doute une chute s'est produite. Mais s'il y a encore de grands changements dans l'accéléromètre de sortie, aucune chute doit être signalée.

La chute des circuits de détection contient principalement de trois parties: l'accéléromètre, le signal analogique de convertisseur de signal numérique (A/D Convertiseur) et d'une unité de traitement des données. Les trois axes de faible micro-accéléromètre MMA7260 de Freescale Semiconductor est utilisé. En changeant le gain interne, cette surface de microcircuits intégrés accéléromètre permet de sélection parmi les quatre différentes gammes avec des sensibilités différentes: 1.5g de 800mV/g, 2g de 600 mV/g, 4g de 300mV/g et 6g de 200mV/g (g est l'accélération causée par la gravité). La puce a également un bord unipolaire tension condensateur de filtrage qui peuvent conditionner les signaux. En outre, il offre un mode veille qui peut fortement réduire sa consommation d'énergie. Cette fonctionnalité est très utile, car elle peut augmenter la durée de vie de batteries utilisées pour l'alimentation.

Un microprocesseur de Microchip Technology, le PIC16LF877, est utilisé pour traiter les données de l'accéléromètre. Ce microcontrôleur a 14.3K octets utilisés pour le pro-

gramme, 368 octets SRAM haute vitesse est utilisée pour les données, 256 octets relativement faible vitesse EEPROM est utilisée pour les données, et 8 10-bit convertisseurs A/D canaux. Le microcontrôleur peut fonctionner jusqu'à une fréquence de 20MHz. Le convertisseur A/D peut encore travail, même le microcontrôleur est en mode veille. Ceci peut être utilisé pour enregistrer la batterie. Le A/D chaînes PIC16F877 sont tous les convertisseurs 10-bit. Pour plus de commodité et d'efficacité, que la haute 8 bits sont utilisés. Ainsi, la production varie de 0 à $255(2^8)$, conformément à une plage de tension de V_{REF-} to V_{REF+}. V_{REF-} dans ce circuit est le terrain et la V_{REF+} est la tension d'alimentation du circuit (3.3 V).

Afin de lire les données en un temps réel pour le débogage, un bloc d'affichage est mis en œvre avec une à deux chiffres conduit à sept segments. Le maximum dégradée actuel du microcontrôleur est de 25mA, alors que les cours pour chaque segment de la LED sont 30mA, de sorte que le microcontrôleur n'est pas en mesure de conduire la LED directement. Pour la recherche, toutes les données obtenues par l'accéléromètre doivent être enregistrer dans un ordinateur. Ainsi, une interface RS-232 est employée dans ce circuit de communication entre ces circuits et un ordinateur avec un port série.

La sortie de l'accéléromètre est un signal analogique, et il doit être converti d'un signal numérique en les convertisseurs A/D inclus dans le microcontrôleur. La vitesse de ce processus, appelé échantillon fréquence, est limitée par le matériel. Dans le projet, une fréquence d'échantillonnage de $160.25Hz$, correspondant à une durée totale de $6.24ms$, est employée.

Après l'échantillonnage, les données seront d'abord filtré par un filtre pour réduire le bruit. Bien que filtre passe-bas est habituellement utilisée pour filtrer les très haute fréquence du bruit, la 47e commande médiane filtre est utilisé ici. La sortie de l'accéléromètre est proportionnelle à la force exercée sur le capteur au lieu de l'accélération de la sonde.

Cette non nulle de sortie peut être retirée par un filtre passe-haut. Cela explique pourquoi un passe-haut FIR (Finite Impulse Response) du filtre d'ordre 126 normalisées avec une fréquence de coupure de 0.02 (1 correspond à la fréquence de Nyquist) est utilisé ici.

Ensuite, la valeur absolue de la production sera additionnée pour estimer la dépense énergétique. Enfin, le système permettra de comparer cette valeur avec un seuil prédéfini $EE_{threshold}$ seuil. Si la valeur calculée est plus petite que le seuil, aucun chute sera communiqué. Si non, le système analyser l'orientation de la personne au début et à la fin à l'aide des trois des chaînes de données de sortie de la médiane filtre.

Le circuit de détection de chute fabriqué a été testé et les données de sortie de l'accéléromètre a été enregistrées dans un ordinateur. De la mesure des résultats, on peut constater que l'algorithme utilisé dans ce système peuvent distinguer efficacement les chutes et d'autres activités quotidiennes. Le calcul la dépense d'énergie est un bon facteur de représenter l'intensité d'une activité. Avec ce facteur, les activités quotidiennes habituelles peuvent être aisément distinguées des chutes.

3. Positionnement sans fil

Guidés par un énorme marché potentiel et des recettes, il existe un intérêt croissant dans la technique de positionnement sans-fil. La différence du système radar qui détermine le temps de propagation et direction de signaux radio réfléchie d'un passif cible, la technique positionnement sans fil ici référence à une détermination de la position entre deux ou plusieurs actifs de terminaux sans fil, tels que l'aéronautique équipement de mesure de distance (DME) et VHF omnidirectionnel (VOR), qui ont été utilisés pendant une longue période. Selon les exigences de précision et d'architectures de systèmes, il existe principalement trois paramètres de base du signal qui peut être mesuré pour le position-

nement: la force du signal reçu(RSS), temps de vol (TOA) et angel d'arrivée (AOA).

Pour la méthode basée sur le positionnement du signal reçu (RSS), il existe principalement deux types de techniques utilisées. Une classe à trilatérale méthode estimée entre plusieurs stations de base et la cible. Sachant que la force du signal reçu à un récepteur est une fonction de la distance de l'émetteur. En général, il y a beaucoup de murs, de meubles, de fenêtres et de portes dans un environnement intérieur, et il y a des gens sont alentour, il est assez difficile d'obtenir précisément la distance uniquement basée sur le modèle de propagation indoor. Les mesures montrent que la réception la force du signal à un certain lieu est plus forte que les autres en dépendant de sa position. En conséquence, les autres emploient la méthode correspondant en temps réel du signal mesuré avec une base de données créées au début. Le avantages pour un système de positionnement utilisant RSS des mesures sont évidents. étant donné que presque tous les émetteurs pour la communication sans fil ont une partie de contrôle de gain automatique qui peut être utilisé pour lire le RSS. Les équipements de communication sans fil peuvent être utilisés pour le positionnement RSS directement. Par conséquent, le coût des équipements pour ces systèmes est très minime. Même si exactitude de ce système n' est pas très haute, il est suffisant pour de nombreuses applications. Les principaux problèmes de ces systèmes sont qu'ils ont besoin beaucoup de travail afin de créer une base de données et ils dépendent fortement de leurs environnements.

Le déploiement des systèmes basés sur TOA ou TDOA sont principalement utiliser pour mesurer le temps nécessaire pour que le signal de voyage de la station de base à la cible. Comme on le sait, le signal radio se propage à la vitesse de la lumière. Lorsque le temps de propagation est obtenu, la distance entre la station de base et de la cible peut être calculée. Avec de nombreuses stations de base disponible en même temps. La position de la cible peut être calculée avec des méthodes telles que trilateration. L'avantage évident de positionnement des systèmes utilisant la mesure du temps est qu'ils peuvent fournir

une meilleure résolution et précision que les autres systèmes de positionnement basés sur des flux RSS ou AOA. D'autre part, la précision de mesure du temps dépend fortement de matériel de système, ce qui signifie plus de frais.

Pour les systèmes basés sur des méthodes de positionnement AOA, il mesure premièrement l'arrivée de la direction signal à partir de plusieurs stations de base. Ils supposent que toutes les stations de base sont dans le même sens que l'arrivée du signal. En conséquence, la position de la cible peut être trouver. Le système de positionnement AOA est très simple à mettre en uvre l'exception de la grande antenne directionnelle. Comme les autres systèmes de positionnement, le bruit et surtout multi effet qui affaiblis les performances. Quant à l'environnement intérieur, La méthode AOA n'est généralement pas utilisé seul pour le positionnement, car il y a beaucoup de réflecteurs, et il est très difficile de donner une précision acceptable avec cette méthode. AOA est souvent mise en uvre en collaboration avec des flux RSS ou des méthodes de mesure du temps comme un complément.

Bien que les systèmes de positionnement basés sur la mesure du temps puisse potentiellement fournir une meilleure précision que ceux basés sur le RSS de mesure, les anciens systèmes de positionnement coûtent beaucoup plus cher. Depuis la méthode de positionnement RSS peuvent répondre aux exigences de notre système, il a été employé dans ce projet.

L'idée du système est de couvrir toute la zone de service avec un réseau sans fil. Beaucoup stations centrales seront déployées à l'intérieur de la zone de positionnement et de communication. Quand une personne de moins de surveiller tombe et qu'il est détecté, le capteur porté par la personne sera enregistrer par la RSS accessible de toutes les stations de base. Ensuite, cette information est transmise à une station de base RSS avec les plus fortes, la station de base transmet ces informations à un serveur par internet. Ces

informations seront analysées afin d'obtenir la position de cette personne.

Prenant le coût et la simplicité en considération, une simple division de fréquence multiplex (FDM) est employée dans ce projet pour couvrir l'ensemble de la zone. Toutes les bandes de fréquences sont divisées en k différents sous bande de fréquence qui peut être utilisé par différentes stations de base simultanément. Alors k est le nombre de stations de base dans un group de stations de base, où k est utilisé les différents sous bande de fréquence, respectivement. Le transporteur de détection d'accès multiple avec évitement des collisions (CSMA/CA), qui a été largement utilisé pour les réseaux locaux sans fil (WLAN) est utilisé pour les moyennes d'accès contrôle.

Selon l'architecture du système, le circuit est conçu et mis en œvre avec les antennes, émetteurs-récepteurs sans fil, ainsi que pour les circuits de conversion de puissance électrique.

Deux types d'antenne polarisée circulairement et un type de PIFA ont été conçus et testés. Ici, la polarisation circulaire est obtenue par l'introduction d'une paire de tronqué coins de la simple antenne patch. Le degré de séparation des deux fréquences résonnées pour les deux modes est déterminé par la taille d'un tronqué paire. Une compacte antenne polarisée circulairement avec coins tronqués a été conçue par l'incorporation d'un groupe de quatre flexions créneaux horaires. Ce type d'antenne peut avoir une réduction de taille de plus de 50%.

La plate-forme sans fil utilisée dans ce projet pour le positionnement, ainsi que pour la communication sans fil sont mis en uvre avec la puce RF ADF7021 d'Analog Device et le PIC16LF877 de Microchip entreprise. ADF7021 est de faible puissance et à bande étroite émetteur. Ses gammes de tension d'alimentation de 2.3V à 3.6V. Comme le même pour les autres circuits, 3.3V est utilisé comme tension d'alimentation. Il peut travailler

en deux bandes de fréquence: 80MHz à 650MHz et 862MHz à 950MHz. Il soutient gaussien et soulevé cosinus filtrage afin de réduire la bande passante du signal transmis de manière à réduire les interférences en dehors de sa bande passante. 2FSK, 3FSK, 4FSK et MSK modulation peuvent être utilisés. Il supporte un débit de données allant de 0.05kbps à 32.8kbps. Il a une puissance maximale de 13dBm (Pour comparaison, le montant maximal de transmettre la puissance de sortie en IEEE802.11 est 20dBm ou 100mW).

Une puce de convertisseur de force société Maxim a été utilisée pour l'alimentation de stations de base. Il supporte une tension d'entrée allant de 5.5 V à 23V. Il dispose d'un maximum de courant de sortie de 2A. Par ailleurs, un court-circuit de protection thermique et de protection de l'arrêt sont également fournis.

Le positionnement de l'algorithme utilisé est une sorte de méthode d'empreinte digitale. Il consiste principalement en deux étapes. La première étape est de construire une carte électronique de l'ensemble de la zone qui est nécessaire pour couvrir le système. Cette carte est enregistrée dans une base de données dans le serveur central. L'autre étape est avoir une application de positionnement pratique, où les emplacements des balises sont fournis par le système. Dans cette étape, les balises RSS vont d'abord enregistrer l'information de toutes les stations de base et de transmettre cette information à la station de base avec le plus fort signal.

Des mesures ont été faites dans notre laboratoire en École Polytechnique de Montréal, où il y a beaucoup de gens qui se promènent dans la journée. Une étiquette qui est connecté à un ordinateur par le biais de l'interface RS-232, est fixé RSS pour recevoir des renseignements provenant de plusieurs stations de base et transmet ces informations à l'ordinateur. Les informations RSS de chaque station de base ont été enregistrées par la marque pour environ 12 heures, de 9h00 am à environ 9h00 pm, avec un

taux d'échantillonnage de 1000 valeurs / seconde. Le nombre total d'informations RSS d'une station de base est enregistré dans 24 dossiers. Chaque enregistrement de fichier RSS d'information est de 30 minutes. Les distances entre la balise et ceux de base sont d'environ 6 mètres à 15 mètres. Les distances entre les stations de base de gamme de 5 mètres à 15 mètres.

Les résultats des mesures effectuées montrent que plus il y a de stations de base et plus détaillées base de données électroniques captées, nous pouvons obtenir une plus grande précision. Avec 8 de station de base, il existe une probabilité de plus de 95% que la balise peut être placée à son plus proche point de grille de référence. Vu le problème des coûts, quatre stations de base peuvent fournir une précision de localisation assez pour le positionnement des personnes dans ce projet. La longueur des temps d'échantillonnage presque n'a pas beaucoup d'impact sur les performances du système en utilisant les correspondant à la méthode de distribution. En comparant le résultat avec un temps de prélèvement de longueur et de 4 secondes, le résultat de la durée de 55 secondes, que peu d'amélioration est observée.

4. Conclusion

Dans cette thèse, un système de détection de chute d'énergie basée sur le calcul des dépenses a été analysé, conçu et fabriqué. Une série de mesures ont été faite pour analyser la performance de la proposé la méthode de détection de chute. L'ensemble du système se compose essentiellement de deux parties: la triaxiaux capteur d'accélération et de l'unité de traitement des données. Cela peut rendre l'ensemble du circuit de petite taille pour les gens de l'usure de leur corps. Les résultats des mesures effectuées montrent que ce système est capable de distinguer une chute avec d'autres activités quotidiennes.

Pour valider le concept proposé, basé sur le positionnement sans fil RSS a été analysé dans une salle d'environnement. Quelques considérations particulières, telles que la polarisation d'antenne, ont été présentées. Plusieurs unités sans fil et de plusieurs antennes de polarisation différentes ont été conçues et fabriquées avec la technologie standard PCB. L'influence de plusieurs facteurs a été étudié et testés. Parce que la force du signal sans fil dans un environnement intérieur fluctue avec le temps, il est difficile d'obtenir une bonne performance basée sur le RSS. Une nouvelle méthode d'estimation de position, la méthode probabilité correspondant a été proposée pour améliorer la performance du système.

À l'avenir, l'effet du corps humain sur la performance de l'antenne devrait être étudié. également, petites antennes avec des performances acceptables doivent être étudiées. En outre, les mesures en ces travaux ont été réalisées dans un environnement de laboratoire, tout ce système est destiné à travailler en d'autres types d'environnement, comme un bâtiment de soins infirmiers.

TABLE OF CONTENTS

LIST OF FIGURES

LIST OF NOTATIONS AND SYMBOLS

AOA: angle of arrival

ASK: amplitude-shift keying

CDM: code division multiplexing

$CSMA/CA$: carrier sensing multiple access with collision avoidance

CRC: cyclic redundancy check

DME: distance measuring equipment

$E-911$: Enhanced-911 service

FCC: Federal Communications Commission

FIR: finite impulse response

FDM: frequency division multiplex

$FDMA$: frequency division multiple access

GPS: The Global Positioning System

g: acceleration due to gravity

$GFSK$: gaussian frequency-shift keying

HMM: hidden markov models

$IRISYS$: infra-red integrated system

ISM: industrial, scientific and medical frequency band

ITU: International Telecommunication Union

$ITU-R$: international telecommunication Union radiocommunication sector

$K-NN$: k-nearest neighbor

LOS: light of sight

LED: light-emitting-diode

MAP: maximum a posteriori

NRZ: non-return-to zero

$PIFA$: planar inverted-F antenna

PLL:	phase locked loop
ppm:	parts per million
PN:	pseudo noise
RSS:	received signal strength
$RSSI$:	received signal strength indicator
SVM:	support vector machine
SNR:	signal to noise ratio
TOA:	time of arrival
$TDOA$:	time difference of arrival
VHF:	very high frequency
VOR:	VHF omnidirectional range
$WLAN$:	wireless local area network

LIST OF TABLES

CHAPTER 1

BACKGROUND AND INTRODUCTION

Falls can be quite dangerous, especially for the elder. Statistics show that more than one third of adults ages 75 and older fall each year(Duthie, 1989). The frequency of falls for those relatively dependent elderly, such as those who live in nursing buildings, is much higher. It has been estimated that more than 50 percent people living in nursing homes fall every year. And more than 40 percent of these people have the unfortunate occasions to fall more than once(Tideiksaar, 1997). A study on fall victims has shown that more than 60 percent of those who fell and remained helpless over 72 hours without assistance suffered from death, while only 12 percent were helpless for less than one hour(Gurley, 1996).

In the North America, behind the developed economy, the proportion of people over 65 is increasing. According to a report from the National Institute of Health in the US, people born during the baby boomer in 1960s' and 1970s' are going to retire in three years. With the current amount of doctors, one doctor has to take care of 2500 elder people at that time. Also, being paid very low, more than 71 percent of nurses quit their jobs in the first two years of their work. How to take care of the increasing amount of the elder has been one of those critical issues faced by our society.

Fortunately, with the rapid development in wireless technology and electronic industry, it is possible for us to design an automated monitoring system for the elder. With the help of such a system, the alarm of a fall as well as the position information could be provided and as a result, immediate assistance can be guaranteed. The elder who falls down can take advantage of the medicine's "golden hour", in which the probability of a good outcome is increased if the person receives treatment within the first hour of the

incident.

The goal of our research is to design and develop a monitoring network that can detect a fall and pinpoint the position simultaneously. Also, with other types of sensors, the system can also be used to monitor other health or vital parameters of a person, such as body temperature, heart beat rate and blood pressure.

1.1 Fall Detection

The detection of falling is an interesting technical topic and extensive research on fall detection has been done recently. According to the way how a fall is detected, all fall detection methods that have been proposed for fall detections in previous research activities can be divided into mainly two types. One is based on wearable sensors, by which people under monitor wear or hold some sensor devices to detect their activities. And the other is based on equipments deployed in the environment, by which usually people do not have to wear or hold devices while monitoring devices are deployed in the environment.

1.1.1 Wearable Device Method

With the fast-ever development, the size of modern sensors becomes more and more small while the cost becomes lower and lower. This development has allowed the utilization of miniature, low powered sensors for fall detection. Devices with sensors, such as accelerometers, tilt sensors as well as vibration sensors, have been already employed on people's bodies to detect their posture and/or movements. For instance, the accelerometer can be used to detect the acceleration of the body, which is a function of activity. When a body falls down, due to the gravitation, there is a period of vibration

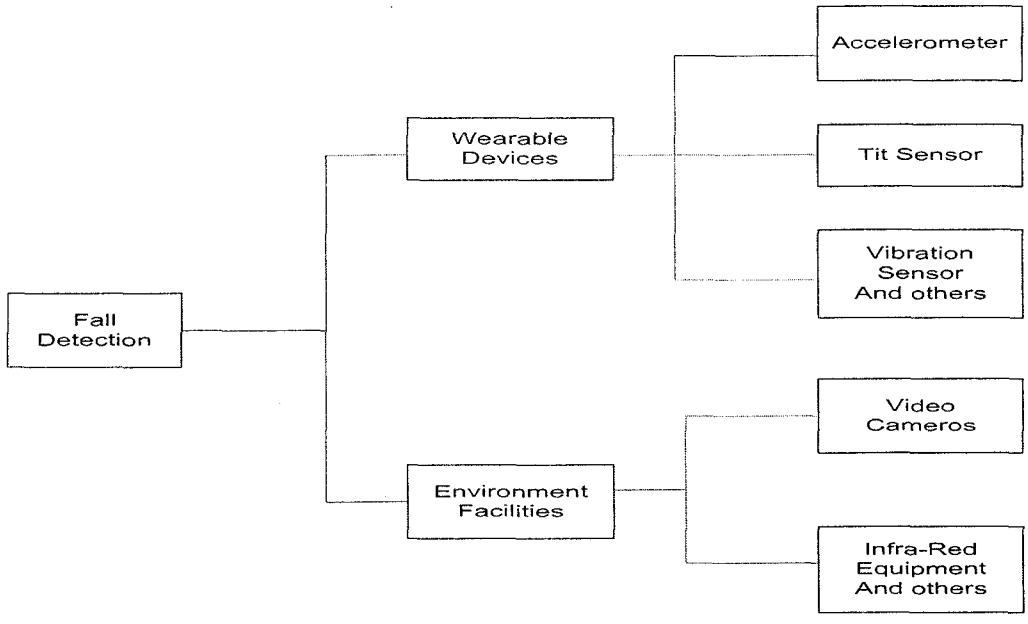

Figure 1.1 Fall detection methods.

and acceleration, which can be detected as a sign of fall. Other sensors, such as tilt sensors can be used to monitor the posture, such as standing and lying, of the body in order to detect falling. As shown in Figure 1.2, according to the data processing methods, this method can be further divided into two categories: based on analytical method such as energy expenditure method and pattern recognition method.

In previous research work, G. Willianms developed a fall detection system, which used a piezoelectric shock sensor to detect the fall impact and a mercury tilt switch to monitor

$$Fall\ Detection \begin{cases} Analytical\ Method \begin{cases} \text{Activity index} \\ \text{Energy Expenditure} \\ \text{etc.} \end{cases} \\ Pattern\ Classification \begin{cases} \text{K-Nearest Neighbour} \\ \text{Support Vector Machine} \\ \text{etc.} \end{cases} \end{cases}$$

Figure 1.2 Data processing method for fall detection system.

the orientation of the person(Williams et al., 1998). The system obtains an activity index by integrating the signals from the shock sensor with respect to time. The activity index is proportional to the forces exerted on the device. When a suitably larger impact is monitored, the orientation of the person by the tilt switch will help the system to determine if a fall happened. In 2001, M. J. Mathie described a system using accelerometers for objectively and continuously monitoring patient activities inside a home environment(Mathie et al., 2001). The patient's posture, energy expenditure(Caspersen et al., 1985a) and movement can be classified by this system. Similarly, U.Lindemann proposed a fall detection system using two orthogonal two-axial sensors(Lindemann et al., 2005). With a sample rate of 200Hz, the output signal of the sensors is filtered by a low-pass filter with a cutoff frequency of 80Hz. With three thresholds: when the sum-vector of acceleration in xy-plane exceeds 2g, when the sum-vector of velocity as integral of acceleration from x-,y- and z-components right before the initial contact is higher than 0.7m/s; and when the acceleration sum-vector of all spatial axes together is higher than 6g, the system is able to distinguish falls with other daily activities. Also with a tri-axial accelerometer, in 2002, M. J. Mathie developed a device for fall detection using a signal energy threshold approach(Mathie et al., 2002). In this detection system, the tri-axial accelerometer consisted of two orthogonally mounted bi-axial piezo-resistive sensor, which measured the acceleration due to gravity as well as that due to body activities. The sample rate of the accelerometer is 45 Hz.

Machine learning and pattern classification techniques have been a hot topic in recent research. A lot of people have tried to use this technique to detect falls. T. Zhang embedded a tri-axial accelerometer inside a cellphone, using pattern classification method, such as 1-Class Support Vector Machine (SVM), Kernel Fisher Discriminant and K-Nearest Neighbor (K-NN) algorithm, for fall detection(Zhang et al., 2006a)(Zhang et al., 2006b). Suhuai Luo presented a fall detection system consisting of three dual-axial accelerometers to detect body acceleration in three planes(Luo and Hu, 2004). They used a gaussian

filter to remove the high frequency noise from the output of the sensors. Then dynamic motion pattern analysis is used to detect the fall event. Followed by C. Doukas in 2007, with accelerometers and using the method of SVM, a platform for detecting patient falls were developed(Doukas et al., 2007).

The main advantage of these systems is that they are very easy to deploy at a very low cost. Also people's privacy usually can be protected. The disadvantage of these systems is that people have to wear those sensors in a correct way all the time when they are monitored. It is possible that people might forget to wear them or even loose them. If they are not worn in the right way, they might not able to work correctly. At the same time, those sensors might cause some discomfort. Generally these systems also require certain calibration which might take a long time before they are used.

1.1.2 Environment Facility Method

The research using the environment facility method, which is to deploy some equipments in the environment, is mainly focused on computer vision techniques. With this method, fall detection sensors are deployed in the environment where targeted people are monitored. Usually video cameras, infra-red sensors as well as sound sensors are employed. And among them, video cameras or video sensors are used the most. Nowadays, video cameras have been quite popular for surveillance and home care system. With the video processing technique, people have attempted to develop computer-vision system to track people's different activities. One of the most important applications for that is the fall detection system. Several approaches exist in the automatic fall detection based on computer-vision system. Based on what these systems track, they can be classified as Body Tracking System and Head Tracking system. And based on the criteria they used for fall detection, they can be categorized as Inactivity Analysis, Motion Sequence Analysis and Motion Velocity Analysis, as shown in Figure 1.3.

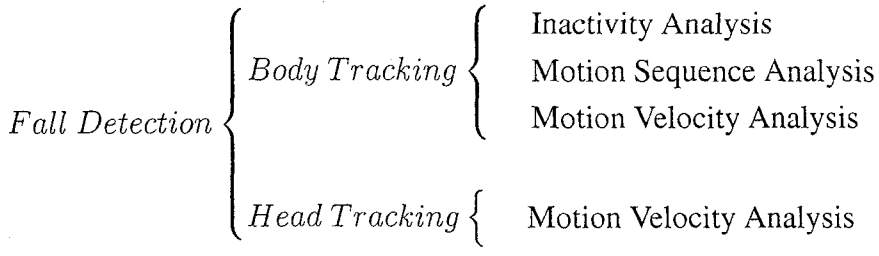

Figure 1.3 Approaches of fall detection based on vision system.

Computer vision has been increasingly involved in home assistive systems. Many methods based on video processing have been proposed to recognize people's posture and activities. Nait-Charif H. and McKenna presented a method using ceiling-mounted, wide-angle cameras with vertically-oriented optical axes that can detect inactivity outside usual zones of inactivity (Nait-Charif and McKenna, 2004). For instance, a person staying in a chair or on the bed probably is just resting, while a person lying on the floor for a relative long period probably have fallen and need help. This method focused on detecting people lying down in an unusual place. In 2006, Bart, J. and Rudi, D. further developed this method with an extensive context model(Bart and Rudi, 2006). A 3D camera which is based on the time of flight is used to provide low resolution depth images. Taking the orientation, location as well as the time and duration of a person's inactivity into consideration, this method can integrate different types of knowledge in determining falls and reduce the probability of false alarms.

There are other methods that not only detect the inactivity but also analyze the motion sequence in a period time. Anderson, D. has proposed a method to extract features from a silhouette and employing Hidden Markov Models(HMM) for activity recognition. The method performs the feature extraction based on the point that when a person is standing, the width to height ratio is very small while the person falls down on the ground, this ratio becomes much larger. Then, the observations over a period are taken as a sequence to train and perform classification using HMM. HMM is also used by Toreyin, BU to model people's activities(Toreyin et al., 2005), where wavelet transform of the one-dimensional

aspect ratio signal is used as the feature signal in HMM based classification and two three-state HMMs are used to classify the motion of a person.

All the above methods to detect falls are based on tracking the person's silhouette or bounding box, while many people have proposed methods to track people by 3D head trajectory, because usually the head is visible and has a larger movement in a fall. Rougier, C. and Meunier, J. have presented a fall detection system employing 3D head trajectory extracted from video information(Rougier and Meunier, 2006)(Rougier et al., 2006). The system detects the fall by measuring the vertical velocity and the horizontal velocity which have thresholds for falls.

Beside these systems based on video cameras, fall detection systems based on other sensors such as infra-red sensors (or thermal imaging sensors) are also presented. The SIMBAD system proposed by Sixsmith, A. and Johnson, N.(Sixsmith and Johnson, 2004) used infra-red integrated system(IRISYS) thermal imaging sensors to locate and track a thermal target, providing the size, location and velocity information. The system used elliptical-contour gradient-tracking method to localize and track targets. And vertical velocity estimates obtained from the sensor array are used in a neural network to detect falls.

The advantages of these systems are that they are able to detect many events at the same time and generally they can provide more information than those standard sensors. Also, they do not bring any discomfort to those people monitored and they can provide location information simultaneously. However, they usually cost much more than those methods based on wearable sensors and they usually have to employ data processing techniques that are prone to errors and are complicated for computation.

1.2 Wireless Positioning

Driven by a huge potential market and revenue, there is an increasing interest in wireless positioning techniques. As a very large number of applications and services are based on location awareness, distance measurement and positioning capability have become necessary for many wireless communication systems. As an example, the Federal Communications Commission (FCC) in the US has issued an order that required all wireless service providers to provide subscriber location information for the Enhanced-911 service (E-911). It is mandatory that all the wireless service providers have to give the mobile position within 100 meters of its actual location for at least 67 percents of all wireless Enhanced-911 calls.

Different from the radar system that determines the propagation time and direction of radio signals reflected back from a passive target, the wireless positioning techniques here refer to a position determination between two or more active wireless terminals, such as the aeronautic Distance Measuring Equipment (DME) and VHF omnidirectional range (VOR) that have been used for a long time. Probably the best known example is the Global Positioning System (GPS). Although it has been widely used, this system can not be used directly in indoor environment. Because there is a high attenuation when the GPS signal goes through walls of high-rising buildings(Dedes and Dempster, 2005). Moreover, because of the multipath effects in indoor environment, the positioning performance will be degraded. Nevertheless, the principles these systems used for positioning can also be applied in indoor positioning systems.

Depending on the accuracy requirements and system architectures, there are mainly three basic signal parameters that can be measured for positioning: Received Signal Strength (RSS), Time of Flight (TOA) and Angel of Arrival (AOA).

$$Wireless\ Positioning \begin{cases} Received\ Signal\ Strength(RSS) \\ Time\ Measurement \begin{cases} \text{Time of Arrival (TOA)} \\ \text{Time Difference of Arrival (TDOA)} \end{cases} \\ Angle\ of\ Arrival(AOA) \end{cases}$$

Figure 1.4 Wireless positioning methods

1.2.1 Received Signal Strength (RSS)

Generally speaking, received signal strength at a receiver is a function of distance from the transmitter. Therefore, the received signal strength contains information about the distance between the transmitter and the receiver and the position information of the receiver, which can be used for positioning.

There are mainly two types of techniques used for positioning based on received signal strength. One class involves trilateration method with estimated range information between several base stations and the target. The second class employs matching real-time measured signal strength with a database created before.

In free space, the relationship between the received signal strength and the distance between the transmitter and the receiver is shown in the following equation:

$$P_r = \frac{P_t G_t G_r \lambda^2}{(4\pi)^2 d^2} \tag{1.1}$$

where P_r is the received power, P_t is the transmitted power, G_t and G_r are the transmitter antenna gain and the receiver antenna gain respectively, λ is the wavelength of the transmitted signal and d is the distance between the transmitter and the receiver. In order

to consider the path loss, the above equation can be rearranged as:

$$P_l = \frac{P_r}{P_t G_t G_r} = (\frac{\lambda}{4\pi d})^2 \tag{1.2}$$

In order to include the multipath and shadowing effects in an indoor environment,Sixsmith, A. and Johnson, N. has proposed a propagation model for indoor environment as(Sixsmith and Johnson, 2004):

$$P_l = \frac{P_0}{d^n} = \frac{\lambda^2 d_0^{(n-2)}}{(4\pi)^2 d^n} \tag{1.3}$$

or in a logarithmic scale, the path loss P_l in dB at a distance d from the transmitter can be described as:

$$P_l(dB) = 20log_{10}(\frac{\lambda}{4\pi d_0}) - 10n \cdot log_{10}(\frac{d}{d_0}) \tag{1.4}$$

where P_0 is the path loss at d_0 from the transmitter and n is an exponent depending on the environment. It was reported in the range from 1.2 to 6.5 for indoor environment with a frequency of 900MHz. So when the transmitted power is known, the target can approximate its distance from the base station with its the received signal strength from that base station. Then the target can be located in a circle for two dimensions or a spherical surface for three dimensions with the base station in the center. With several base stations, the target is able to find its location from the geometry of the intersection of circles (two dimensions) or spheres (three dimensions) as shown in Figure 1.5.

Because usually there are many walls, furniture, windows and doors in an indoor environment, and there are people walking around, it is quite difficult to get precise distance only based on indoor propagation model. In order to get a better performance, the other type of methods that employs comparison between real-time measured signal strength from several base stations and recorded data in a database created previously is more popular. These methods are usually referred to as pattern recognition or fingerprinting.

Although it is very difficult to develop a model for radio propagation in an indoor en-

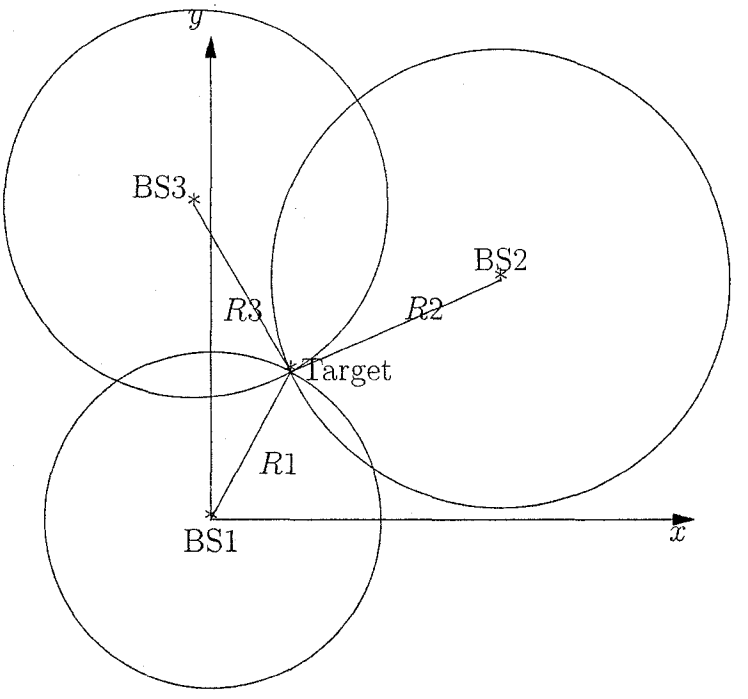

Figure 1.5 Trilateration for positioning with RSS

vironment, measurements show that the received signal strength at a certain place still strongly depends on its position. It is just like fingerprints that can be used to find persons because different people have different fingerprints. We can use the received signal strengths to find the location. These methods usually involve two phases usually referred to as off-line phase and on-line phase. At first, all the area covered by the positioning system is divided into many grids composed of many points. The received signal strengths from all available base stations at each point are recorded in a database. As a result, all the multipath and shadowing effects are already included in the database. Then in the on-line phase, the target will collect all the received signal strengths available and these collected signal strength information will be compared with those recorded in the database. According to some algorithm, distances between the real-time measured signal strengths and those in the database will be calculated. The position whose recorded signal strengths has the smallest distance from the real-time measured ones will be considered as the real position of the target.

The advantages for positioning system employing RSS measurements are obvious. Since almost all the transceivers for wireless communication have an automatic gain control part, which can be used to read out the RSS, existing equipments for wireless communication can be used for RSS positioning directly. Therefore, the cost of equipments for these systems is very low. Even though the accuracy is not very high, it is sufficient for many applications. The problems are that these systems require a lot of work to create the database and they highly depend on their environments. If some changes happen that affect the radio signal propagation, the database has to be rebuilt.

People from Microsoft Research have proposed a radar system for indoor positioning(Bahl and Padmanabhan, 2000). This system uses the RSS information measured by IEEE802.11 wireless network devices at many location inside a building. It combines empirical measurements with signal propagation modeling for estimating user location. An accuracy of $3 \sim 4.3$ meters with a probability of 50% has been reported.

1.2.2 Time of Arrival and Time Difference of Arrival

As is known, the radio signal propagates at the speed of light. So if the time when the signal transmitted from a base station is known, and the target measures the time when it arrives, the time it takes for the signal travel from the base station and the target can be obtained. Further, the distance between the base station and the target can be calculated. With many base stations available at the same time, the position of the target can be calculated with some methods such as trilateration described in Figure 1.5.

However, positioning systems based on time of arrival(TOA) require accurate synchronization for all base stations and the target involved in positioning. This is a big drawback for many applications. Systems based on time difference of arrival(TDOA) do not have this problem, although they need one more base station for positioning. For this kind of

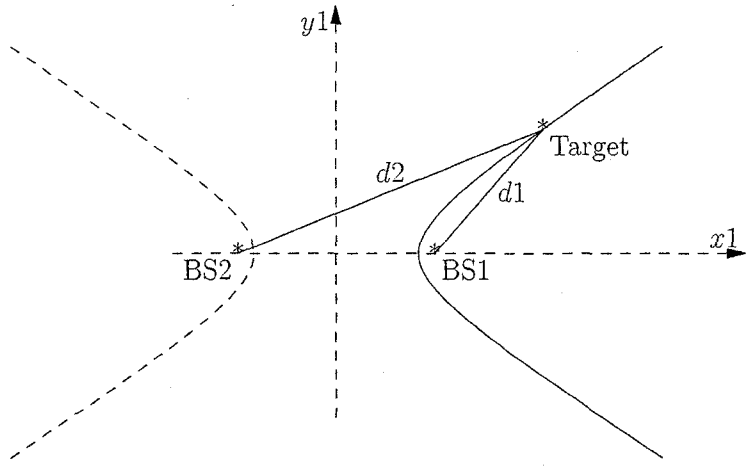

Figure 1.6 Locus of TDOA with two base stations

systems, the target doesn't need to be synchronized with those base stations, although base stations involved in a positioning event have to be synchronized. The target just has to determine the difference of arrival time of those radio signals from different base stations. As we know, the locus of points difference of distances from two base stations is a hyperbola as shown in figure 1.6. The target measures the different arrival time Δt of radio signals from two base stations. Since radio signal propagates at the speed of light, the difference of distances from the two BS to the target can be determined as: $\Delta d = d_1 - d_2 = \Delta t \times c$, where c is the speed of light. The locus determined by this is a branch (the solid line if $\Delta d > 0$, or the dashed line if $\Delta d < 0$)) of a hyperbola. So if there is another available base station, the position of the target can be determined in a two dimensional space, as shown in figure 1.7. TDOA is quite similar to TOA. In fact, it has been shown that TDOA can be considered as TOA with a clock bias(Shin and Sung, 2002).

The obvious advantage of positioning systems employing time measurement is that they can provide a better resolution and accuracy than other positioning systems based on RSS or AOA. On the other hand, the precision of time measurement highly depends on system hardware. For TOA method, all the base stations and the targets have to be

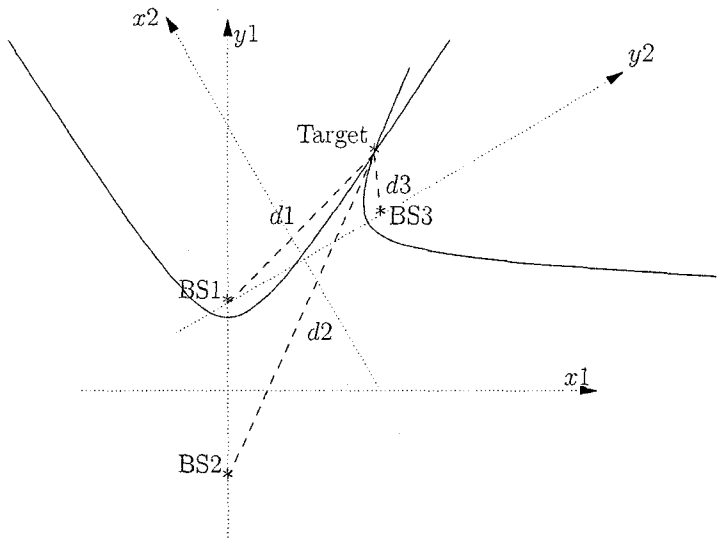

Figure 1.7 Positioning based on TDOA in a two dimensional Space

synchronized, and for the TDOA method, all the base stations have to be synchronized. In order to get a good performance, stable clock at a frequency high enough should be used to measure the time. Also, wider bandwidth should be employed to get a better distance measurement. Apart from the system parameters, multipath effect and additive noise are very important factors that can induce ranging errors.

The PinPoint 3D-iD Indoor Location Positioning System is designed with time measurements for positioning a large number of tags in an indoor environment(RF Technologies, 2001). In this system, the base stations or interrogators transmit a test signal, and the tag simply changes the signal's frequency and transponds it back to the base station. The distance can be obtained by measuring the time delays. An accuracy of $1 \sim 3$ meters is specified.

1.2.3 Angle of Arrival

Other than trying to measure the distance between the base stations and the target, the target location can be found with angle of arrival information. Figure 1.8 presents the

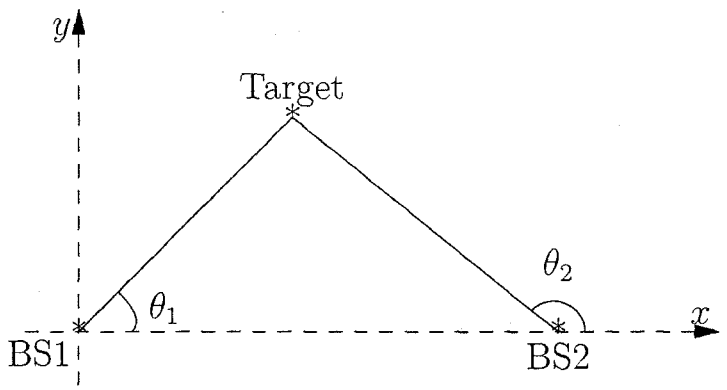

Figure 1.8 Positioning based on AOA in a two dimensional space

principle of the method. There are mainly two basic methods for finding the direction of signals. One is based on comparison between the power distribuion of received signal and the antenna pattern. The other is to measure the phase between two successive antenna elements in an antenna array.

For the first case, the target or base stations can rotate a directional antenna to find the peak of the antenna pattern, that is to find the angle of the antenna where the signal with highest power level is received. Then the direction pointed by the peak of the antenna pattern is the arrival direction of the received signal. Besides, because for many antennas, the gain varies much more around the null than around the peak of the radiation pattern, some systems try to find the null of the antenna pattern, instead of finding the maximum. The direction pointed by the null of the antenna pattern is the arrival direction of the received signal. For these systems, highly directive antennas are preferred for good accuracy. Also, large signal to noise ratio(SNR) will give a good performance.

Beside finding the AOA by measuring power peak or power null, the arrival direction can also be found with an antenna array. Figure 1.9 shows a simple example that uses antenna array with two antenna elements to find the signal arrival direction. There are different distances from the target to the two antenna elements. The signal from the target will reach the second antenna element first. As a result, there will be a phase

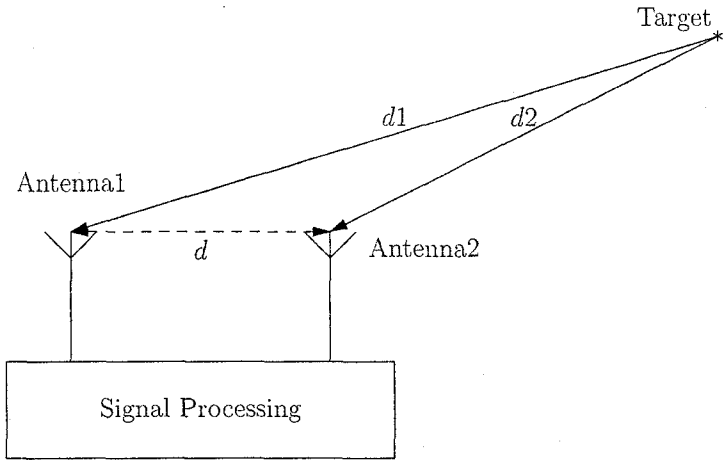

Figure 1.9 Finding direction with antenna array

difference between the signals received by the two antenna elements and the direction can be obtained.

The AOA positioning system is very simple to implement except the high directional antenna. Like the other positioning systems, noise and especially multipath effect degrade the performance. As for indoor environment, AOA method is usually not used alone for positioning, because there are many reflectors and it is very difficult to give an acceptable accuracy with this method. AOA is often implemented together with RSS or time measurement methods as a supplementation.

In addition, some positioning systems also employ infra-red signal and ultrasound for indoor positioning. Infra-red signals has been used in the Active Badges positioning system(WANT et al., 1992), which can find the position of people inside an area of a room size. The Active Bat Location System uses ultrasound signal to measure time flights(Harter et al., 2002). The system measures the distance between a mobile tag, called Bat, to ceiling mounted ultrasound sensors. Because the speed of sound is much lower than that of electromagnetic waves, this system doesn't require a high accuracy timer. It is reported to have an accuracy of 9 cm with a probability of 95%. Ultrasound is also used in the Cricket location system(Priyantha et al., 2000), which is able to position

the target inside a 4 by 4 ft area.

1.3 System Architecture

In the current project, we proposed and implemented a positioning system based on RSS and a fall detection system based on wearable sensors.

A question can be logically asked: since the positioning systems based on time measurement can potentially provide a better accuracy than those based on RSS measurement, why the RSS method is chosen over the TOA or TDOA? The first reason is that positioning systems based on time measurement cost much more than those based on RSS measurement. Because systems based on RSS measurement only have to be able to read out the RSS while those based on time measurement requires very stable and accurate clocks with a high frequency as well as powerful data processing units. Since transceivers for telecommunication usually have a automatic gain control unit, which can be used to read out the RSS, almost all the transceivers in markets can be used for positioning with RSS.

Another reason is that such an accurate positioning is not required for our application. Indeed, in order to find the position of a person how has fallen down, there is no difference between using a system that has a precision of ten centimeters and another one with a precision of two meters. It might be difficult to find a needle with a precision of two meters, but there is no difficulty to find a person within two meters. The difficulty to find people with these two systems is almost the same.

The reason for using wearable devices for falling detection is obvious. It costs much less than other methods. It is very easy to implement. And it is suitable to cooperate with the positioning system.

CHAPTER 2

FALL DETECTION

In this chapter, the theory that how the fall detection system works will be discussed. And a system implementation with a sensor from the company Freescale and a micro-controller as the data processing unit from Analog Device will be introduced.

2.1 Basic Theory

Although the word 'fall' seems very easy in the common sense, it might be difficult to describe it precisely and specify its features for fall detection. It is quite necessary to define the fall precisely while easy for the system implementation. One commonly used definition is 'A fall is a sudden, unintentional change in position causing an individual to land at a lower level, on an object, the floor, or the ground, other than as a consequence of a sudden onset of paralysis, epileptic seizure, or overwhelming external force'(Tinetti et al., 1994). This definition is used for the fall detection system design.

Physical activities can be defined as many bodily movement produced by skeletal muscles that result in energy expenditure(Caspersen et al., 1985b). It has been widely accepted that the energy expenditure can be used to classify daily activities, including falls. Unfortunately, although energy expenditure is quite useful for fall detection, it is not practical to measure it directly. As a result, energy expenditure has to be measured in other ways. It has been demonstrated that there are strong relationships between energy expenditure and the output of accelerometers used to analyze gait and other movements. The best prediction of energy expenditure has been considered to be the summation of

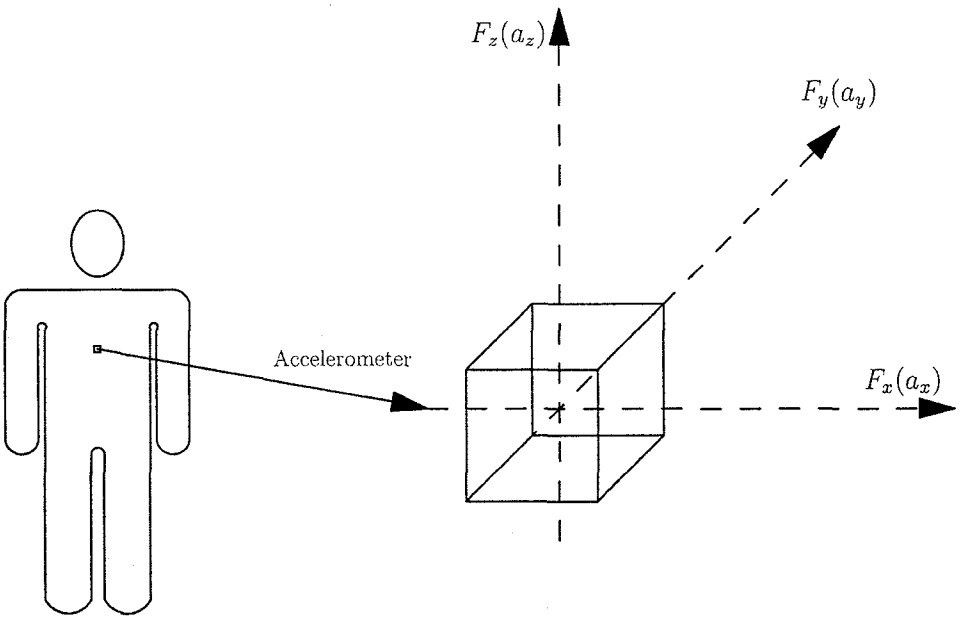

Figure 2.1 Using accelerometer to measure energy expenditure

the absolute value of the three orthogonal forces:

$$\text{Energy Expenditure} \approx \int_{time} (|F_x| + |F_y| + |F_z|)dt \tag{2.1}$$

where F_x, F_y and F_z are the forces exposed on a person in the x, y and z direction. According to Newton's second law, the relationship between an object's mass m, its acceleration a, and the applied force F is:

$$\vec{F} = m \times \vec{a} \tag{2.2}$$

or

$$F_x = m \times a_x \tag{2.3}$$

$$F_y = m \times a_y \tag{2.4}$$

$$F_z = m \times a_z \tag{2.5}$$

Then the energy expenditure is directionally proportional to the integration of acceleration:

$$\text{Energy Expenditure} \propto \int_{time} (|a_x| + |a_y| + |a_z|)dt \tag{2.6}$$

As a result, other than measuring the applied force directly, it can be measured by the acceleration, because accelerometers are very cheap and easy to buy.

However, the energy expenditure alone is not enough for fall detection, because there are many intensive activities, such as jumping, that can have an energy expenditure value similar to that for fall. With the orientation detection, this problem can be solved. Because when fall happens, the orientation of the body has a 90 degree change while for usual activities, there is no change in the orientation of the body.

Besides, after a fall that hurts the person badly, there will not be any intensive activities after. So, after a high energy expenditure value is measured, if the output of the accelerometers is stable, probably a fall happened. But if there is still big changes in the accelerometer output, no fall should be reported.

2.2 Hardware Implementation

The fall detection circuits mainly contains three parts: the accelerometer, analog signal to digital signal converter (A/D Converter) and a data processing unit. The three axis low-g micromachined accelerometer MMA7260QT from Freescale Semiconductor is used(MMA7260Q 3D Accelerometer, 2008). By changing the internal gain, this surface-micromachined integrated-circuit accelerometer allows for the selection among four different ranges with different sensitivities: 1.5g with 800mv/g, 2g with 600mv/g, 4g with 300mv/g and 6g with 200mv/g(g here is the acceleration caused by the gravity). The chip also has a onboard single-pole switched capacitor filter that can condition signals. Besides, it provides a sleep mode that can highly reduce its consumed power. This

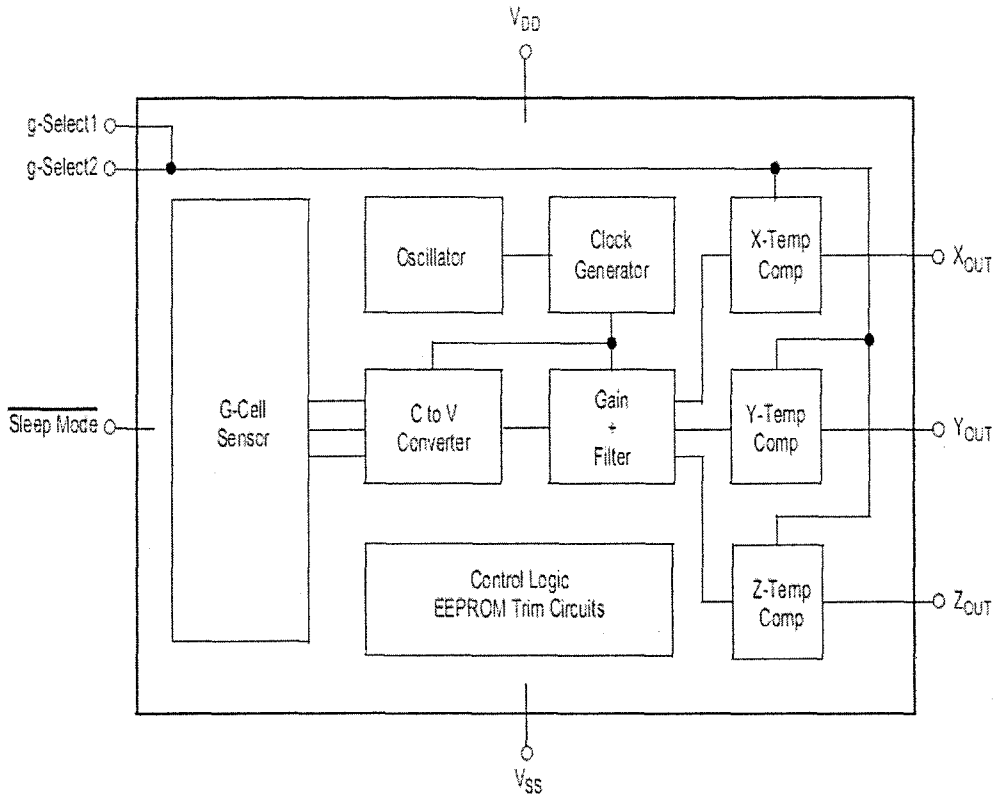

Figure 2.2 The accelerometer MMA7260QT architecture(MMA7260Q 3D Accelerometer, 2008)

feature is very useful, since it can increase the lifetime of batteries used for power supply. Figure 2.2 shows the architecture of the accelerometer(MMA7260Q 3D Accelerometer, 2008).

A microprocessor for Microchip Technology, the PIC16LF877(Microchip datasheet, 2003), is used to process the data from the accelerometer. This microcontroller has 14.3K bytes used for program, 368 Bytes high-speed SRAM used for data, 256 bytes relatively low-speed EEPROM used for data, and 8 10-bit A/D converter channels. The microcontroller can work at up to a frequency of 20MHz. The A/D converter can still work even the microcontroller is in sleep mode. This can be used to save the battery power. The A/D channels in PIC16F877 are all 10-bit converters. For convenience and

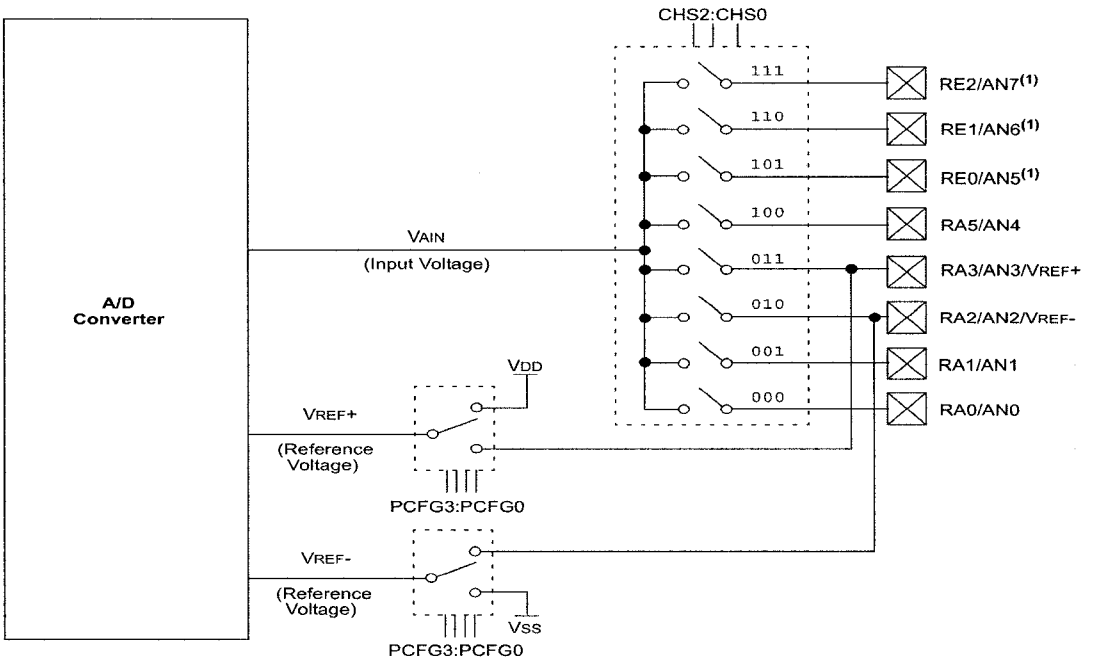

Figure 2.3 The A/D block of the microcontroller(Microchip datasheet, 2003)

efficiency, only the high 8 bits are used. So the output ranges from 0 to 255(2^8) in accordance with a voltage range of V_{REF-} to V_{REF+}. The V_{REF-} in this circuit is the ground and the V_{REF+} is the supply voltage of the circuit(3.3V). As a result, one unit difference in the output digital value of the A/D converter corresponds to a input voltage difference of

$$\Delta V = \frac{3.3V}{2^8 - 1} = 0.0129V \tag{2.7}$$

This is also the minimum input voltage difference recognizable by the A/D converter. For example, when there are two data 18 and 22 read out at time t_1 and t_2 and corresponding to an input voltage of V_1 and V_2 respectively, then, the difference of these two voltages, $V_2 - V_1$, can be calculated by $(22-18) \times 0.0129V = 0.0516V$. Figure 2.3 shows the A/D converter block of the microprocessor(Microchip datasheet, 2003). As recommended, other than connecting the accelerometer and the microcontroller directly, a low pass RC filter is used at the output of the accelerometer to reduce the clock noise.

In order to read out the real time data for debug, a display block is implemented with a two-digit seven segment led. The maximum soured current of the microcontroller is 25mA while the required current for each segment of the LED is 30mA, so the microcontroller is not able to drive the LED directly. The MAX6978 from Maxim company, which has a maximum output current of 55mA, is used as the driver of the LED(Maxim Integrated Products, 2005). It has a industry standard 4-wire serial interface. And the microcontroller can use three or four pins to control the display block.

For research, all the data obtained by the accelerometer has to be recorded in a computer. So a RS-232 interface is employed in this circuits for communication between this circuits and a computer with a serial port. Since the voltage of input/output pins comply with the TTL/CMOS industry standard while the serial port of the computer employs RS-232 voltage standard, they can not be connected directly. The MAX232 from Maxim company is used to convert TTL/CMOS(RS-232) voltage level to RS-232(TTL/CMOS) voltage level. The whole circuits are shown in Figure 2.4.

2.3 Software Implementation

There are mainly two parts concerning the software implementation. One is the processing of the output data of the accelerometer. The other is the communication between the fall detection circuits and a computer.

As presented above, the output of the accelerometer is analog signal and it has to be converted to digital signal by the A/D converters included in the microcontroller. The speed of this process, referred as sample frequency, is limited by the hardware. Figure 2.5 shows the analog model for the A/D block of the microcontroller(Microchip datasheet, 2003). As we can see, the circuit is mainly a RC network. It is obvious that for good accuracy, the charge holding capacitor C_{HOLD} must be fully charged to the input voltage

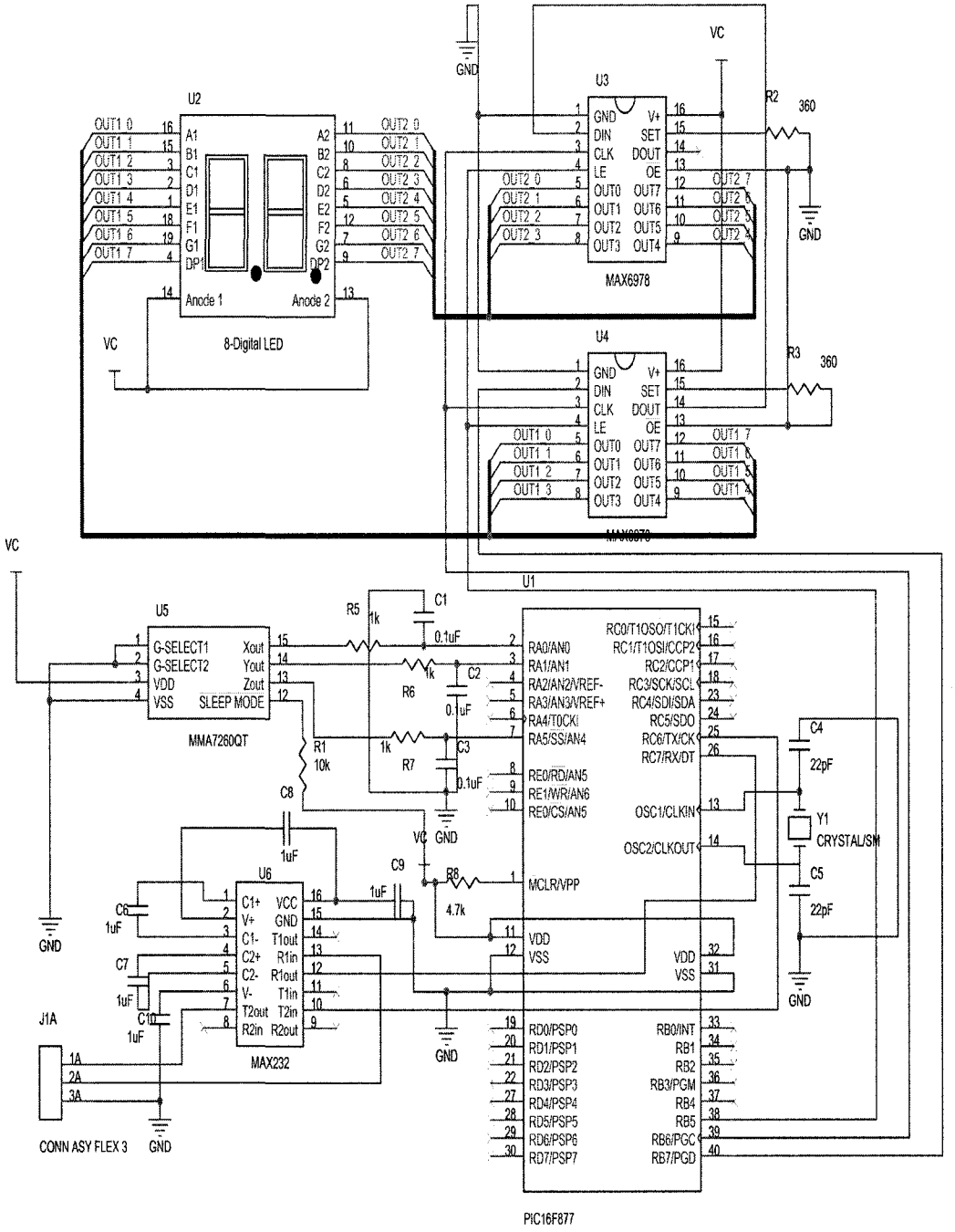

Figure 2.4 The fall detection system circuits

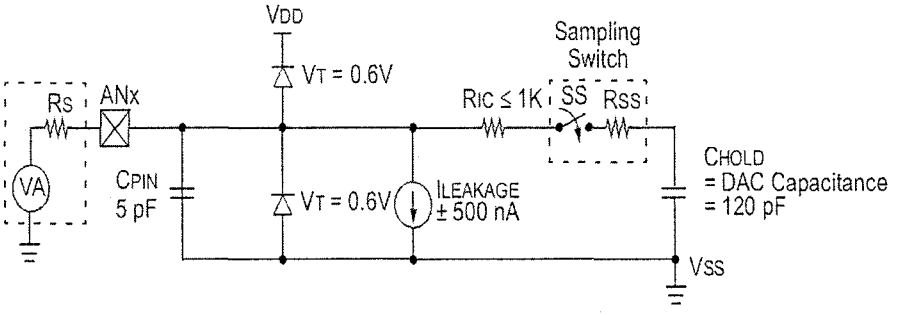

Figure 2.5 The analog model for A/D block of the microcontroller, where VA and R_s is the equivalent circuit of the external circuit, whose analog voltage will be converted to digital signal, C_{pin} is the input capacitance, V_T is the threshold voltage, V_{DD} is the supply voltage, $I_{leakage}$ is the current leakage at the pin due to various junctions, R_{IC} is the interconnect resistance, SS is the sampling switch and C_{HOLD} is the sample and hold capacitance.

level. Figure 2.6 shows a typical RC network and its output. As shown in the figure, the output V_{out} never equals to the input voltage V_{input}.

The voltage on the capacitor is calculated by:

$$V_{out}(t) = V_{in} - V_{in} \times e^{-\frac{t}{R \times C}} \tag{2.8}$$

and the error is obtained by:

$$V_{error} = V_{in} \times e^{-\frac{t}{R \times C}} \tag{2.9}$$

Although it takes infinite time for the capacitor to be 100 percent charged, V_{out} can almost reach V_{input} in a short time with a small error. For example, if an error of $\frac{1}{2}$ LSb[1] is allowed, the required time is reduced to:

$$T_C = -R \times 3C \times ln(\frac{1}{2 \times 2^{10}}) = R \times C \times ln(2048) \tag{2.10}$$

[1]LSb is the least significant bit for a binary number. So, for a 10-bit A/D, $\frac{1}{2}$ LSb error equals to $\frac{1}{2} \times \frac{1}{2^{10}} \times V_{in} = \frac{V_{in}}{2048}$

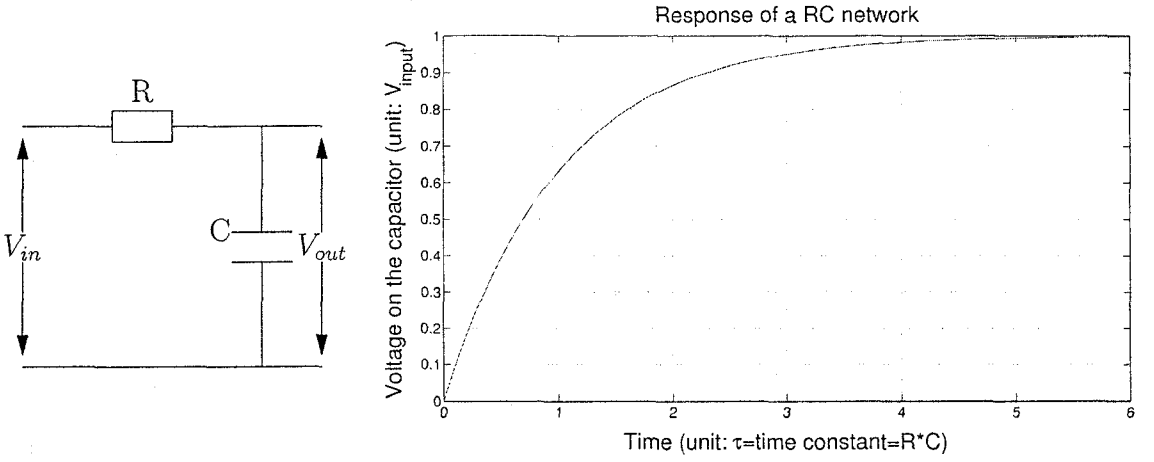

Figure 2.6 A typical RC network and its response versus time

The total time required for the A/D converter to complete one conversion also includes an amplifier settling time and a temperature coefficient. The latter is only required for temperature larger than 25°C. The minimum time required for A/D conversion can be obtained by:

$$T_{Total} = T_C + T_{AS} + T_{CO} \tag{2.11}$$

where T_C is the time required to charge the holding capacitor, T_{AS} is the amplifier settling time and T_{CO} is the temperature coefficient. According to the datasheet, T_{AS} is $10\mu s$ and T_{CO} is 0.05 $\mu s/°C$. Since usually people's body temperature is around 36.5°C, T_{CO} can be obtained by

$$\begin{aligned} T_{CO} &= (Temperature - 25\,°C) \times 0.05\mu s/\,°C \\ &= (36.5\,°C - 25\,°C) \times 0.05\mu s/\,°C \\ &= 0.575\mu s \end{aligned} \tag{2.12}$$

The R_{IC} and R_{ss} together are less than $13k\Omega$(Microchip datasheet, 2003). Assume R_s

is around $50k\Omega$ and when $\frac{1}{2}$ error is applied, the T_C can be calculated by

$$\begin{aligned} T_C &= (R_s + R_{IC} + R_{ss}) \times C_{HOLD} \times ln(2048) \\ &= (50k\Omega + 13k\Omega) \times 120pF \times ln(2048) \\ &= 57.6\mu s \end{aligned} \tag{2.13}$$

As a result, any sample period larger than this value can be used for good accuracy. The R_s value here might be larger, but even if it is around several hundreds $k\Omega$, the T_C is still in the order of $10^{-6}(\mu s)$. This gives us the minimal sampling frequency. In the project, a total period of $6.24ms$, corresponding to a sampling frequency of $160.25Hz$, is employed. Because there are three channels that have to be sampled while there is only one channel that can work at one time, the T_C for each channel is around $\frac{6.24}{3}ms = 2.08ms$. In addition to the accuracy requirement for the A/D block presented above, there are many other reasons for which this sampling frequency is chosen. First, the speed of people's fall is relatively slow compared to the speed of the sampling speed. When the sampling speed is very high, the data do not change among many sampled points. And it will take more memory to store the data. Second, usually the memory of the microcontroller itself is not enough to store and process the sampled signal, so other memory chips will be used. The speed that the microcontroller works with the memory chip also puts a limit on the sampling speed. Third, the microcontroller has to process the sampled signal at the same time that the A/D converter is working. If the processing speed is quite low compared with the sampling speed, the microcontroller is not able to process the data and they system would not work. As a result, concerning accuracy and memory requirement, the period of $6.24ms$ is used for total three channels.

After the sampling, the data will be first filtered by a filter to decrease the noise. Although a low pass filter is usually used to filter out the very high frequency noise, the 47th order median filter is used here. The low pass filter can work well, but the median filter is

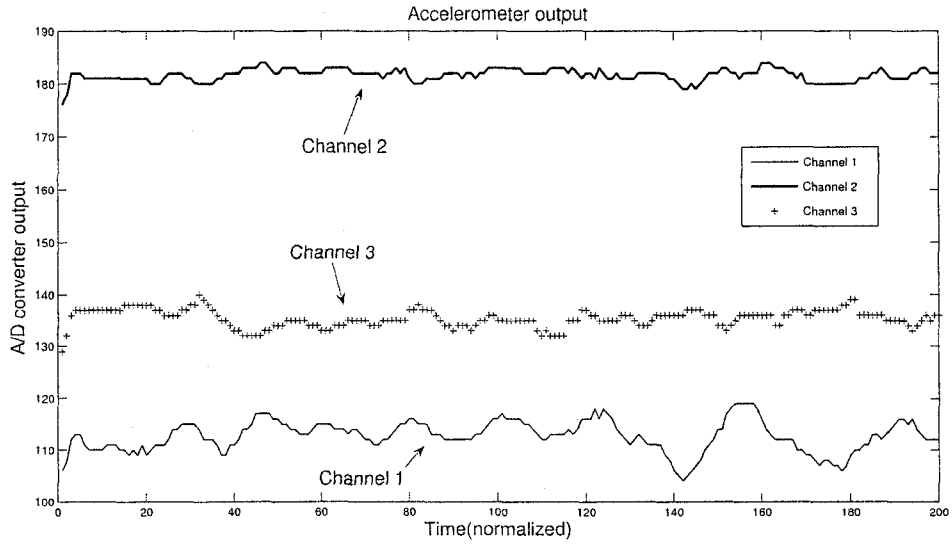

Figure 2.7 Output offset of the accelerometer

more efficient here. The median filter is a non-linear spatial filter for smoothing signals, especial for suppression of impulse noise. The median filter can also be considered as a kind of non-linear low pass filter. By 'non-linear', it means that for different input, the frequency response of the filter is different. Besides, the median filter can preserve the edges. Specifically, what the median filter does is to replace a value with the median of its neighbor values.

A high pass digital filter is needed after the median filter. In fact, the output of the accelerometer is proportional to the force exerted on the sensor instead of the actual acceleration of the sensor. So even the sensor is at rest, there will also be a non-zero output because of the gravity of the sensor. When there is no force applied to the sensor, there will be a typical output of 1.65V(MMA7260Q 3D Accelerometer, 2008). Then when the sensor with a sensitivity of $800mV/g$ is at rest, the output is $1.65V + 800mV/g \times 1g = 2.45V$. Figure 2.7 shows a typical measured output of the accelerometer when a person wearing it in the way shown in Figure 2.1 stands still.

This non-zero output has no relationship with the energy expenditure and it has to be

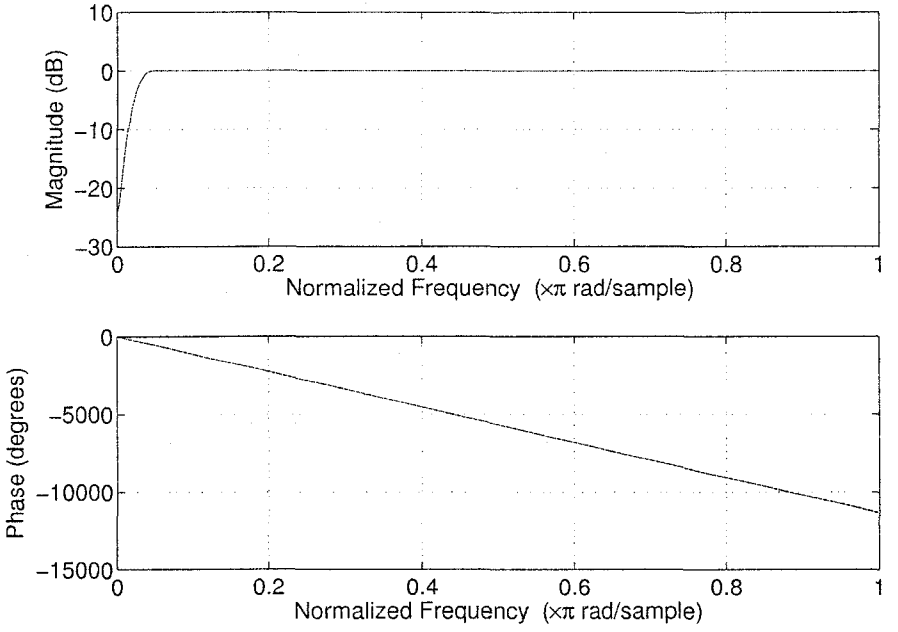

Figure 2.8 Frequency response of the high pass FIR filter.

removed. This part can be considered as a DC component in the output signal. Then it can be removed by a high pass filter. This explains why a high pass FIR(Finite Impulse Response) filter of order 126 with a normalized cutoff frequency of 0.02(1 corresponds to the Nyquist frequency) is used here. Figure 2.8 shows the frequency response of the high pass filter.

Then the data will be processed according to equation(2.6). The output of the three channels for x, y and z-axis will be added together according to equation

$$|\vec{a}| = \sqrt{|a_x|^2 + |a_y|^2 + |a_z|^2} \tag{2.14}$$

Before the further processing, the time window T_{window} for the integral will be presented here first. The actual time window is determined in device calibration. This time window must be wider than the length of time that is taken by all types of falls, or any types of falls can be finished inside this period of time. Also, the time window should not be too

long. Because it will require more memory and complexity for the microcontroller to process it. Further more, if it is too long, two successive activities with small accelerations would be taken as one activity with a large acceleration, resulting in false detection. In this project, a time window of one second is used($T_{window} = 1s$), corresponding to a data number of:

$$\begin{aligned} N_{window} &= \text{Time Window} \times \text{Sampling Frequency} \\ &= \frac{1s}{2.08ms} = 480\text{data} \end{aligned} \tag{2.15}$$

For instance, at the time t_0, the system will process the data further according to the following equation:

$$EE = \int_{t_0 - T_{window}/2}^{t_0 + T_{window}/2} (|\vec{a}|)dt \tag{2.16}$$

Finally, the system will compare this value with a predefined threshold $EE_{threshold}$. If the calculated value is smaller than the threshold, no fall will be reported. If not, the system will analyze the orientation of the person at the beginning and that at the end using the three channels' output data out of the median filter. If obvious changes are found in two channels, then the orientation changes. If changes happen in only one or all three channels, it means that the activity is not finished yet, and the start time and end time for processing will be changed and the data will be processed again. When the orientation of the person changes, the system will start a timer to wait for a predefined time. If within the predefined time period no obvious change in the output of the accelerometer is detected, a fall will be reported and the system will start to do the positioning. If obvious changes can be found inside the period, the system will be reset and no fall will be reported.

In order to save power, the system will not do the algorithm talked above all the time. Instead, the system will calculate the value $|\vec{a}|$ according to equation(2.14) with the orig-

inal sampled signal all the time. If this value is not larger than a predefined threshold $|a_{threshold}|$, the system will stop processing current sampled data. But if the value goes beyond the threshold, the system will go through the above algorithm to check out if a fall happens or not. If the calculated energy expenditure is larger than the threshold $EE_{threshold}$, the system will start a timer. After the timer finishes, the maximum calculated $|\vec{a}|$ and minimum $|\vec{a}|$ will be analyzed to see if obvious changes happen or not. If it happens, it means that the person can still move and no fall will be reported. But if no obvious changes happen, a fall will be reported.

The whole flow chart of the fall detection system is shown in Figure 2.9.

2.4 Measurements and Results

2.4.1 Measurement Setup

Figure 2.10 shows the fall detection test circuit. A power supply of 3.3V is used to feed this circuit. The serial port is connected to a PC with a wire. A windows program shown in figure 2.11 runs on the PC to read the sampled data out of the accelerometer. This circuit is put on a person as shown in figure 2.1. The person performs some daily activities for test. The connection wires for the serial interface and for the power supply is long enough to enable free activities of the person. The LED on the circuit shows real-time sampled signal. And the windows program reads out all those data, which can be saved in a file for further analysis.

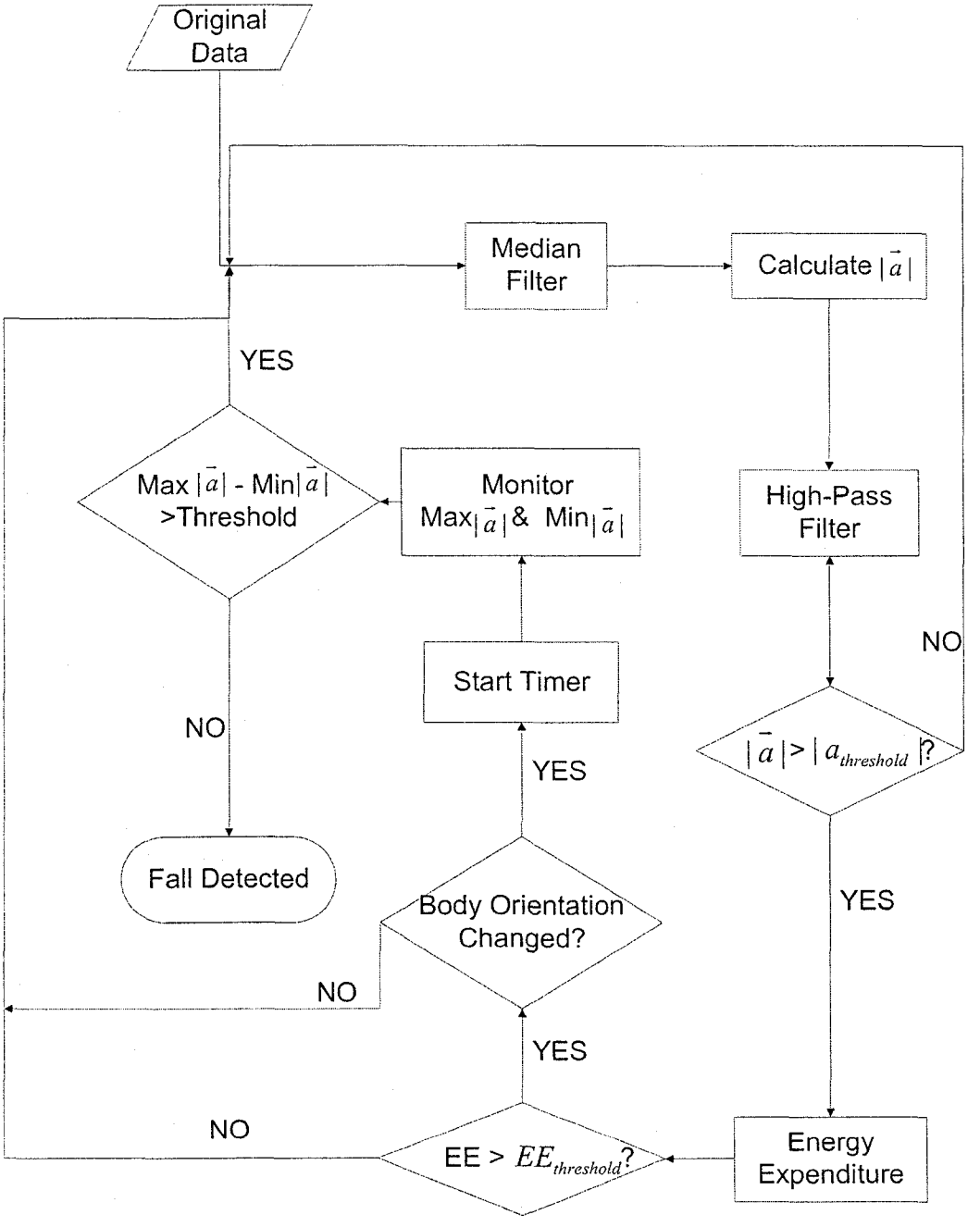

Figure 2.9 Flow chart for the fall detection system

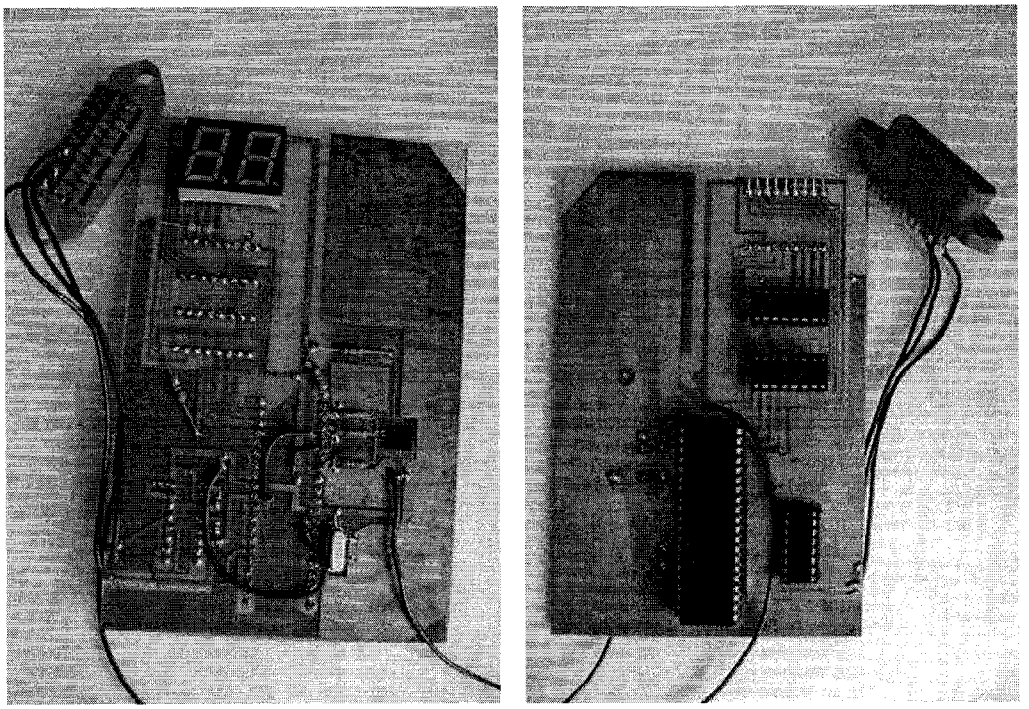

(a) Top view of the test circuit (b) Bottom view of the test circuit

Figure 2.10 The fall detection test circuit

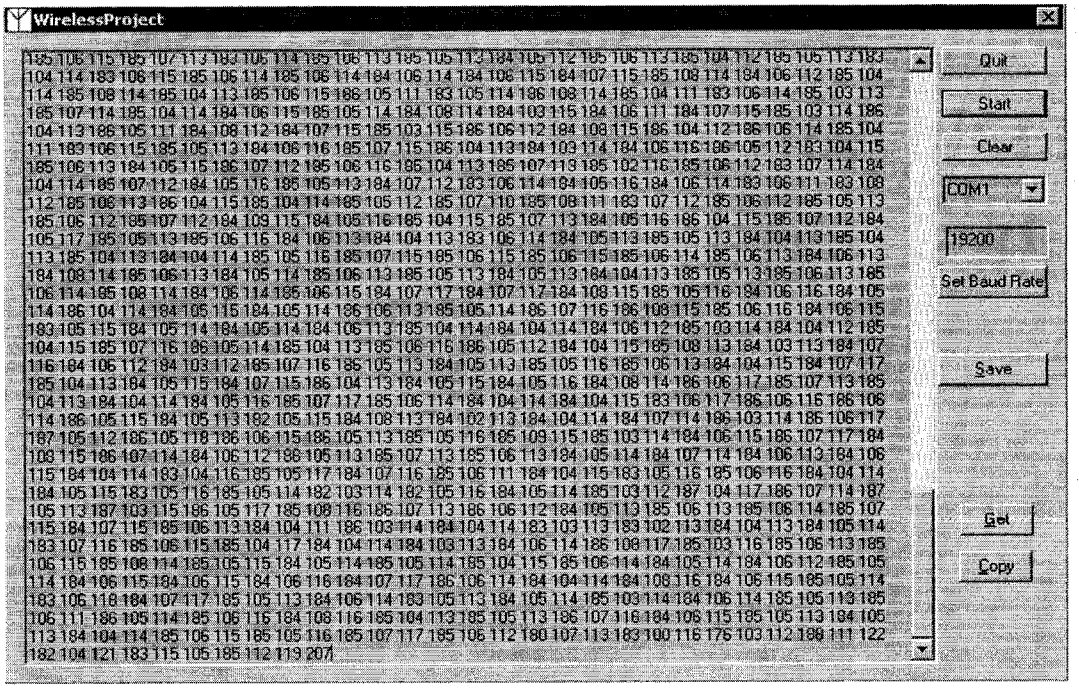

Figure 2.11 Windows program to read the data from the test circuit

2.4.2 Measurement Results

All the sampled data are transmitted to the PC and are saved to files that are processed and analyzed with Matlab afterwards. During the analysis, all the digital signals are represented by the output 8-bit data directly. Those data are not converted to the actual input voltage according to the mechanism of the A/D converter.

Figure 2.12(a) shows the original digital signal obtained by sampling the output of the accelerometer. Although there are low pass filters before the A/D converters in the circuit, a lot of impulse noise can be observed obviously. Figure 2.12(b) shows the output signal of the median filter. It is apparent that the non-linear median filter can get rid of the noise efficiently. If without the median filter, although it is possible that no false falls are reported, the processor will be required to spend more time processing the data, wasting much power. As shown in figure 2.9, the calculated $|\vec{a}|$ or EE can easily exceed their thresholds with those noise, because noise value can be quite large some time, as shown in figure 2.12(a).

Figure 2.13 shows the result of the high pass filter after the median filter. This data shows the output of the channel corresponds to the Z-axis as shown in figure 2.1 during a free fall of a long rod. As presented in section 2.3, with the earth's gravitational effects, before the fall, Z-axis is perpendicular to the ground and there is an offset in the output corresponding to an acceleration of around 1g. After the fall, this channel is parallel with the ground and there is a very small offset in the output because the sensor is not strictly placed in the way shown in figure 2.1 and this channel is not strictly parallel to the ground. For people's usual activities, such as standing, walking, sitting, lying on the bed and so on, one and usually only one axis of x, y and z shown in figure 2.1is almost vertical to the ground. Then the output signal of this channel is much larger or smaller than the other two channels. And the orientation of a person can be easily found. Even if there is no axis vertical or parallel to the ground, the orientation of a person can be

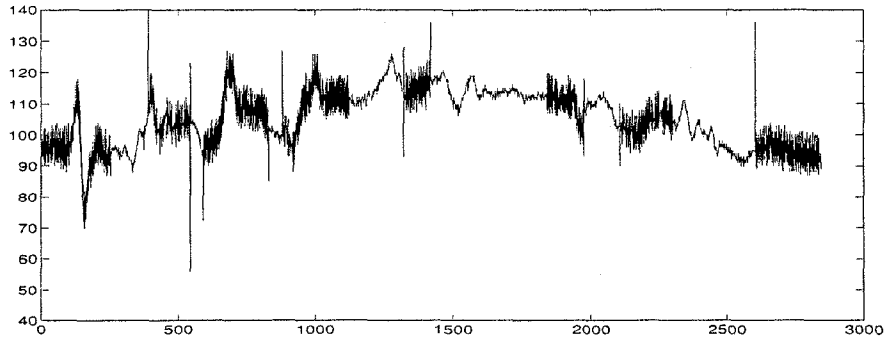

(a) Original sampled signal with noise

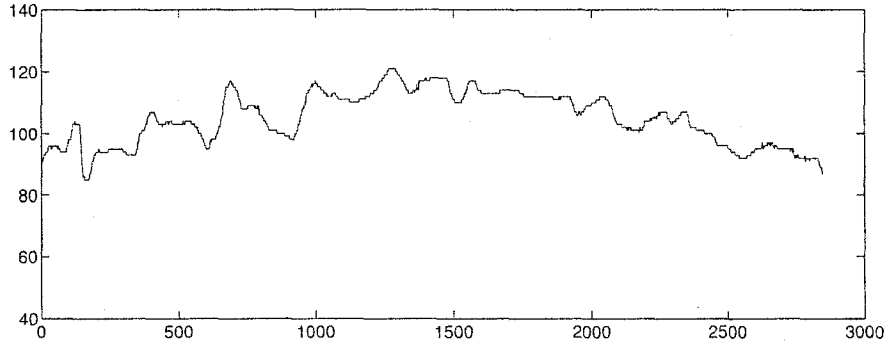

(b) Output signal of the median filter

Figure 2.12 Median filter result

found using vector calculation when the output is stable, which means the person is not moving, because the way that the sensor is worn is known.

Figure 2.13(b) shows the output signal of the high pass filter. It can be seen that after the high pass filter, there is no considerable offset for the time before the fall or after the fall. With this high pass filter, only the actual acceleration will be further analyzed.

Also, it is a free fall of a rod, the falling speed at the beginning is smaller than a real fall of a person. That is why the beginning part of the fall is filtered by the high pass filter here. From figure 2.13(a), it can be seen that this fall period starts at around the 800th point and ends at around the 1300th point. The total period contains 500 points

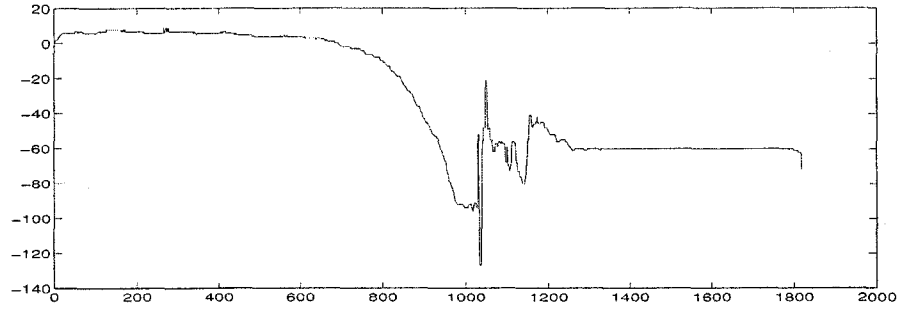

(a) Signal after the median filter

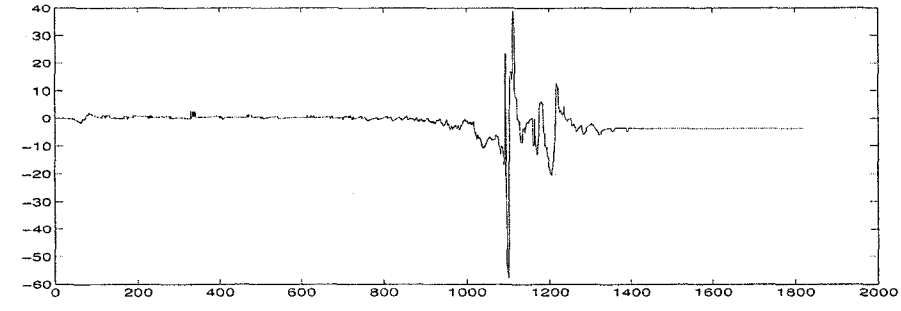

(b) Output signal of the high pass filter

Figure 2.13 High pass FIR filter result

corresponding to around 1 second, which proves that the time window of 1 second is practical.

Figure 2.14 shows the process result of a fall measured in the test. Channel 1 to channel 3 correspond to the three output channels of the accelerometer. From figure 2.14(a), it can be drawn that the channel 3 was vertical and the other channels were parallel to the ground when the person stood. And after the person fell down, channel 1 was vertical and the other two were parallel to the ground. Because there was an offset of the output of the channel that was vertical to the ground, as reported before.

The values of the calculated $|\vec{a}|$ and the energy expenditure are results from Matlab. When the data is processed by a microcontroller, although it can use some data types

such as double or float to process these data, it will take much memory. In order to reduce memory usage, all the digital signal can be scaled down by the same scale factor and the result is essentially the same. As a simple illustration, if there is a number x that satisfy

$$x_1 < x < x_2 \tag{2.17}$$

where x_1 and x_2 are constant, then the following formula also holds:

$$x_1 \times k < x \times k < x_2 \times k \tag{2.18}$$

where k is a positive scaling factor. As a result, an usual activity can be distinguished from falls by processing scaled signals in a microcontroller, if this activity can be distinguished from falls with data processing without scaling.

With only the test result of falls, it is not possible to see how well this system works, because the performance of a fall detection system is determined by how well it can distinguish falls from other daily activities. In the following, measurements and processing results of some typical daily activities are presented.

Figure 2.15 shows the measured data and processing result for a scenario where a person wearing the sensor bent over. The process is from standing to bending and then to standing again. From figure 2.15(b), it can be seen that the data of channel 3 are different from the data of the other channels. It is the output for the person's up-down direction, or the z-direction shown in figure 2.1. And according to previous analysis, the channel 2 is in the person's left-right direction or the x-direction in figure 2.1. The channel 1 is in the person's front-back direction or the y-direction in figure 2.1. By comparing figure 2.15(d) and figure 2.15(e) with figure 2.14(d) and figure 2.14(e) respectively, it shows that the calculated $|\vec{a}|$ is more efficient to distinguish such two kinds of activities, because the peak $|\vec{a}|$ of the fall (approx. 6000) is around 60 times larger than that of the bending (approx. 100), while the calculated energy expenditure of the fall (approx.

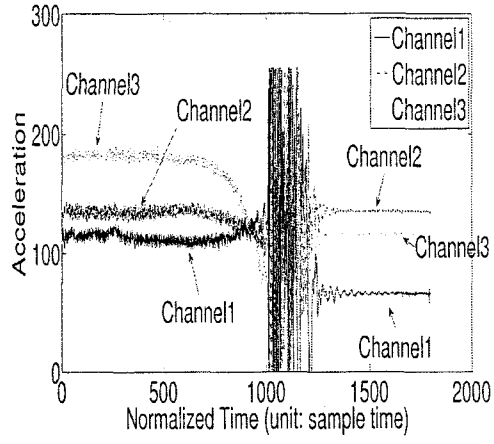

(a) Original sampled acceleration signal

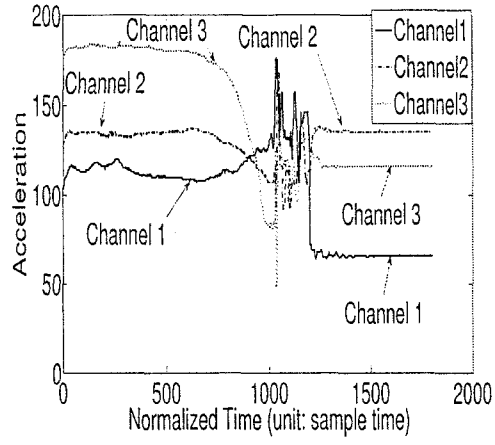

(b) Output of the median filter

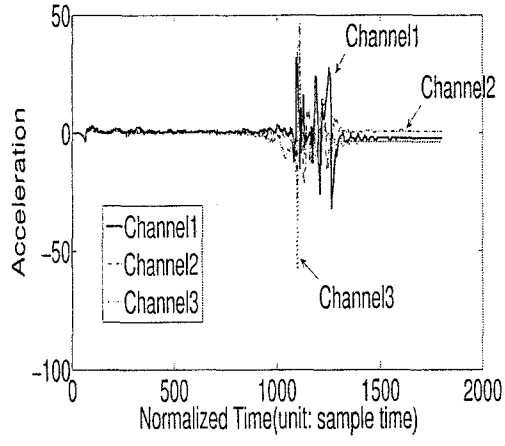

(c) Output of the high pass filter

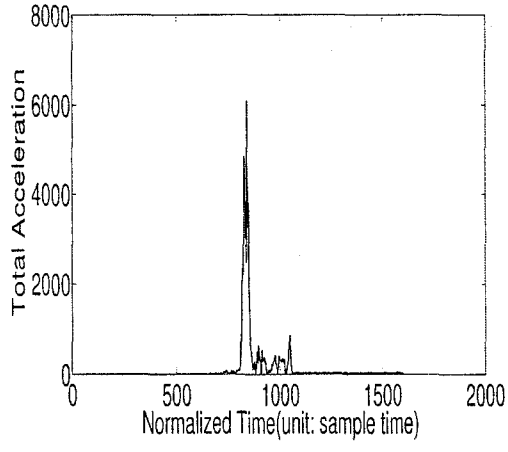

(d) Calculated $|\vec{a}|$

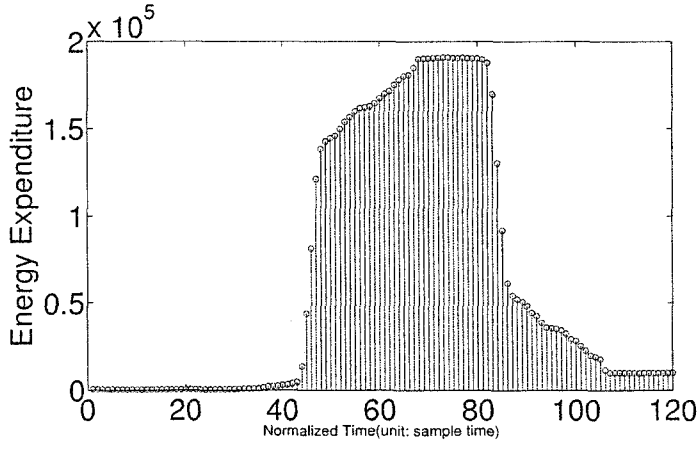

(e) Calculated energy expenditure

Figure 2.14 Data processing result of a fall test

2×10^5) is only about 10 times larger than that of the bending (approx. 2×10^4).

Figure 2.16 shows the data processing result for a scenario where a person wearing the sensor was walking. Because the orientation of the person is not changed and no vigorous exercise there, there is no obvious change in the recorded data for the three axis. Compared with values for the fall, both the peak $|\vec{a}|$ and the energy expenditure here is quite small, and this types of activity can be easily distinguished from falls.

Figure 2.17 shows the data processing result for a scenario where a person wearing the sensor sits down in a chair, and figure 2.18 is for the scenario where a person stands up from a chair. By comparing these two figures, it is obvious that both the peak $|\vec{a}|$ and the energy expenditure for sitting down are larger than that for standing up. This is consistent with the actual situation, because when people sit down, there is a higher velocity and it happens in a shorter time than that when people stand up. The peak $|\vec{a}|$ and the energy expenditure for sitting down are larger than that for bending over, but they are much smaller than that for falls. And this type of activity can also be easily distinguished from falls.

Figure 2.17 shows the data processing result for a scenario where a person wearing the sensor lay down. As the orientation of the person changed, the state in the end is different from that in the beginning, as can be seen in figure 2.19(b). The peak $|\vec{a}|$ and the energy expenditure for this activity are comparable with those for the sitting down test, but are much smaller than those for the fall test.

Figure 2.20 shows the data processing result for a scenario where a person wearing the sensor jumped once. It is easy to see that the channel 3 corresponds to the person's top-down direction, or the z-axis shown in figure 2.1 that is vertical to the ground. In figure 2.20(b), there are two pulses for this direction, which is different from other activities discussed above, where there is only one pulse or even no obvious pulse. The same can

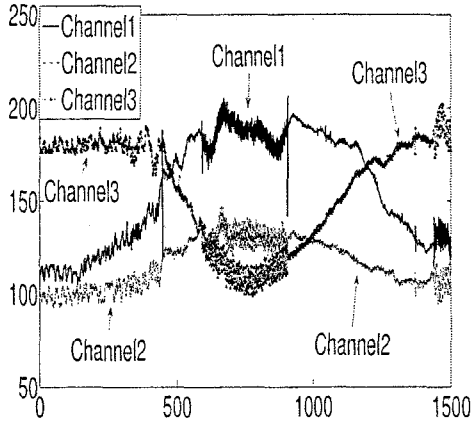

(a) Original sampled acceleration signal

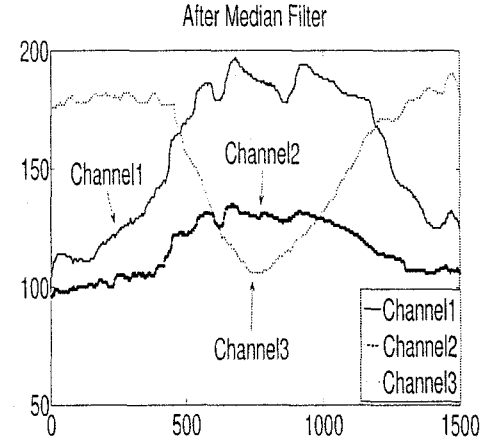

(b) Output of the median filter

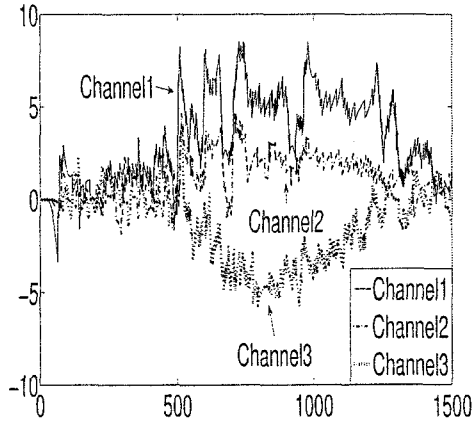

(c) Output of the high pass filter

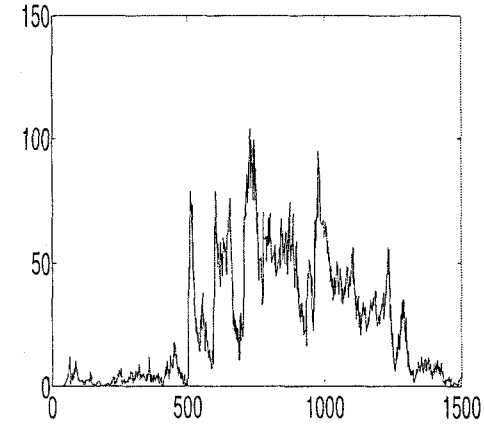

(d) Calculated $|\vec{a}|$

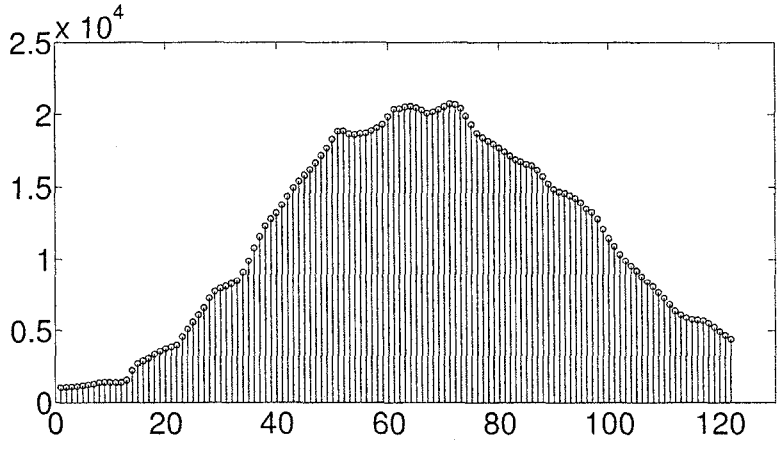

(e) Calculated energy expenditure

Figure 2.15 Data processing result of a bending test

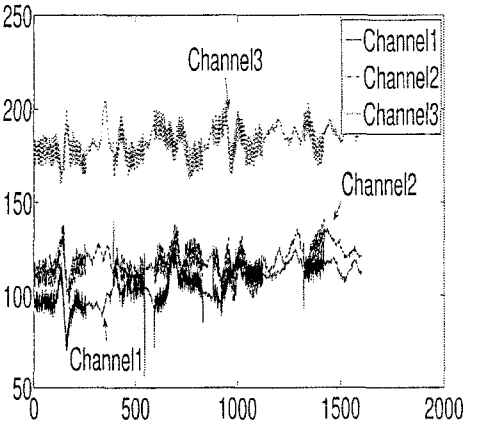

(a) Original sampled acceleration signal

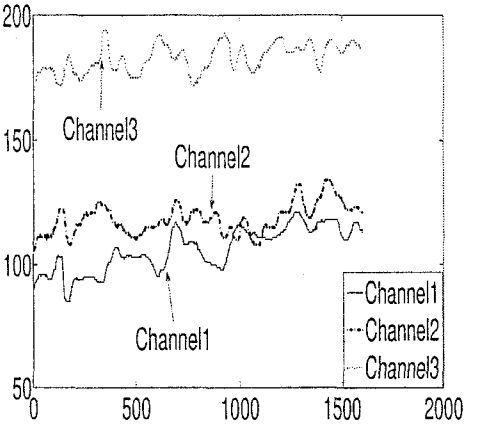

(b) Output of the median filter

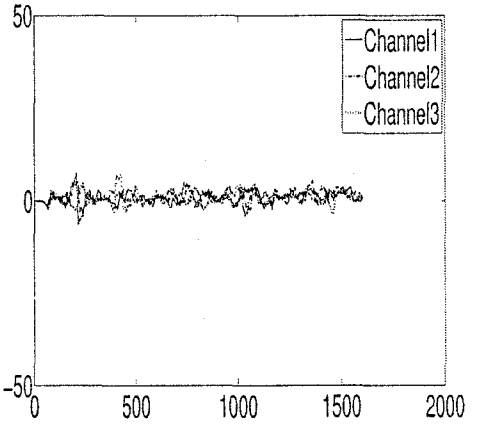

(c) Output of the high pass filter

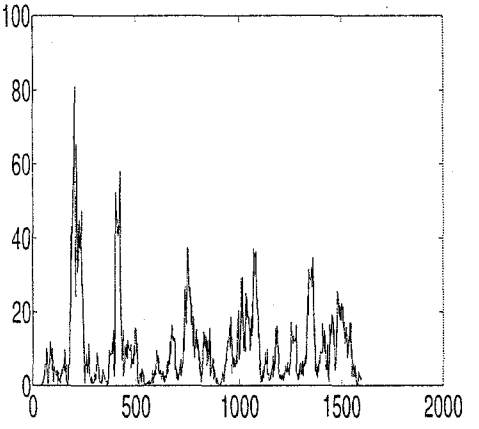

(d) Calculated $|\vec{a}|$

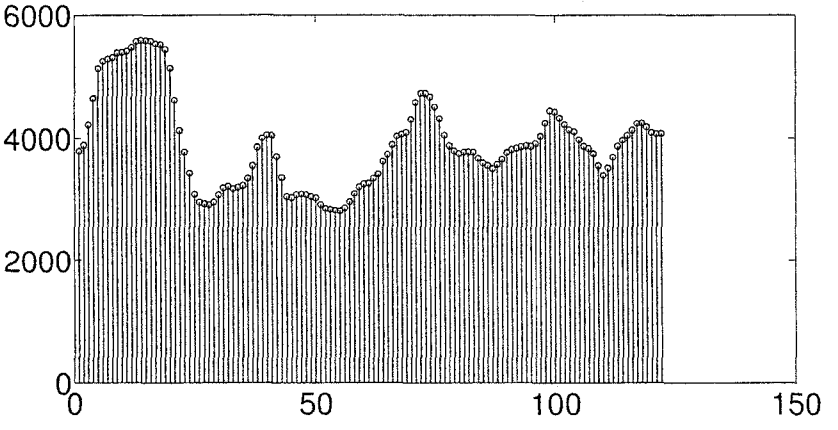

(e) Calculated energy expenditure

Figure 2.16 Data processing result of a walking test

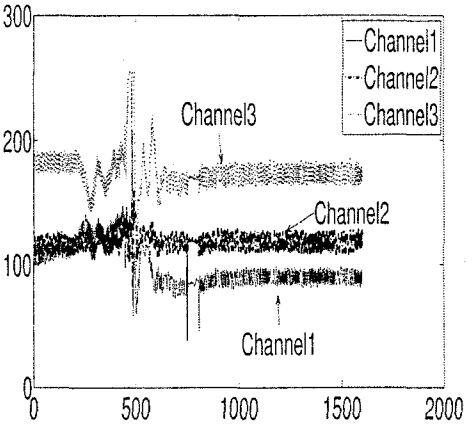

(a) Original sampled acceleration signal

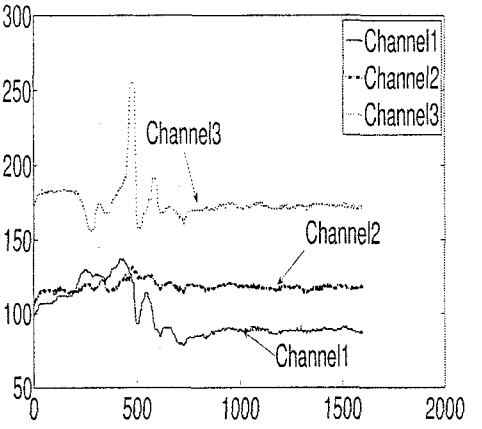

(b) Output of the median filter

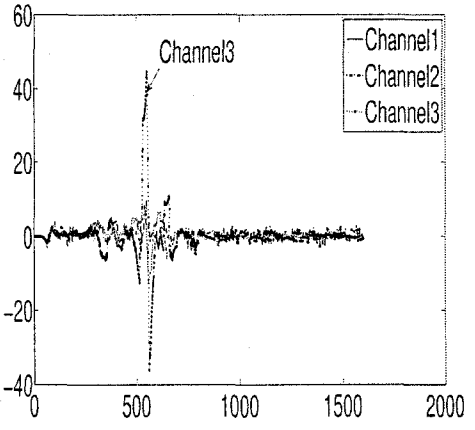

(c) Output of the high pass filter

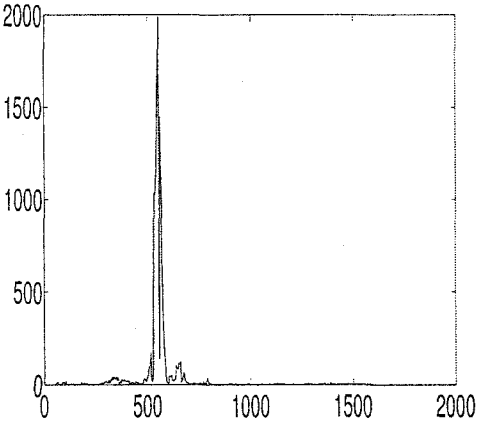

(d) Calculated $|\vec{a}|$

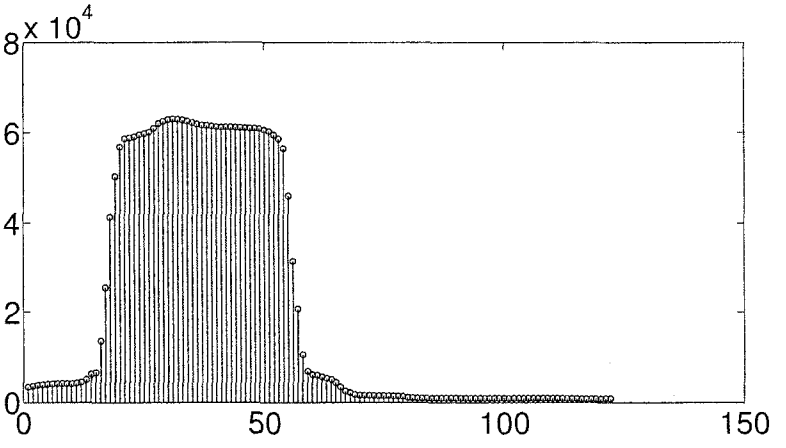

(e) Calculated energy expenditure

Figure 2.17 Data processing result of a sitting down test

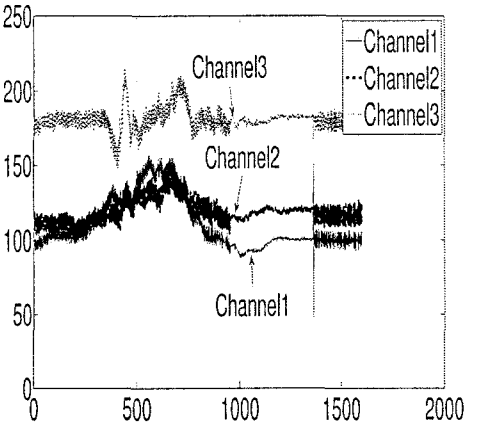

(a) Original sampled acceleration signal

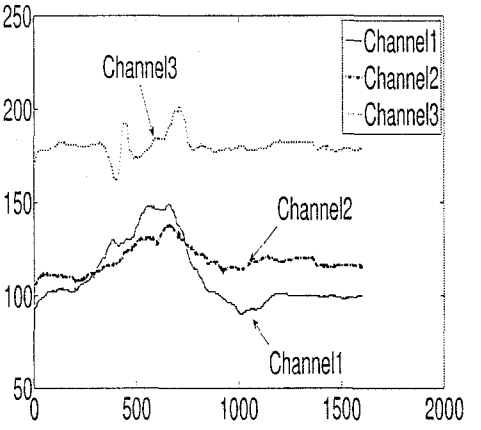

(b) Output of the median filter

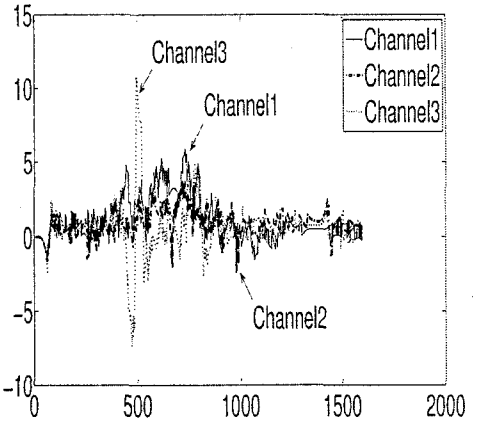

(c) Output of the high pass filter

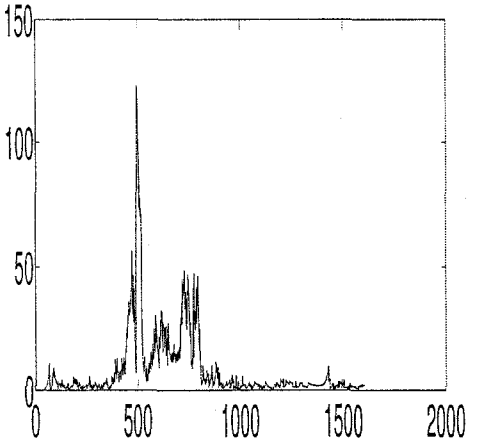

(d) Calculated $|\vec{a}|$

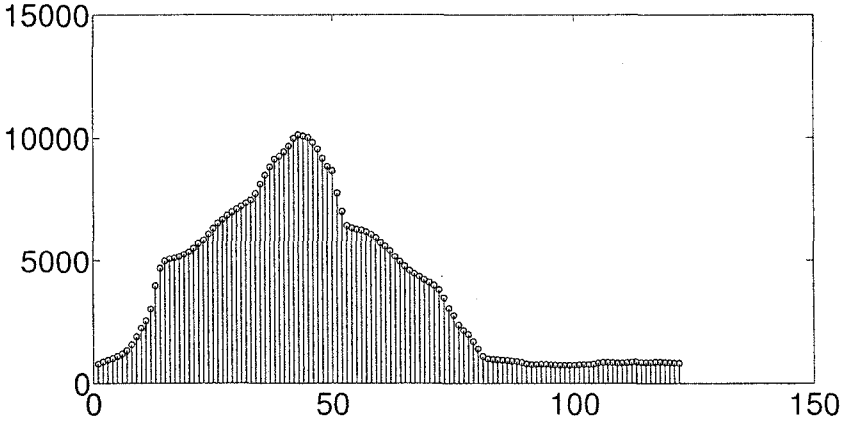

(e) Calculated energy expenditure

Figure 2.18 Data processing result of a standing up test

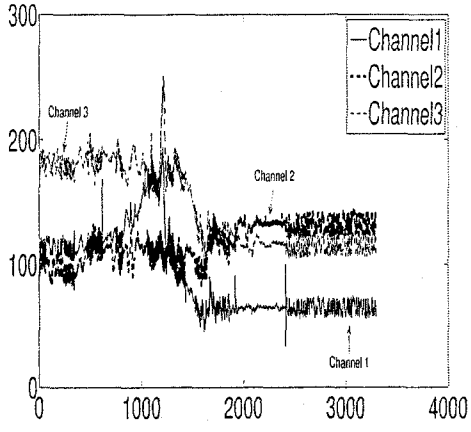

(a) Original sampled acceleration signal

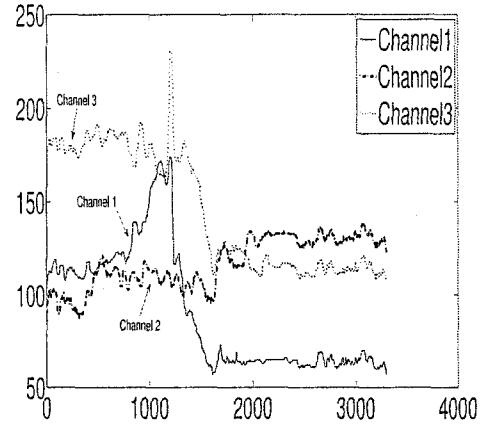

(b) Output of the median filter

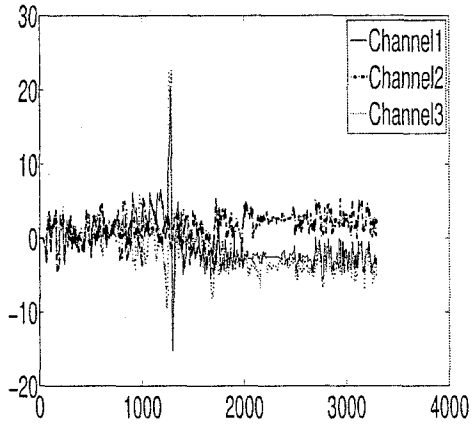

(c) Output of the high pass filter

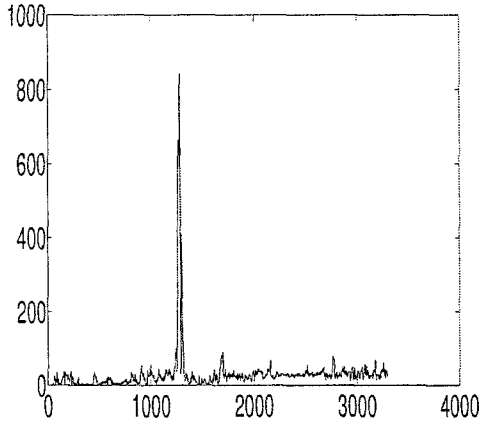

(d) Calculated $|\vec{a}|$

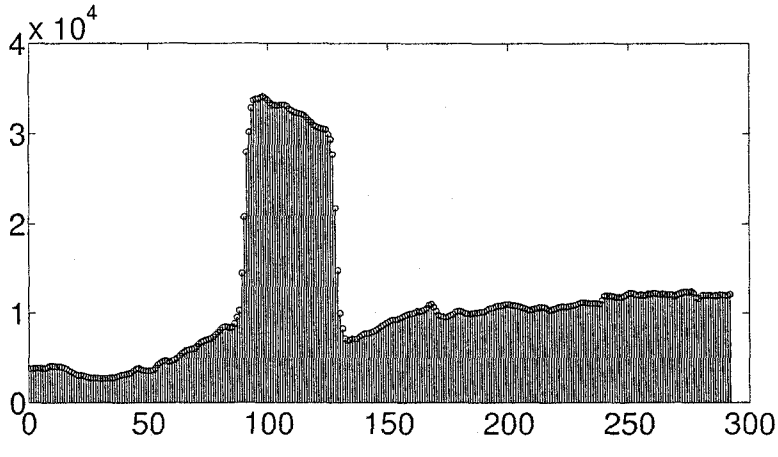

(e) Calculated energy expenditure

Figure 2.19 Data processing result of a lying down test

be found in the $|\vec{a}|$. Because at the beginning, the person propelled himself to jump, introducing a high upward acceleration, and this is the first acceleration for the first pulse. After that, the total gravitation from the earth provided the downward acceleration. According to the mechanism of the accelerometer, it can be considered that there is no force outside applied on it. As a result, after the first pulse, the output of the three channels are almost the same, since there is no offset for all channels. The other pulse comes when the person reached the ground when there is large upward acceleration and the offset from gravitation also comes back. Apart from this, it is more interesting to see that the peak $|\vec{a}|$ for jumping is much less than that for the fall, although the energy expenditure is a little larger than that for the fall. Probably this is because jumping is a kind of conscious activity and some of the shock is absorbed by some special parts of the body to reduce hurt on the body, while fall is unconscious activity and it happens too fast for the body to get ready for it. This characteristic is quite useful to distinguish conscious vigorous activities from falls.

From above results, it can be seen that the algorithm used in this system can efficiently distinguish falls from other daily activities. The calculated energy expenditure is a good factor to represent the intensity of an activity. With this factor, usual daily activities can be easily distinguished from falls. For vigorous activities, since they also have high energy expenditure, it is difficult to distinguish them from falls with this factor. Another factor, the total absolute value of acceleration $|\vec{a}|$, in some way can show the degree to which the person is hurt. This factor can also help to distinguish other activities from falls efficiently, especially distinguish intended vigorous activities from falls, which both have high energy expenditure. Besides, usually people that need help from others are those who fell down and were hurt badly and they can not move. As a result, after falling down, no big fluctuation or changes will be found at the output of the accelerometer. This can also help for fall detection as a compensation.

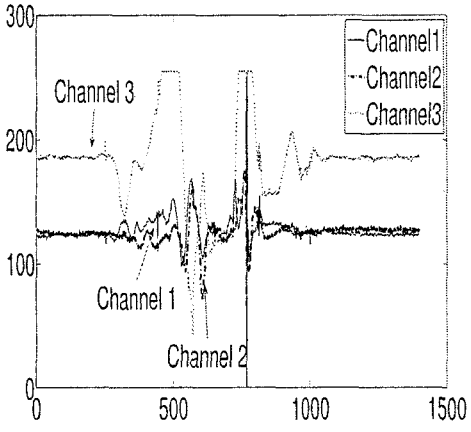

(a) Original sampled acceleration signal

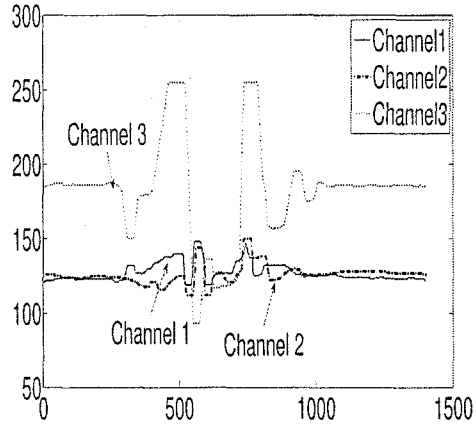

(b) Output of the median filter

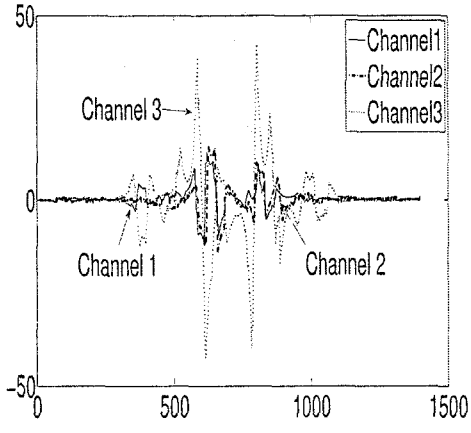

(c) Output of the high pass filter

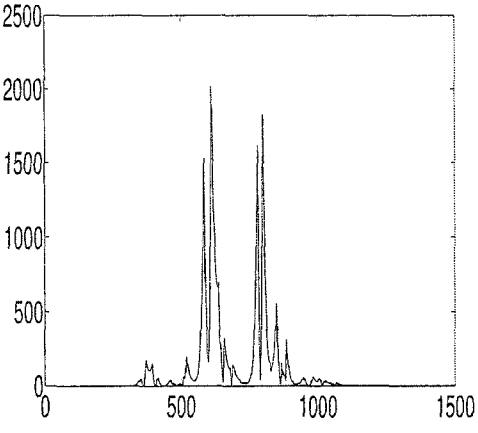

(d) Calculated $|\vec{a}|$

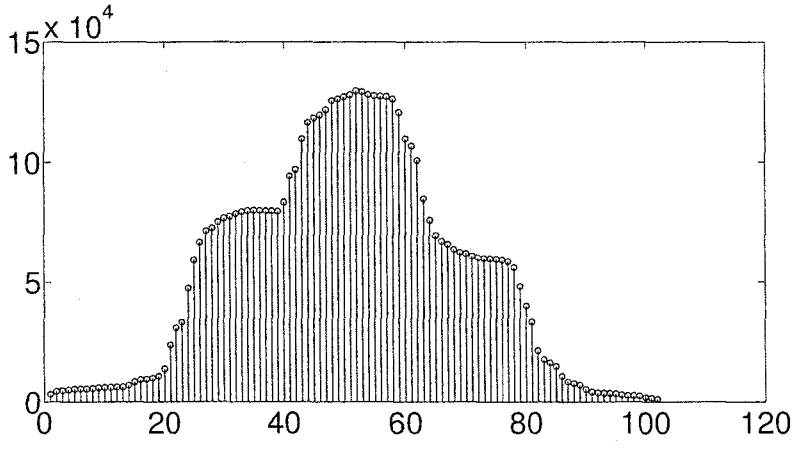

(e) Calculated energy expenditure

Figure 2.20 Data processing result of a jumping test

CHAPTER 3

WIRELESS SYSTEM ARCHITECTURE AND IMPLEMENTATION

In this chapter, the architecture of the wireless positioning system, including network coverage, telecommunication protocols as well as other issues, will be introduced. And the implementation of the whole system includes the wireless telecommunication circuit and the data processing circuit, will also be presented here.

3.1 System Architecture

The idea of the system is to cover the whole service area with a wireless network. Many base stations will be deployed inside the area for communication with tags[1] and for monitoring. When a person under monitor falls down and is detected, the tag worn by that person will record the RSS from all accessible base stations. Afterwards, this information is transmitted to a base station with the strongest RSS, the base station will transmit this information to a server by internet. Figure 3.1 shows the whole system architecture.

3.1.1 Network Architecture

The wireless network must be able to cover all the area where people under monitoring could be detected. And for every tag worn by a person, there must be at least one base station that the tag can communicate with. For a good positioning precision, the more base stations whose signal can be received by the tag, the better the system would be.

[1]Tag referred to the whole circuit worn by a person under monitor

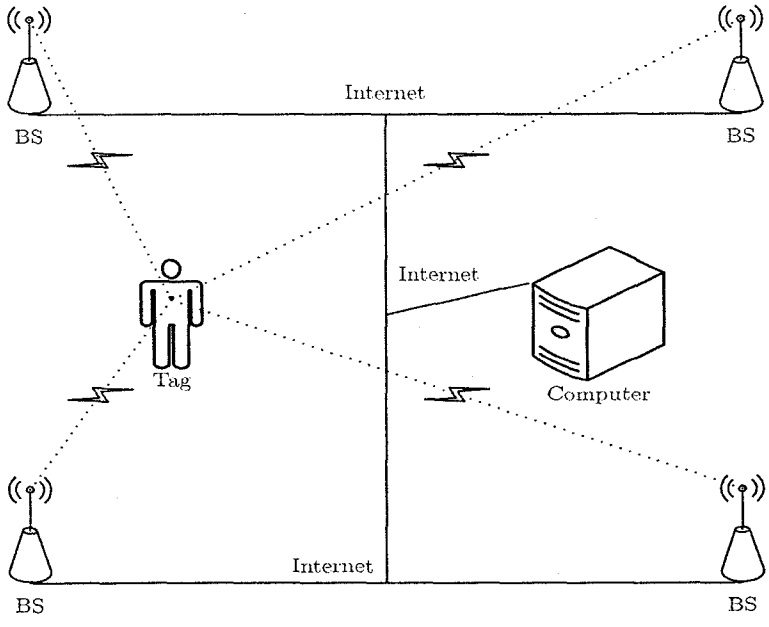

Figure 3.1 Whole system architecture

At the first glance, it is apparent that the more base stations are employed, the better performance the system can provide. Generally this is true, but the cost of the whole system will increase and interference among base stations has to be considered carefully.

The code division multiplexing(CDM) could be used for this network to get a good performance. However, this technique has some requirement on the transceiver, that is, the transceiver has to be specially designed. Since the RSS is used for positioning, very simple transceiver at a very low price can also be used to reduce the cost of the system, where as in this work, a simple frequency division multiplex(FDM) is employed. All the available frequency band is divided into k different sub frequency band that can be used by different base stations simultaneously. Then k is the number of base stations inside a cluster where k base stations use the k different sub frequency band respectively. In cellular systems, this technique is used to increase the utility efficiency of the frequency spectrum. However, this technology here is to reduce the interference among users.

Figure 3.2 shows three schemes for FDM with different cluster size.

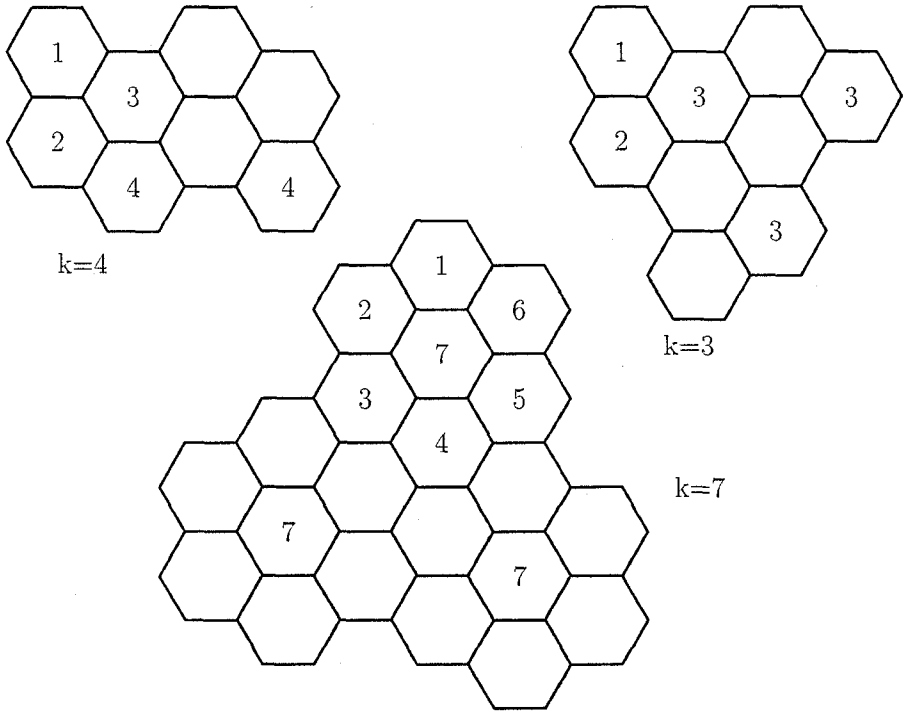

Figure 3.2 Frequency division multiplexing

The cluster size, or the number of sub frequency band can not be selected randomly. It is decided by the following equation:

$$k = i^2 + i \times j + j^2 \tag{3.1}$$

where i and j are both integers and only one of them could be zero. Then the minimum k is 3 when $i = j = 1$. In our project, the larger k, the longer time it takes for a tag to get access to a base station, because the tag has to search the frequency band to find available base stations. However, a tag can not be covered by two base stations with the same working frequency band. Because if so, there will be a strong interference and the performance will be degraded. So the number of sub frequency band also determines the maximum number of base stations that a tag can reach for positioning. Although for digital cellular systems, larger k might impair the efficiency of frequency spectrum, it is not the case for this project. Because the frequency band for a base station is further

divided for many channels, larger k means smaller sub frequency band for each base station and less channels can be used inside a base station. But for this project, the frequency division multiple access(FDMA) is not used, and only one uplink channel and one downlink channel were used for each base station. So large k will not impair the system performance.

3.1.2 Medium Access Control

The medium access control here refers to the schemes for users in an area covered by a same base station to communicate with the base station. In this case, the transmission medium is shared by all the users inside the cell of the base station. And the transmission medium is broadcast in nature. For every area covered by a base station, there are two channels with two different frequency band. One channel is the downlink channel and is used by the base station to broadcast information and support positioning mechanism for all tags in that area. This channel can be divided into several logic channels. For example, all the control frames and payload that the base station needs to send to a tag are all included in frames using this channel. The other channel is the uplink channel and is shared by all tags covered by that base station that need to communicate with the base station.

Carrier sensing multiple access with collision avoidance(CSMA/CA) is used for medium access control. This scheme has been widely used for wireless local area networks(WLAN) and it works as follows:

When a tag needs to transmit a frame, it will monitor the wireless medium first by receiving information from the base station and then sense the uplink frequency band. If the wireless medium is busy, it will defer its transmission and it will calculate a random backoff time to schedule a reattempt. If the medium is free for a certain period T_s, the

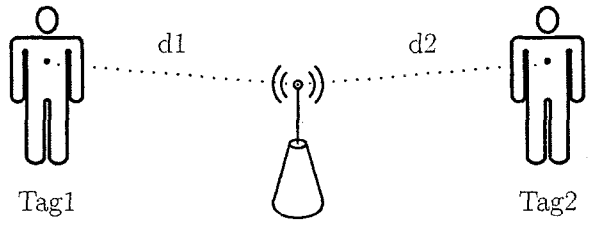

Figure 3.3 Hidden tags

tag can transmit its frame, using cyclic redundancy check(CRC) coding. If the base station successfully received the frame, it will check the CRC and send an acknowledge frame back. If the tag doesn't receive an acknowledge frame, the frame will be retransmitted. For those tags that have scheduled a reattempt, they will start a timer and keep monitoring the medium. All tags have to keep quiet during the period T_s after a frame transmission has been completed. After that period, if the timer of a tag with a reattempt expires, it is allowed to transmit its frame.

Because tags may not be able to hear each other when they try to transmit a frame, the following scheme is used to reduce the probability of collision:

A tag needs to transmit a long frame will send a short control frame first, which includes the source address, destine address and the length of time for the following transmission. If the base station receives this frame successfully, it will send back another short control frame, including the same information. The base station will keep broadcasting this information until it is completed. As a result, all other tags receiving this information will use this with physical carrier sensing when they need to transmit a frame. This is due to the fact that tags may not be able to hear each other in the wireless environment. Figure 3.3 shows an example.

Because the distances between the two tags are larger than the distances between them and the base station, it is possible that both the tags can communicate with the base station but they can not receive signals from each other. Let us suppose that when tag1

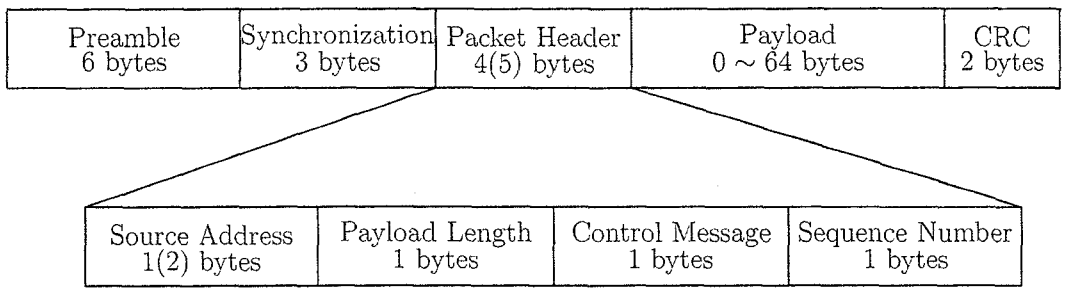

Figure 3.4 The packet format

senses the wireless medium before its transmission, and the tag2 is transmitting its frame. Then tag1 will consider the wireless medium free and transmit its frame. Thus collision will happen. With the scheme described previously, tag1 will receive information from the base station and get to know that the medium is busy and the probability of collision will be reduced.

Figure 3.4 shows the packet format used in this project. This format is used by both the tag and the base station. The only difference between the frame format for tags and that for base stations is the length of the packet header. The address for base stations is 1 byte long while the address for tags is 2 bytes long, because there are much more tags compared with base stations. Then inside a building, there can be as many as $2^8 = 256$ base stations and $2^{16} = 65536$ tags. Then payload length can range from 0 to 64 bytes. This limitation on the length of addresses is to reduce the time it takes when a tag attempts to communicate with a base station, so as to reduce the power consumption of the tag. For example, when the frame is a control message, the payload length can be 0 while a tag transmit RSS information for positioning, this length can be 32 bytes.

3.1.3 Power Consumption Consideration

The tag that people wear is supposed to be of a very small size, then only some small batteries can be used to power it. But those small batteries usually do not have much

energy inside. It will be a big problem if the batteries can not work for a long time. In order to avoid changing the batteries too often, some scheme should be employed to reduce the power consumption of the tag.

For this project, the wireless circuit of a tag is only used for positioning, so it can only work when the fall detection system detects a fall. And only the fall detection sensor works all the time. Then the battery can work for a very long time. But in this case, only the tag can offer to communicate with a base station and all communications have to be initialized by a tag. It is not possible for a base station to initialize a communication with a tag.

Sometimes, the base station needs to have the capability to initialize communication with a tag. There are two methods to implement this procedure in this project. The tag can inquire with the base station in some certain frequency, for example, the tag can communicate with the base station every five minutes. Considering the power consumption issue, another better way is to broadcast all the identification numbers of tags that base stations need to communicate with. This information can be included in the payload section as shown in figure 3.4. Because the length of the payload can be 64 bytes long, the maximum number of tags a base station can page for is 64bytes/2bytes per address=32. Since a tag can know if base stations are looking for it by only receiving message from a base station, the time it takes for this process is short and the power consumption is reduced.

It is also possible to provide a switch that the person can use to turn off the whole circuit before he or she goes to sleep, but people might forget to turn the system on when they get up. However, since the fall detection circuit has to keep working all the time, some special designed circuit can be used to reduce its power consumption. For example, an analog high pass filter can be used to filter the output of the accelerometer. The output signal is used to provide a wake up signal. In some period, like at night, the

microcontroller of the fall detection circuit can keep in sleep mode until a wake up signal is received. In this case, only the accelerometer keeps working all the time.

3.2 System Implementation

According to the system architecture, the circuit is designed, implemented and tested, including antennas, wireless transceivers as well as power conversion circuits for power supply.

3.2.1 The Antenna

In indoor wireless environment, usually there is no light of sight(LOS) between the base station and the tag that communicate with each other. Also, the orientation of a person wearing a tag can vary with time, for instance, one can lie in the bed, or bend over or stand, the direction of the antenna of that tag will vary with time. Then linear antennas can not be used for both base stations and tags, because if the antenna of a base station has a 90 degree difference with that of a tag, the tag might not be able to receive the signal from the base station because of polarization, even if they are very close to each other. And the circular polarized antennas may not be suitable for both base stations and tags either. Because signals from a left/right circular polarized antenna can only be received by an antenna with the same polarization. And when a left/right circular polarized signal is reflected, it can change into right/left circular polarization respectively. In order to solve these problems, four types of antennas, including both circular polarized antennas and linear polarized antennas, have been simulated and three types of them have been fabricated and investigated in this project.

A microstrip antenna is a resonator type antenna. Usually the microstrip antenna is of

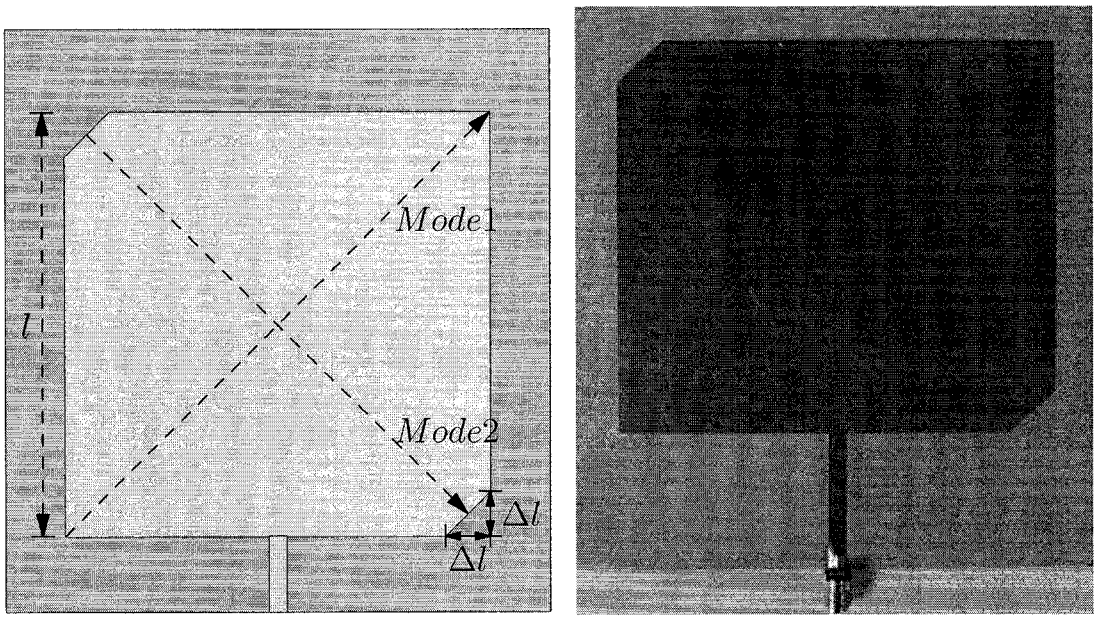

(a) Degenerate mode patch antenna (b) Fabricated antenna

Figure 3.5 Singly fed circularly polarized microstrip antenna($l = 9.378cm, \Delta l = 0.99cm$)

low weight, and of thin profile. It is easy to be fabricated and integrated with integrated circuits at low cost. So the microstrip antenna is chosen for this project. In the following, a singly fed circularly polarized microstrip patch antenna, a small circularly polarized microstrip patch antenna with bent slots, a printed inverted-F antenna and also a simple monopole antenna are presented.

General rectangular microstrip patch antenna has a length of around half wavelength of its center working frequency. The height of the substrate and the dielectric constant have great influence on the efficiency and bandwidth of the antenna. It can be considered as a cavity with electric walls on the top and bottom and magnetic walls along the periphery.

Usually it can be assumed that only the $\mathrm{TM}_{10}(z-axis)$ mode is excited for a rectangular microstrip antenna. It can generate circularly polarized radiation by exciting two orthogonal radiation modes with a 90 degree phase difference. And a 90 degree in phase can be generated by a delay line or a hybrid. But a more compact structure can be adopted

to generate circularly polarized radiation. Figure 3.5 shows a singly fed circularly polarized microstrip patch antenna. This structure doesn't require a hybrid or a phase-delay line, so it can be small in size.

Here, the circularly polarization is obtained by introducing a pair of truncated corners(JAMES and HALL, 1989). The degree of separation of the two resonate frequencies for the two modes is determined by the size of the truncated pairs. As shown in figure 3.5(a), two modes with equal amplitude and a 90 degree phase difference can be supported in the diagonal planes with appropriate truncated corners that satisfy the equation:

$$|\frac{\Delta S}{S}| \times Q_o = \frac{1}{2} \tag{3.2}$$

where ΔS is the size of the truncated area, S is the size of the square patch and Q_o is the unloaded Q factor of the two orthogonal modes [2]. And the two resonant frequencies of the orthogonal modes are:

$$f_{o1} = f_o \tag{3.3}$$

$$f_{o2} = f_o \times (1 - 2 \times \frac{\Delta S}{S}) \tag{3.4}$$

where f_o is the resonant frequencies of the square path without perturbation, f_{o1} and f_{o2} are the resonate frequency of the two modes. Since the circularly polarization is generated by the combination of the two orthogonal modes, low Q factor can give a good axial ratio bandwidth. Besides, thick substrate can also slightly increase this bandwidth.

The substrate of the antenna shown in figure 3.5 is RO3203($\varepsilon_r = 3.02$) with a thickness of 60mil from Rogers Company. Figure 3.6 shows the simulated axial ratio. The axial ratio is almost 0 dB around the center frequency 909MHz. Figure 3.7 shows the simulated radiation pattern.

[2]The unloaded Q factors of the two orthogonal modes are equal to each other: $Q_{o1} = Q_{o2} = Q_o$

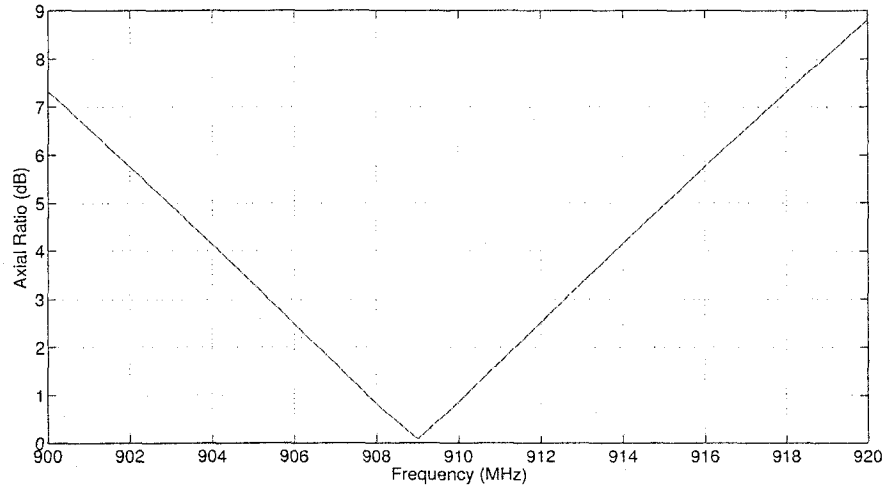

Figure 3.6 Simulation result-Axial Ratio of the patch antenna

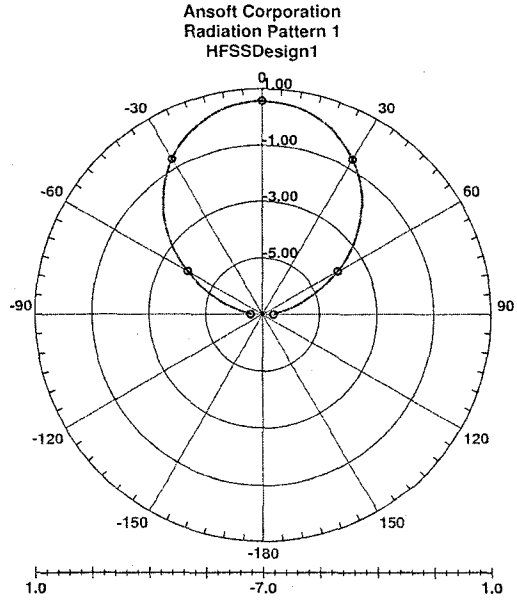

Figure 3.7 Simulation result-Radiation Pattern of the patch antenna

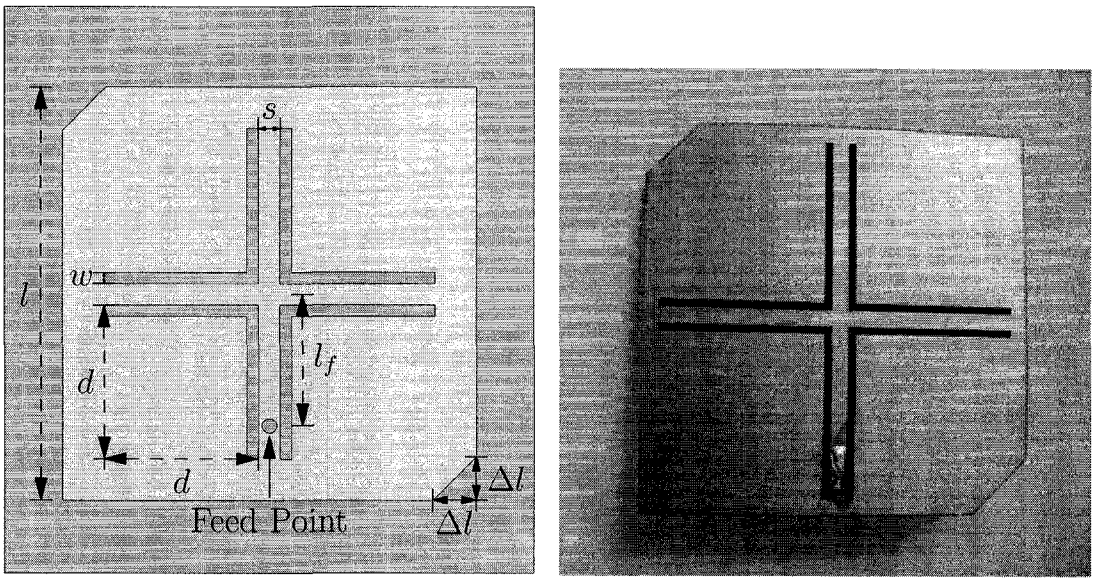

(a) Compact patch antenna (b) Fabricated antenna

Figure 3.8 Compact circularly polarized microstrip antenna with bent slots

Since the substrate RO3203 has a low dielectric loss tangent (0.0016) and a large thickness, this antenna has a relatively high efficiency (around 92%). Because the length of this square patch antenna is inversely proportional to the resonant frequency, it is very large. It can not be used for the tag circuit that people can wear and it can only be used for base stations. Although compact microstrip antenna can be achieved with substrates having a large dielectric constant ε_r, it is not easy for system integration because the substrate for the antenna might be different from that for the circuit. Besides, the bandwidth will also become small with a substrate having a high dielectric constant.

In order to make the tag circuit smaller, a microstrip antenna with small size has to be designed. Compact microstrip resonate antenna can be designed by some shorting posts(Hirasawa and Haneishi, 1991). But this type of antennas suffers from a degradation in their radiation pattern and a very poor gain. Another way to reduce the size of a microstrip antenna is to increase the path length of its surface current with some slots in the patch. Here, a compact circularly polarized antenna with truncated corners has

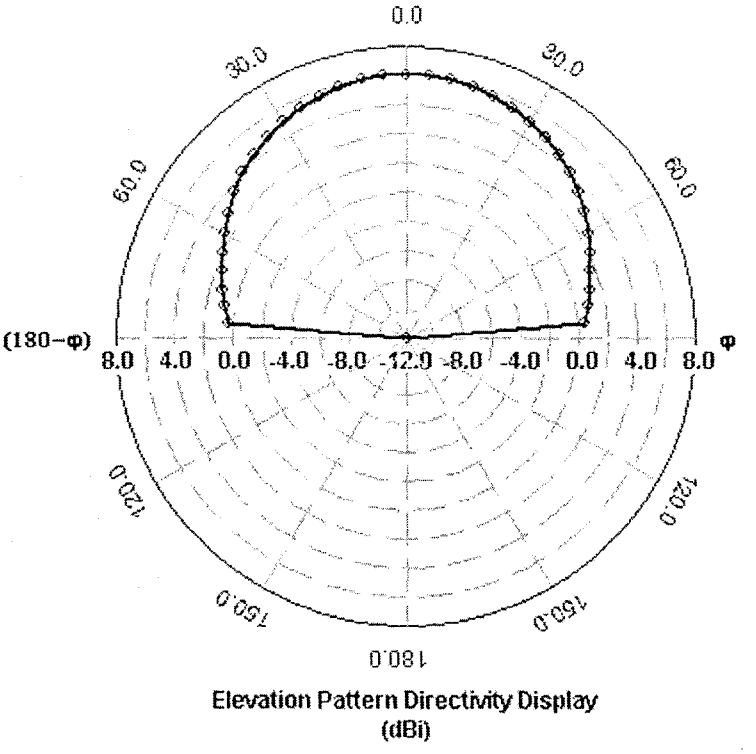

Figure 3.9 Simulation result-Radiation Pattern of the microstrip antenna with bent slots

been designed by embedding a group of four bending slots(Chen et al., 1998). It can have a size reduction of more than 50%. The antenna uses FR4 as its substrate, which is also the substrate for the whole circuit. Then the whole system can be easily integrated together.

Figure 3.8 shows the compact antenna configuration: $l = 49.08mm, \Delta l = 6.64mm, l_f = 19.2mm, w = 1mm, s = 2mm, d = 21.43mm$. Based on the reflection parameter, this antenna has a bandwidth of more than 20MHz. The radiation pattern and the axial ratio are shown in figure 3.9 and figure 3.10, respectively.

This antenna has a very small size. Its side length is reduced to almost half of the regular one and its area is reduced to one quarter of the regular size. Because the substrate FR4 has a large dielectric loss($tan\delta = 0.02$) and a very small size compared with traditional

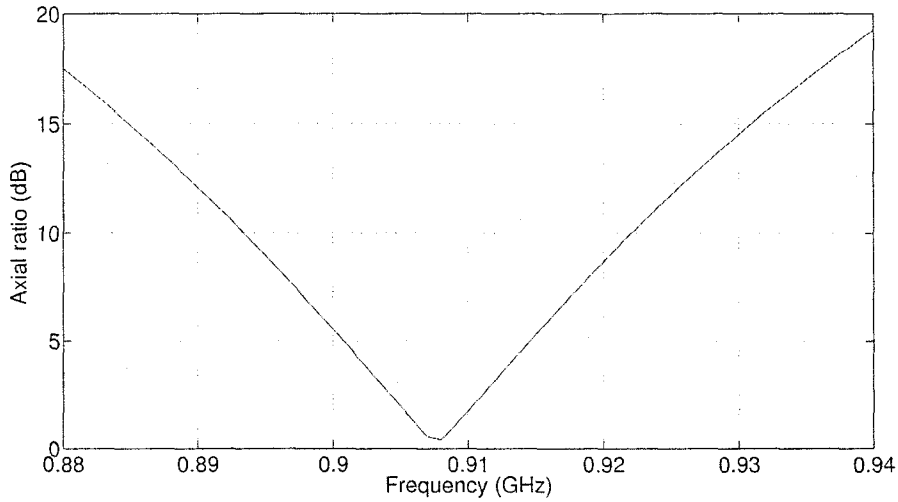

Figure 3.10 Simulation result-Axial Ratio of the microstrip antenna with bent slots

microstrip antenna, the antenna gain is very low and it has a poor antenna efficiency.

In order to investigate the effects on received signal strength of different types of antennas, a kind of monopole antenna, a planar inverted-F antenna(PIFA), has been designed and fabricated. Figure 3.11(a) shows the configuration of this antenna($l = 54.8mm$, $w = 1mm$, $l_f = 3.8mm$, $w_1 = 2mm$, $l_2 = 2.65mm$, $l_1 = 0.9mm$, $l_3 = 0.8mm$). It is fed by a 50 Ω transmission line, the wide line at the bottom in figure 3.11(a). The tapered line is used to match the 50 Ω line to the antenna. The resonant frequency of this antenna can be easily tuned by putting solder on its end(figure 3.11(b)) to reduce its resonant frequency or cutting this microstrip line to increase its resonant frequency.

Figure 3.12 shows the simulated and measured S_{11} parameters of the antenna as shown in figure 3.11(a). And the radiation pattern(directivity) is shown in figure 3.13.

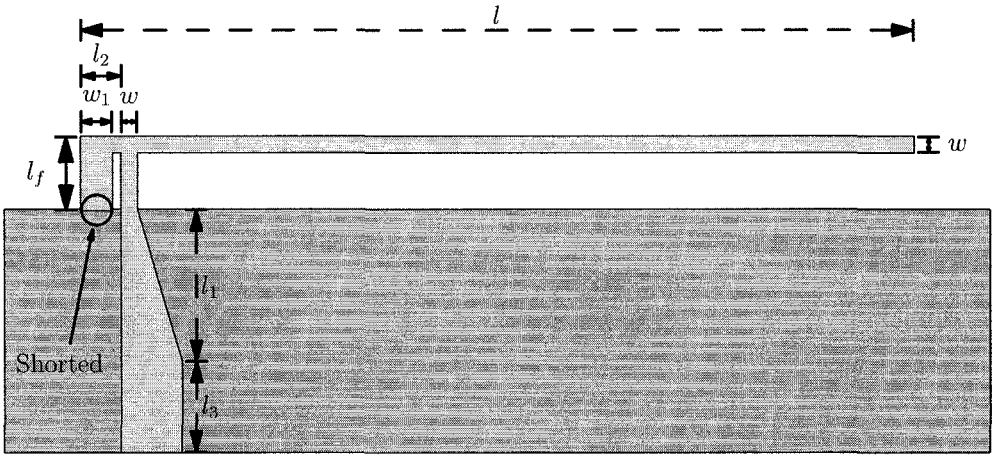

(a) Planar inverted-F antenna

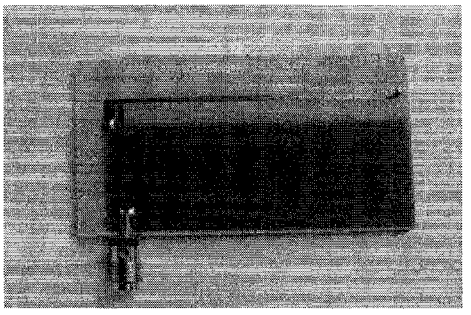

(b) Fabricated antenna-Top

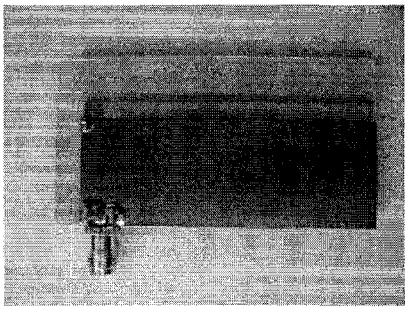

(c) Fabricated antenna-Bottom

Figure 3.11 Compact linearly polarized microstrip antenna(PIFA)

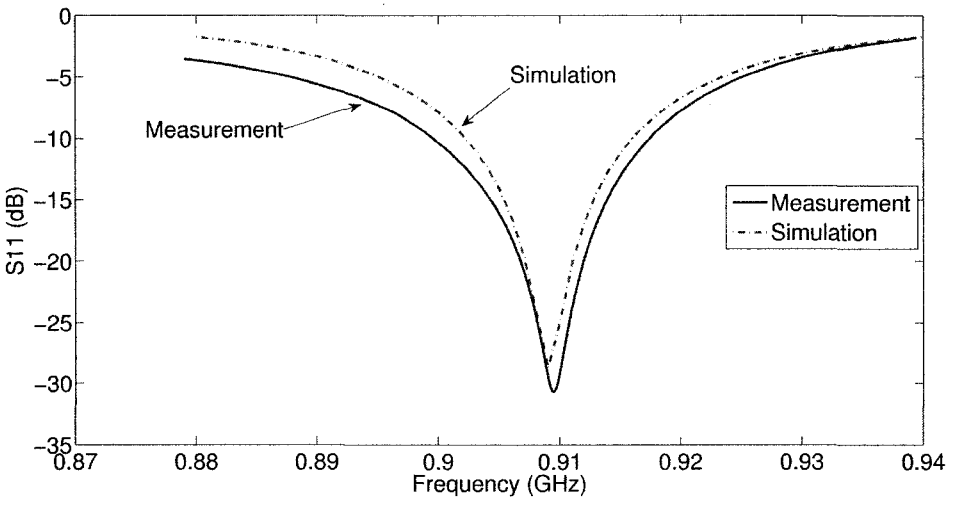

Figure 3.12 S_{11} parameter for the PIFA

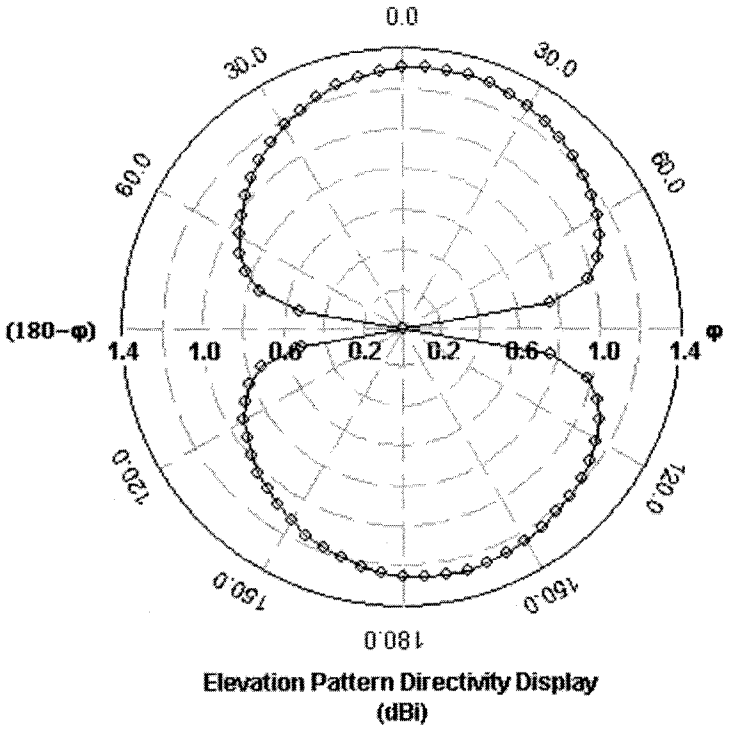

Figure 3.13 Radiation pattern of the PIFA

3.2.2 Wireless Unit

The wireless platform used in this project for positioning as well as for wireless communication is implemented with the RF chip ADF7021 from Analog Device and the PIC16LF877 from Microchip, which is used for the fall detection system.

The ADF7021 is a low power, narrow-band transceiver. Its supply voltage ranges from 2.3V to 3.6V. As the same for other circuits, 3.3V is used as power supply voltage. It can work in two frequency bands: 80MHz to 650MHz and 862MHz to 950MHz. It supports gaussian and raised cosine filtering to reduce the bandwidth of the transmitted signal so as to reduce interference outside its bandwidth. 2FSK, 3FSK, 4FSK and MSK modulation can be used. It supports a data rate ranging from 0.05kbps to 32.8kbps. It

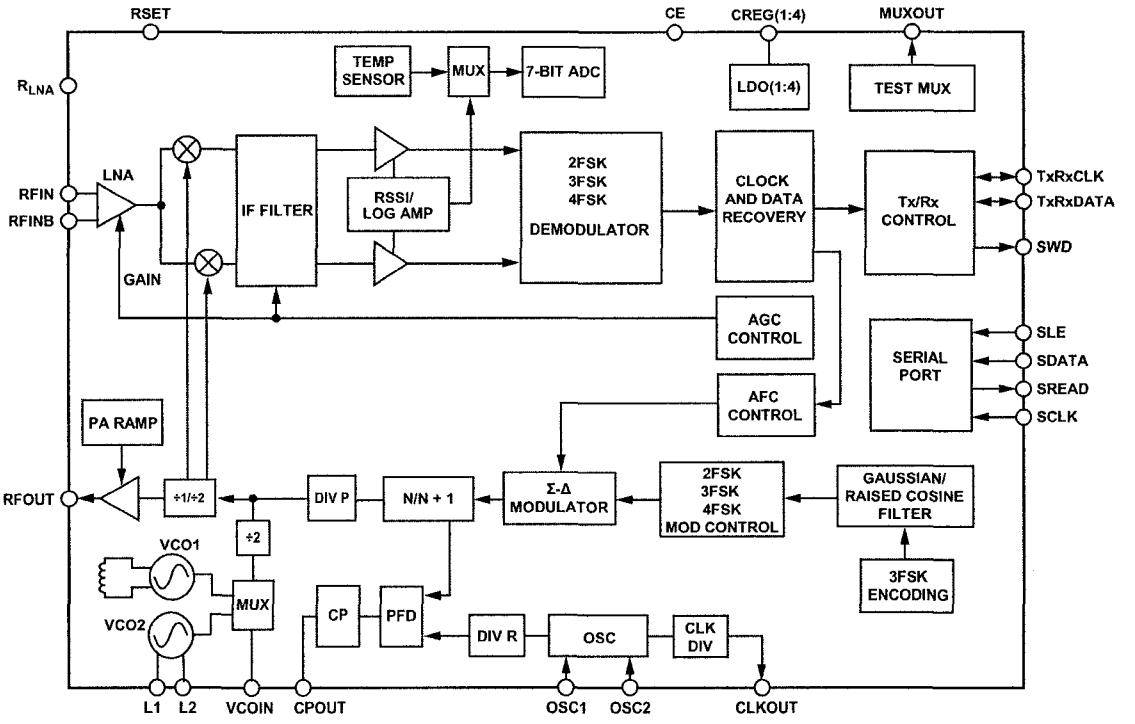

Figure 3.14 Transceiver architecture (Analog Device, 2007).

has a maximum output power(maximum unmodulated power) of 13dBm[3].

As seen in its block diagram shown in figure 3.14, the transmitter uses a direct frequency modulation transmitter architecture. It employs a frequency-agile fractional-N Phase Locked Loop(PLL) to generate digital frequency modulation. The PLL tends to keep the VCO frequency stable. It should be noted that if the base band modulating signal falls inside the PLL bandwidth, which is about the reciprocity of the synthesizer lock time, the PLL will track out the modulation. The low noise PLL is reported to have an output resolution of less than 1 ppm(parts per million). The transmitter doesn't have a internal filter for the RF signal. An external bandpass filter can be used to reduce interference outside its frequency band, especially to suppress the harmonic emissions of the power amplifier. In our project, a simple T-stage low-pass filter(shown in figure

[3]For comparison, the maximum transmit output power in IEEE802.11 is 20dbm, or 100mW

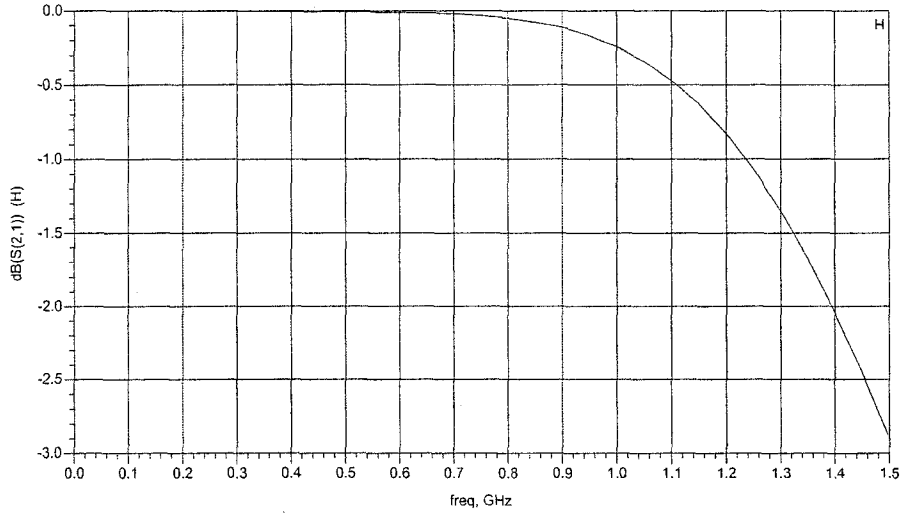

Figure 3.15 Frequency response of the T-stage filter

3.19) has been used. The frequency response of this filter is shown in figure 3.15.

The receiver part of the chip uses a low-IF(100kHz) receiver architecture. A fifth-order butterworth polyphase filter(complex filter) is employed to filter out adjacent channel and image interferences. The mixer frequency of the receiver is $f_{RF} - 100kHz$, then image frequency is 200kHz below the desired signal, that is $f_{RF} - 200kHz$. This interference is rejected by the asymmetric frequency response of the polyphase filter. The performance depends on how well the amplitude and phase balance accuracy between the I and Q channels are. A real-time on chip image rejection calibration can be performed to improve this performance. This architecture can greatly reduce the '1/f' noise as well as the DC offset and self-mixing LO leakage. And it doesn't require a high performance front-end RF filter. The disadvantages of this architecture are that the out-band rejection is limited by the poly phase filter that is implemented with hardware in order to reduce cost.

In this project, the 902MHz-928MHz ISM(industrial, scientific and medical frequency band) frequency band is employed. It is defined by ITU(ITU stands for International

Telecommunication Union) Radiocommunication Sector(ITU-R) and can be used without licence. This frequency band is used for several reasons. First, considering the antenna size, which is proportional to its wavelength, antennas for higher frequency system can have a smaller size. High frequency is preferred to reduce the size of the system, especially for the tag worn by people under monitor. Another important factor is that the path loss is dependent on frequency. Compared with higher frequency systems, with certain distance, lower frequency systems usually have a lower path loss in an indoor environment(Malik, 2006). In a wireless telecommunication, this means either a larger area can be covered or the transmitted power can be reduced. However, high path loss is preferred in wireless positioning systems based on RSS. This kind of positioning systems can provide higher accuracy in an environment with a higher path loss. The reasons are presented in Chapter 4. Then in general, high frequency is desirable for this application. However, high frequency will reduce the covered area by a base station, which means more base station will be required and hence increases the total cost. Also, RF components working at a higher frequency cost more than those at a lower frequency. At present, the WLAN(Wireless Local Area Network) is widely used, which uses the 2.4GHz and 5GHz ISM bands according to the IEEE802.11a/b/g standards. If these ISM bands are used in this project, very complicated protocols must be used to avoid interference with current WLAN applications, or there would be strong interference. For higher ISM frequency band(higher than 24GHz), the cost of RF devices will cost a lot. Then as a compromise, the 902MHz-928MHz frequency band is used.

The frequency band 905MHz $\sim$ 913MHz with a channel bandwidth of 25kHz is used for this work. The specified data rate employing GFSK(Gaussian Frequency-Shift Keying) with a frequency deviation of 5.0kHz is around 9.14kbps. NRZ(Non-Return-to Zero) is used for base band coding. A crystal oscillator of 8.192MHz with a stability of 10ppm is used as the frequency reference. A loop filter with a bandwidth of 100kHz and a phase margin of 45 degree have been designed for the PLL. The whole circuit as shown in

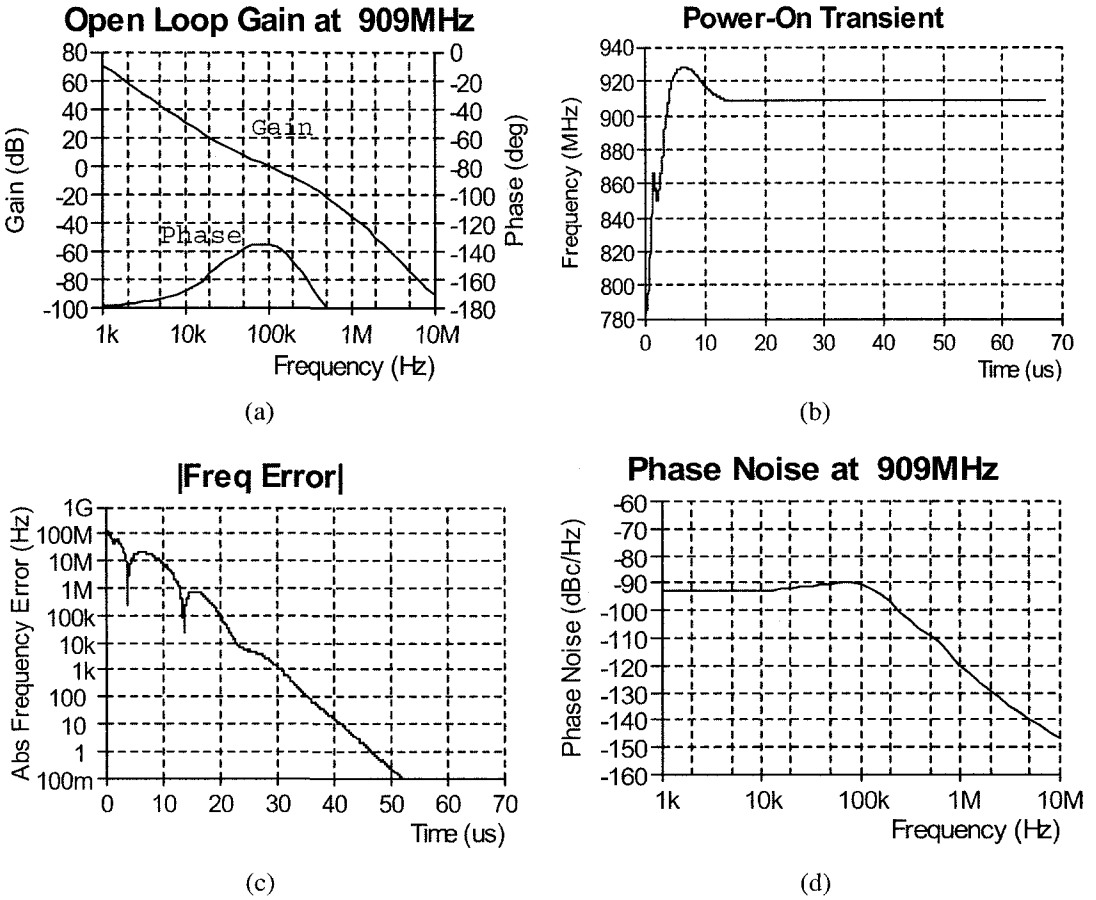

Figure 3.16 PLL performance

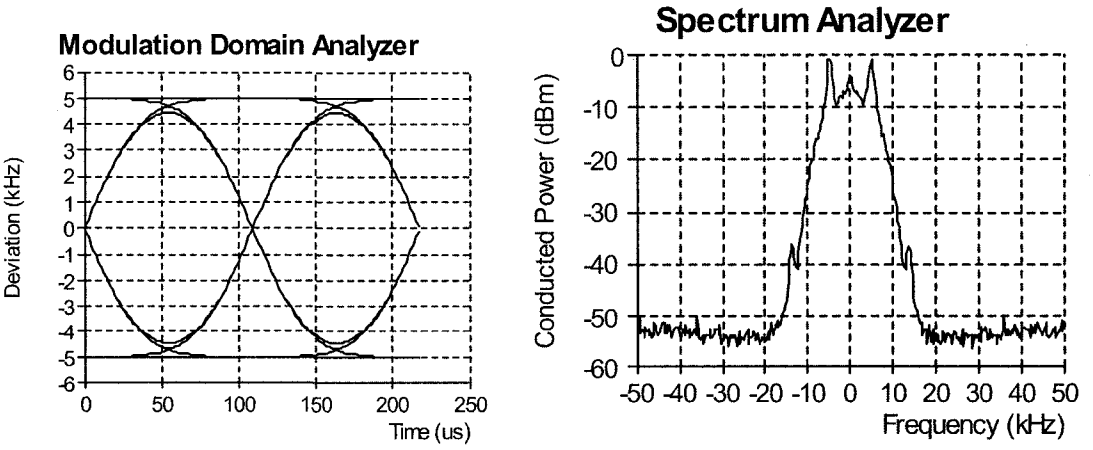

Figure 3.17 Transmitter performance

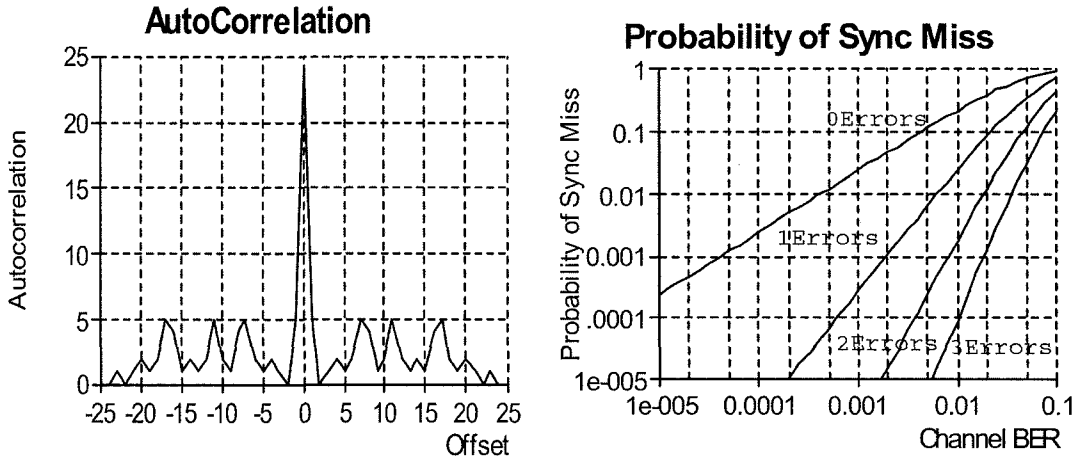

(a) (b)

Figure 3.18 Synchronization performance

figure 3.19 has been simulated with the software ADI SRD Design Studio from Analog Device.

Figure 3.16 shows the simulation results for the PLL. Figure 3.16(a) shows the loop bandwidth and the phase margin, which is around 45 degree. The transient response of the this PLL is shown in figure 3.16(b).

The simulation results for the transmitter part are shown in figure 3.17 and the synchronization performance of the receiver part is shown in figure 3.18. A kind of PN(Pseudo Noise) code has been used as the data source to generate the power spectrum in figure 3.17(b). The 24 word, 0x123456, has been used for the synchronization. The auto correlation function shown in figure 3.18(a), and the synchronization error probability with different number of errors shown in figure 3.18(b), are all based on this word.

The whole circuit of the wireless tag is shown in figure 3.19 and the fabricated one is shown in figure 3.20.

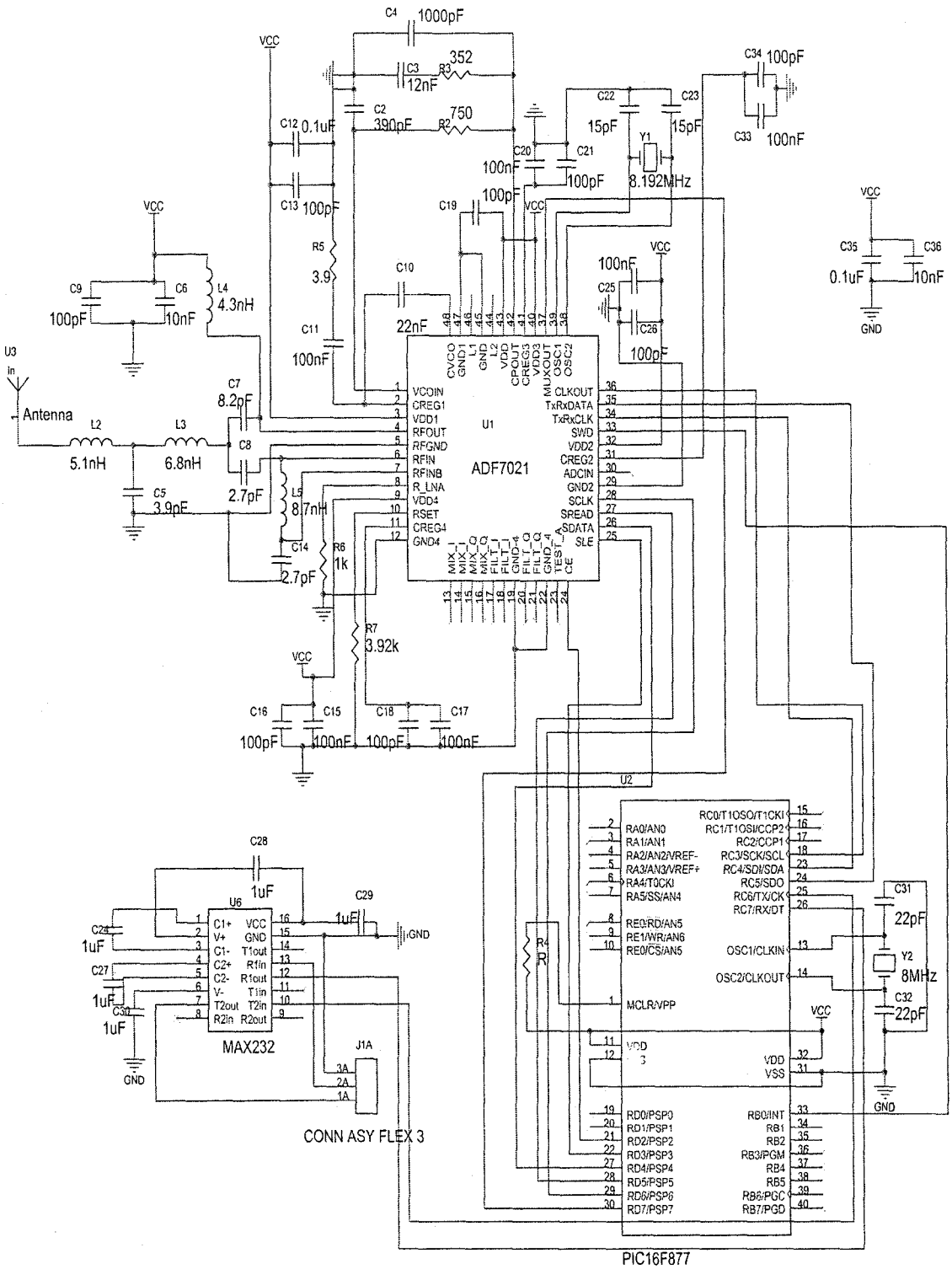

Figure 3.19 The basic circuit for the wireless unit

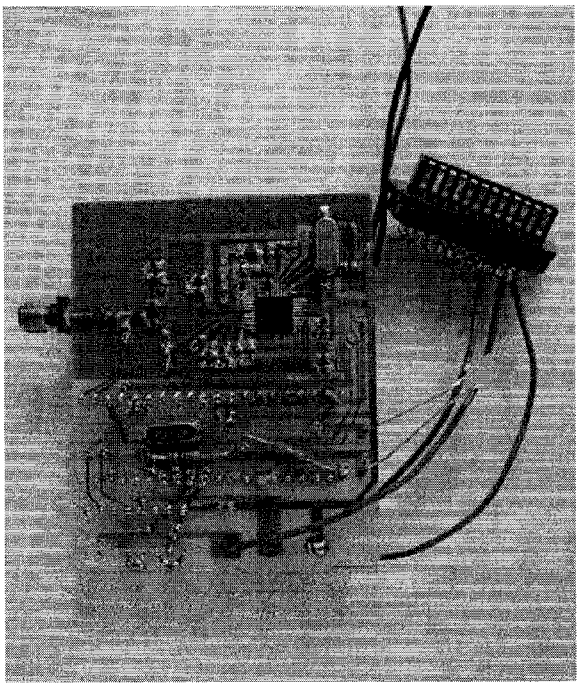

Figure 3.20 The wireless unit

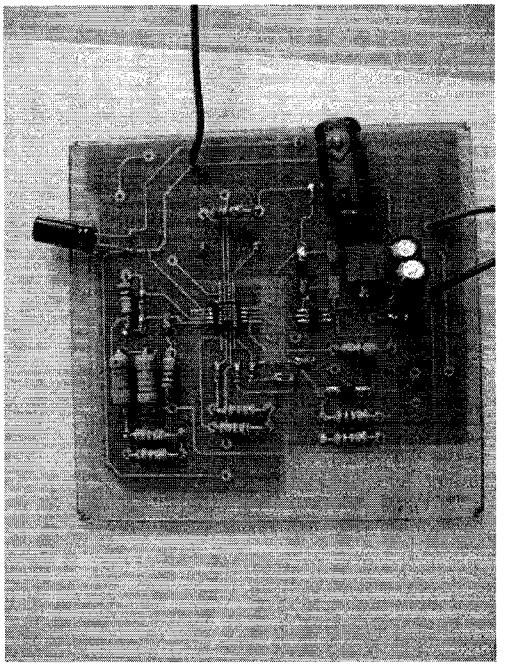

Figure 3.21 The power converter circuit

3.2.3 The Power Supply

The power supply is an important issue for wireless sensor networks. In this project, the supply voltage for all circuits is 3.3V. Concerning the wireless unit worn by people, since it is designed to reduce its power consumption as low as possible, it doesn't require a lot of power. The very small button battery can be used. However, this doesn't work for base stations, which keep working all the time and hence require a lot of power. A transformer can be used to supply them with the household electricity, but this method might be expensive because the transformer is usually more expensive than the cost of a base station circuit. In order to solve this problem, a power converter has been designed to supply the base station with those batteries with high voltage, because they usually have more power than those batteries with low voltage.

A buck converter chip from Maxim company has been used for this power converter. It

supports an input voltage ranging from 5.5V to 23V. It has a maximum output current of 2A. Besides, short-circuit protection and thermal-shutdown protection are also provided. The circuit is shown in figure 3.22 and the fabricated circuit is shown in figure 3.21.

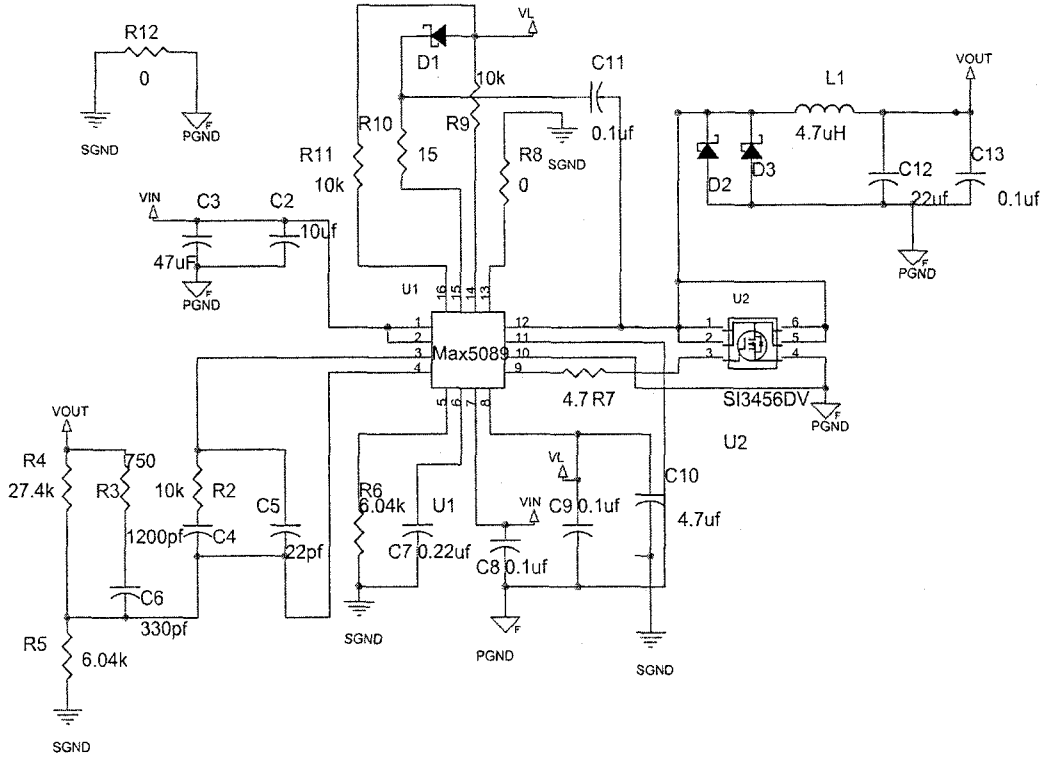

Figure 3.22 The circuit for the power converter (output=3.3V)

CHAPTER 4

POSITIONING ALGORITHM AND PERFORMANCE

This chapter is mainly focused on the positioning based on RSS. There are mainly two kinds of elements that affect the positioning performance. The first element is the environment which is not possible to change. The second element is the algorithm which it is possible to optimize to obtain a good performance. There are mainly three parts in this chapter. First, key factors that affect the positioning accuracy are introduced. Then the measured RSS properties are presented and analyzed. Finally, the positioning algorithm and its performance are discussed.

4.1 Key factors on accuracy

In essence, wireless positioning based on RSS is a kind of parameter estimation problem. And the position of a target is the parameter that needs to be estimated. Although the algorithm for positioning is quite different from the modulation-demodulation in wireless

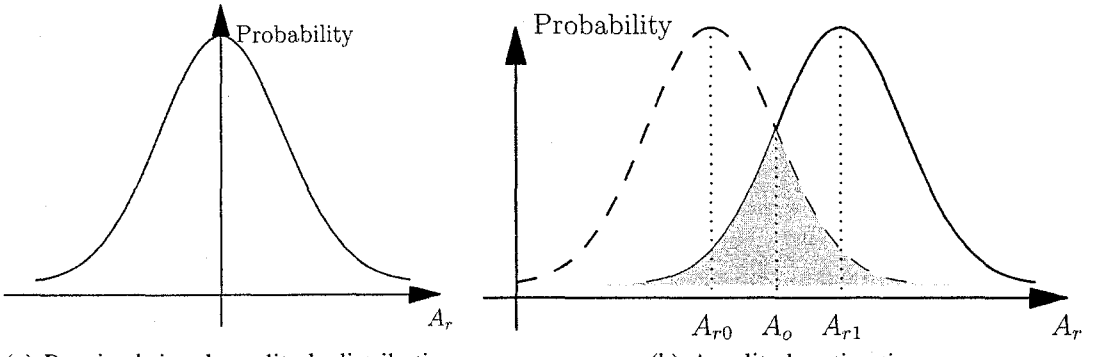

(a) Received signal amplitude distribution (b) Amplitude estimation

Figure 4.1 Simple ASK estimation

telecommunication, they are similar to each other in the mathematical point of view, because they both can be considered as parameter estimation problems. For example, with ASK(amplitude-shift keying) modulation, digital data are represented in the amplitude of a carrier wave. When transmitting logic 1, a signal amplitude of A_{t1} is transmitted and when transmitting logic 0, another signal amplitude of A_{t0} is transmitted. Because of the effects of the wireless channel, the received signal amplitude is no more a single value. It can be described with a distribution as shown in figure 4.1(a). The received signal can be simply decided by comparing the signal amplitude with the value shown in figure 4.1(b). If the signal amplitude is larger than A_o, the transmitted signal will be considered as a logic 0, or it will be considered as a logic 1. When a logic 0(1) is transmitted but the received signal amplitude is larger(smaller) than A_o, an error will occur. The theory for positioning based on RSS is also quite similar. In wireless positioning system based on RSS, the RSS at a certain place can also be described by a RSS distribution. Different places will have different RSS distributions. SupposeLet us suppose that the RSS distribution is as shown in figure 4.1(a), and the RSS distribution of two places, adjacent to each other are as shown in figure 4.1(b)(p_0 with the dashed curve and p_1 with the solid curve)[1]. Then when the RSS at point p_0 is larger than A_o, it will be considered being at position p_1 and when the RSS at point p_1 is smaller than A_o, it will be considered being at position p_0. It is obvious that the size of the area covered by shadow determines the error probability. If this size is large, the error probability is large, and vice versa.

It is important to note that the positioning accuracy is kindly determined by the size of the intersection of the two probability distributions. There are several factors that can affect this intersection size.

First, the standard deviation is an important factor. Large standard deviation means the random variable has a high probability to be far away from its expected value. Figure 4.2

[1]It should be noted that the RSS distribution is not like the curve shown in figure 4.1, but the theory is similar.

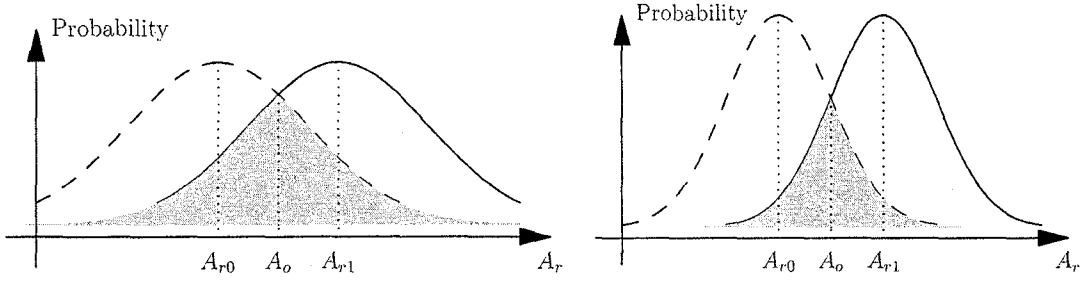

(a) Large standard deviation (b) Small standard deviation

Figure 4.2 Effects of standard deviation of RSS

shows two situations where the parameters are all the same except the standard deviation of their RSS. It is clear that large standard deviation means a large error probability and small standard deviation results in a small error probability. When the standard deviation is very large, there would be almost no difference among the RSS at different places. The RSS will be of no help for positioning. When the standard deviation is very close to zero, the RSS of every point will corresponds to a unique value and the error probability becomes zero.

The RSS standard deviation is a main factor that determines the positioning accuracy of a wireless system based on RSS. This factor is determined by the environment where the system works. Inside a certain environment, different places will have different RSS standard deviations and a same place will also have different RSS standard deviations at different time. The hardware can cause some error when they read out the RSS. The wireless channels can also be affected by other factors, like temperature and humidity. However, usually errors caused by these factors are small. The main source of this deviation is caused by people's activities inside the environment, such as people walking around, changing the wireless channel response, people penning and closing doors, changing the position of furniture like chairs, and so on. Unlike the outdoor environment, indoor environment usually is not spacious and people's activities can have much influences on indoor wireless channels. In an indoor environment, high positioning accuracy can be obtained if there is not much people's activities. If the RSS standard deviation is

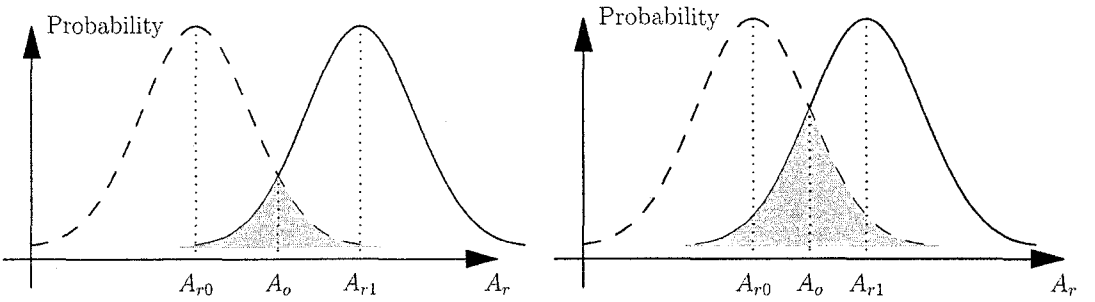

(a) Large signal strength distance (b) Small signal strength distance

Figure 4.3 Effects of signal strength distance

zero, it is possible to have an accuracy of 100%.

The x-axis in figure 4.2 and figure 4.3 represents the signal strength. As shown in figure 4.3, the size of the intersection area of the two curves can be reduced by "moving" the two curves far away from each other, and then the error probability can be reduced. There are two factors that decide this strength distance: the loss factor(here it means the loss of signal power in dB per unit length) of the electromagnetic waves and the position distance between the two points. Correspondingly, there are mainly two methods to "move" the two curves far away.

The first method is simply to change the positions of the two points where RSS is measured. If the two points are far away, the signal strengths received in the two points should be far away. In fact, this means effects of the grid size. As introduced in 1.2.1, the whole covered area of a positioning system based on RSS is divided into many grid points. The RSS from all available base stations measured at those points are stored. Real-time measured RSS are compared with these "fingerprints" to decide its real position. This means that large grid size can have a small error probability. However, this doesn't always make sense. As a special case, when there is only one of this grid point in the whole area, there won't be any positioning errors, but apparently this doesn't make any sense. Also this conclusion is not true if we estimate the positioning accuracy with

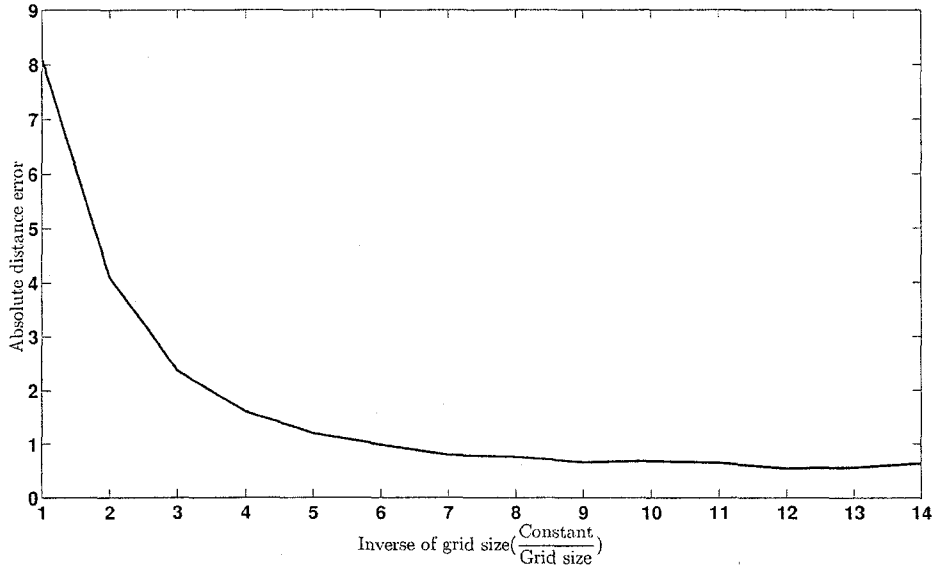

Figure 4.4 Grid size effects on absolute error distance

the absolute error distance, which is calculated by the following equation:

$$d_{error} = |p_{real} - p_{estimated}|^2 \tag{4.1}$$

where p_{real} is the real position of the target, $p_{estimate}$ is the estimated position of the target and d_{error} is the absolute distance error.

Then in order to investigate the problem that whether the positioning accuracy can be improved by reducing(increasing) the grid size or not, a simulation using Monte-Carlo method is employed. The simulation is performed in a one dimensional space, that is a line with fixed length. The distribution of RSS is assumed to be normal. Although the distribution of RSS in practice is not strictly normal, this doesn't affect the result, because all positions employ the same distribution. In the simulation, a random position inside the line with uniform distribution is used to represent the real position of a target. Then the estimated position of this target is determined by the method of maximum a posteriori(MAP, or posterior mode). The absolute error distance is then calculated with

equation 4.1.

The result is shown in figure 4.4. Now it is apparent that the positioning accuracy can be improved by reducing the grid size, but small grid size doesn't always mean a good performance. It can be seen that, when the inverse of the grid size(constant/grid size) in figure 4.4 is larger than 6, the performance is not improved very much. Obviously, the limit of the absolute distance error, as the grid size approaches zero(the inverse of the grid size approaches infinite), almost becomes a constant other than zero. There is a corresponding threshold of the grid size for a positioning system in a certain environment. Different environment might have different threshold. When the grid size is larger than this threshold, reducing the grid size can greatly improve the positioning performance. When the grid size is smaller than this threshold, the positioning performance can not be improved much by reducing the grid size. Also, for some applications, there is no need to have a small grid size. For example, if the accuracy in an application requires an accuracy of 10 meters, then there will be no need to have a grid size of 1 meter.

Since the distance between the two curves in figure 4.2 and figure 4.3 is also determined by the loss factor of electromagnetic wave propagation, these two curves can be 'moved' far away from each other if the loss factor can be changed. The x-axis in figure 4.2 and figure 4.3 represents the signal strength. If there is a big difference of RSS between the two points adjacent to each other, their distribution of RSS will not have a large intersection area, and then the error probability is small. The difference of RSS between two points is determined by the difference of their distances from a base station and also by the loss factor of the electromagnetic wave propagation. The first element, the difference of their distances from a base station is fixed and can not be changed. Then the only method left is to change the loss factor. With a larger loss factor, a better performance can be obtained. This means that if there are some obstacles among those grid points for fingerprint, there will be a large loss factor and the performance can be improved. Also, if the environment is filled with water or other material that have

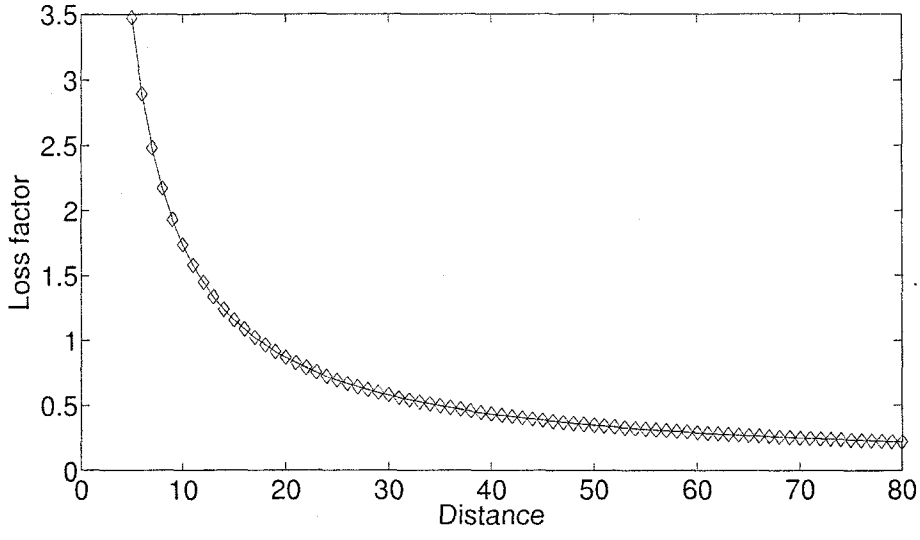

Figure 4.5 Loss factor versus distance between the tag and the base station

a larger loss factor than air does, the system can provide a better accuracy, although this will reduce the size of the coverage area. However, this is usually decided by the architecture of the environment and is difficult to change. One possible way for general indoor environment is to put the base stations on the ground of floors. The effects of the ground might introduce a large loss factor.

It should also be noted that, with the definition of loss factor here(see section 4.1), this factor is also dependent on the distance between the tag and the base station, that is, the loss factor is position sensitive. The reason for this is from the propagation law of the electromagnetic waves. The equation for path loss of electromagnetic waves(1.4) is rewritten here:

$$P_{loss}(dB) = 20log_{10}(\frac{\lambda}{4\pi d_0}) - 10n \cdot log_{10}(\frac{d}{d_0}) \tag{4.2}$$

It is obvious that the path loss is not a linear function of the distance d. The loss factor

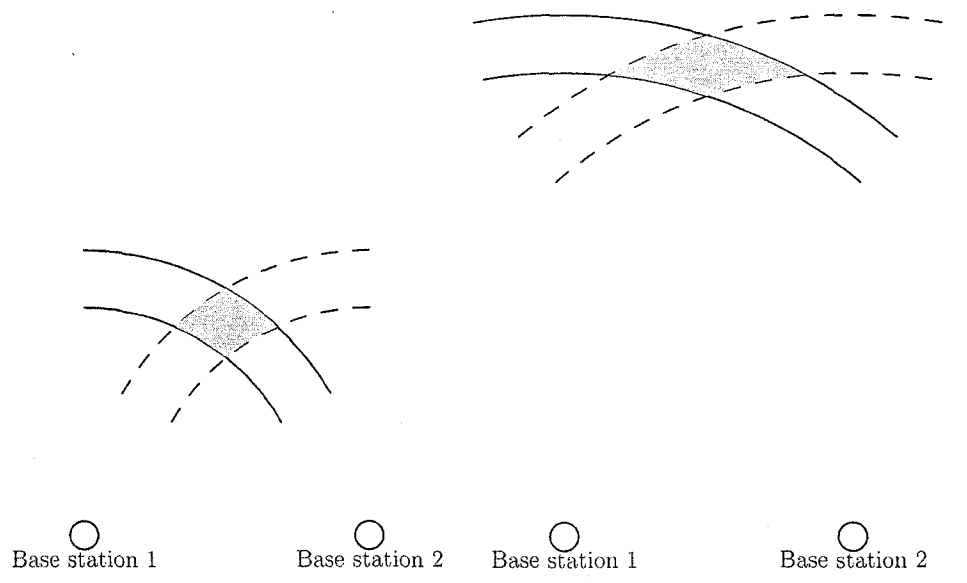

(a) The tag is close to the two base stations (b) The tag is far from the two base stations

Figure 4.6 Geometry effect on positioning accuracy

is the derivative of the path loss. It can be calculated by the following equation:

$$\begin{aligned} \text{Loss Factor} &= -\frac{\partial P_{loss}}{\partial d} \\ &= -\frac{\partial(20log_{10}(\frac{\lambda}{4\pi d_0}) - 10n \cdot log_{10}(\frac{d}{d_0}))}{\partial d} \\ &= \frac{10n}{d \times ln10} \end{aligned} \tag{4.3}$$

This shows that the loss factor is inversely proportional to the distance. This result is plotted in figure 4.5. As a result, different locations will have different loss factor depending on their distances from base stations, hence have different accuracy performance. For instance, when a tag is 20 meters from a base station, 1 meter's distance difference will result in around 1dB difference in RSS from that base station. When the distance is 80 meter, 1 meter's distance difference will only result in around 0.17dB difference in RSS. Then if a tag is far away from a base station, the RSS of the tag from that base station will has a small loss factor, and a poor accuracy occurs. A good accuracy can be obtained when the tag is close to base stations.

In an environment that has more than one dimensions, the position of tags can affect the positioning accuracy in another way. Figure 4.2 and figure 4.3 explain the fundamental positioning theory in a one dimensional space. In a more than one dimensional space, another factor that can affect the positioning accuracy comes up. Figure 4.6 shows the geometric dispersion of position in a two dimensional environment. In this figure, the distance between the two base stations is the same, but the distance between the tag and the base stations is different. The shaded area represent the uncertainty of the position. The RSS at positions of the targets in figure 4.6(a) and figure 4.6(b) are assumed to have the same standard deviation. Obviously, the size of the shaded area of the two figures are different. The area uncertainty in figure 4.6(b) is significantly greater than that in figure 4.6(a). This conclusion can be easily extended to a three dimensional environment, where the shaded area becomes significant.

Besides the factors discussed here that have much influence on the performance of a wireless positioning system based on RSS, there are some other factors, such as the number of base stations that a tag can reach, the length of RSS measurement time. These factors will be discussed later in this chapter.

4.2 RSS Properties

Compared with outdoor environment, the wireless channel in an indoor environment is more complicate. Different indoor environment can have different properties, because generally they have different architectures, they are built with different materials, there are different number of people inside and those people inside have different kinds of effects on the electromagnetic wave propagation. The properties of RSS in an indoor environment have a decisive influence on the performance of a whole wireless positioning system. Based on measurement, several important properties of RSS have been found.

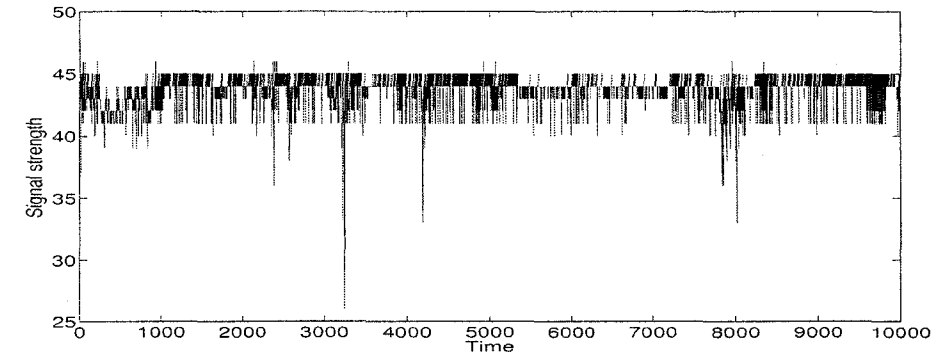

(a) Measured RSS

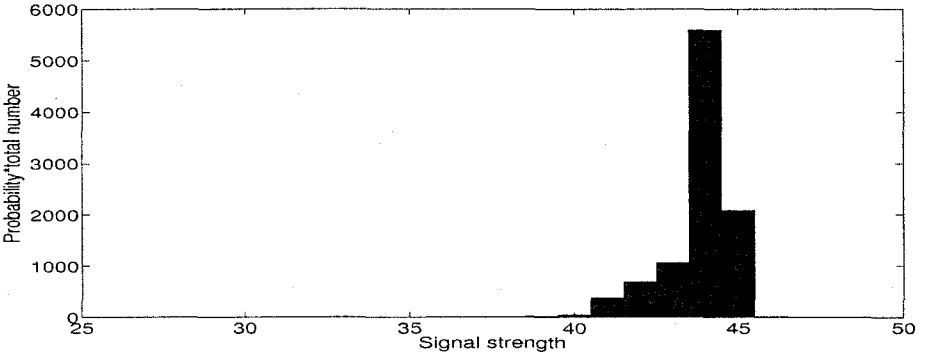

(b) Measured RSS distribution

Figure 4.7 Typical RSS measured in indoor environment

The RSS in an outside environment is usually considered to be normally distributed. And in some papers the RSS in an indoor environment is also considered to be normal. However, our measurements show a different result.

First, measurements show that the distribution of RSS in an indoor environment is not symmetrical. Figure 4.7(b) shows a typical distribution of RSS from measurement in an indoor environment[2]. Figure 4.7(a) shows the measured RSS changing with time. The expected value of this measurement is around 43.78 and the standard deviation is around 1.18. The minimum measured RSS is 26 and the maximum measured RSS is 46. As can be seen in the figure, the RSS tends to become smaller other than larger. And the RSS

[2]The RSS values shown here all have an offset

distribution has a 'tail' in its left side. Apparently this won't be a normal distribution. Since the variance of the measured RSS is mainly caused by the change of environment, such as people's activities, this shows that the usual changes in environment tend to increase the attenuation of the signal strength. Also, even sometimes the received signal strength becomes larger, there is no much increase in the signal strength, because the largest RSS is only about 3dB larger. However, the signal strength can be reduced to a value much smaller than its expected value. As shown in this figure, the smallest RSS is only 26, which is about 18dB lower than its expected value. In previous works, this property has been used to improve the positioning accuracy.

Another important property of RSS in an indoor environment is that usually there might be more than one signal strength values whose probabilities are local maximum and is comparable with the peak probability. This is illustrated in figure 4.8(b), where there are two signal strength values that have local maximum probabilities and they are comparable to each other. This makes the positioning based on RSS more challenging. In previous work, It is proposed to use the mean value of RSS as the fingerprint of a location and this value is used for positioning. However, the property of RSS shown here will degrade this method.

Generally, one of those signal strength values is the real 'fingerprint' of the location. Usually this is the largest value. Other signal strengths that have local maximum probabilities are caused by people's activities. People's daily activities have a great influence on the indoor wireless channel. The curve in figure 4.8(a) is like a two stairsteps and can be divided into two parts by their RSS value. During the first part of this measurement, the measured RSS is close to 55, where is the first local maximum probability in figure 4.8(b). And during the second part of this measurement, after time 1.2×10^4, With many measurements, a common characteristic among them has been found: all the RSS values that have local maximum probabilities correspond to a continuous period of time, during which the measured RSS is close to that RSS value. This is because of people's

activities. For example, suppose a person comes to stand in the way through which the wireless signal is transmitted. Then the wireless signal is likely to be attenuated by the body. And the tag will receive a signal strength smaller than its normal value. If the person stands there for a period long enough, this situation will continue and measured RSS will be close to the smaller value during that period. This will result a local maximum probability as in figure 4.8(b). This maximum can be very large if the period is very long compared with the total measurement time. If another person also walks around a place in the way of the wireless signal, then the signal will be further attenuated and another local maximum probability will occur. If the person stands in the way all though the measurement time, the real RSS value will be hidden and the performance will be greatly degraded.

Although this property gives a big challenge in positioning performance, this problem can be addressed to some extent. As discussed above, this is mainly caused by people's activities. And people usually have their schedules. For example, people usually go to work during Monday to Friday, people will go out of their offices at noon for lunch, and so on. People have their own schedules and habits. Then the wireless channels influenced by people will have corresponding trends. For instance, if at a certain position inside an indoor environment and at a certain time, say, ten o'clock in the morning of Tuesday in a week, the RSS from a base station is 10dB less than its normal value, then there is a high probability that the RSS from that base station is also around 10dB less than its normal value at the same time in the next week. As a result, this property can be used to improve the system performance.

Besides the two important properties of RSS distribution above, measurements show that the standard deviation of the RSS at a certain position varies with time. Figure 4.9 shows the measurement result. The measurement is performed in a laboratory during a period of almost one day, from around nine o'clock in the morning to around nine o'clock in the evening. The RSS at a fixed position has been measured by a tag and

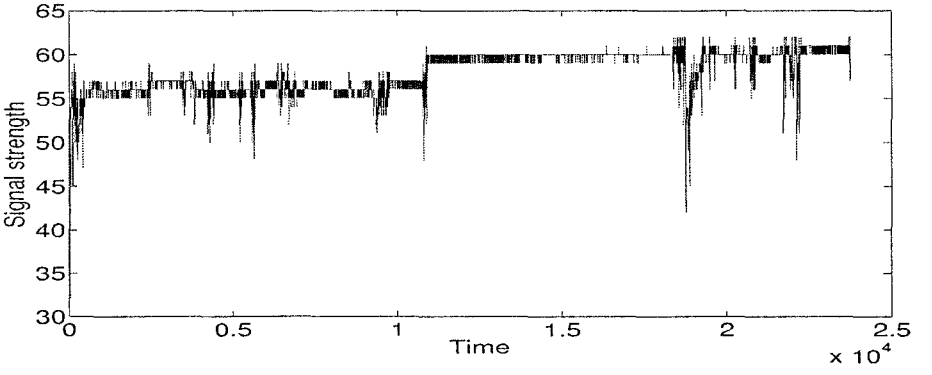

(a) Measured RSS

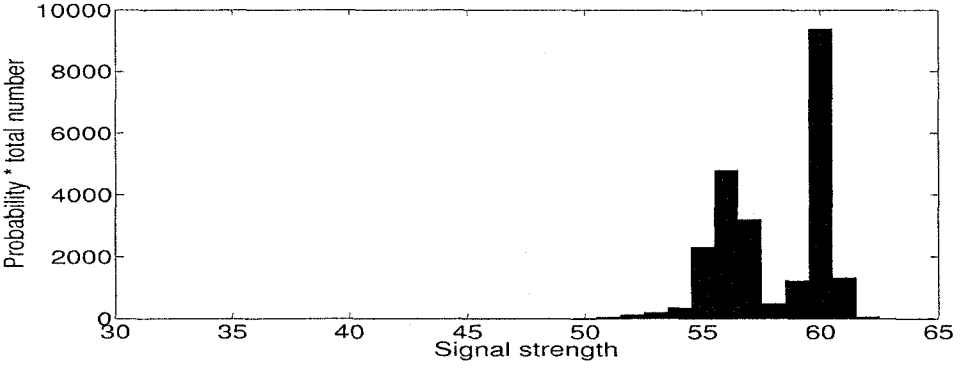

(b) Measured RSS distribution

Figure 4.8 More than one peaks of RSS measured in indoor environment

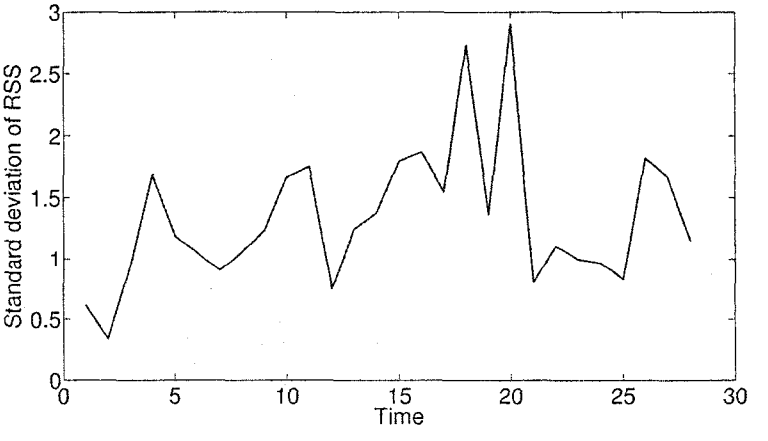

Figure 4.9 Standard deviation varies with time

data are transmitted into a computer for processing. Measured RSS during a period of thirty minutes are considered as a group and its standard deviation is calculated. A total of twelve groups have been recorded and their standard deviations have been calculated respectively and are shown in figure 4.9. It seems that the standard deviation changes randomly between 0.3 and 2.9 all through the time. It should be noted that the curve in figure 4.9 is dependent on the time length that is used to calculate the standard deviation. If the time length changes, the minimum standard deviation, the maximum standard deviation and all the curve in figure 4.9 will also change. However, the fact that the standard deviation of RSS varies with time doesn't change.

There is a relationship between these two RSS properties. As mentioned above, the large variance of RSS is mainly caused by people's activities. The standard deviation comes from the variance of RSS and hence is because of people's activities. When the standard deviation is larger, probably more people's activities are involved in the environment, and vice versa. Large standard deviation will lead to a poor performance. Then, this means that the performance of a wireless positioning system is not only dependent on the position of the tag, but also dependent on the time when the positioning process is performed.

4.3 Antenna polarization

In usual point to multi-point wireless telecommunication systems, linearly polarized antennas have been used at both the base stations and the mobile users. In most cases, the antennas in mobile devices are not oriented in a way that they are not physically aligned to the direction of the antenna in the base station. Any polarization misalignment between the transmitting antenna and the receive antenna will result in a loss in signal strength. If there is a line-of-sight path between a mobile device and a base station, the loss caused by antenna polarization mismatch can be calculated by the following

equation:

$$Loss_{\text{Polarization mismatch}} = 20log(cos\theta) \tag{4.4}$$

where θ is the angle between the two antennas' polarization.

In practice, especially in an indoor environment, there are shadow fading and multipath effects. Signal strength is dependent on blockages and multipath reflections of the environment. In many cases, there might be no line-of-sight path between a base station and a mobile device, and the signal transmission between them is based on multipath channels. Signals from the transmitting antenna probably have been reflected several times before they reach the receive antenna. Signal polarization can be changed when they are reflected. Because of the following reasons, using linearly polarized antennas in both base stations and tags is not a good choice.

Firstly, since our wireless positioning system is used to position the people that fall down and need help, usually it is impossible for these people to control the antenna direction of their tags after they fall down. Then the angle between direction of a tag's antenna and that of a base station is beyond our control. This angle will become a random variable. Since the loss caused by polarization mismatch is a function of this angle, this loss is also a random variable. Because different levels of signal strength correspond to different locations, this randomly varying loss will lead to an error in position.

In addition, in an indoor environment, serious multipath reflections exist. The signal arriving the receive antenna doesn't only consist of the signal from line-of-sight(if it exists), but also consists many signals that are reflected by objects in the environment, which result in multipath. If those objects that reflect the signal are not aligned with the polarization of the incident signal, the polarization direction of the incident signal will change. As a result, the signals that arrive at the receive antenna doesn't only consist of signals with the same polarization direction of the transmit antenna, but also consist of many signals with a different polarization direction. Then the polarization mismatch

loss still exist. And the received signal strength is also dependent on the environment, including people's activities nearby, which is not controllable. Apparently this will lower the positioning accuracy.

In order to improve the positioning performance, other than using linearly polarized antenna only, linearly polarized antennas and circularly polarized antennas or dual polarized antennas can be used together to combat this problem. Usually these techniques are used to improve signal quality. But here it needs to be noted that these techniques can be used to reduce the dependence of RSS on antenna direction. For example, suppose at a location, by changing the receive antenna direction, the maximum received signal strength is P_{Max}, and the minimum received signal strength is P_{Min}. Then the goal is to make $|P_{Max} - P_{Min}|$ as small as possible.

Using dual polarized antennas is often referred as polarization diversity. Usually these antennas have two outputs for the two polarization elements. Systems with dual polarized antennas will analyze the received signal and some algorithms are used to process the two channel input signal to get the strongest signal level. With a dual polarized antenna, the loss due to polarization mismatch can range from 0 to 3dB. Circularly polarized antennas only have one output port. The signal at the output of the port is a combination of all arriving signals. The loss of polarization mismatch with this kind of antenna is dependent on their axial ration.

Apparently, dual polarized antennas will make the system more complicated than circularly polarized antennas do. Besides, because the receive antenna is also used as the transmit antenna, some switches have to be used to control them, which will introduce some loss and increase the cost of the system. As a result, a combination of linearly polarized antennas (for tags) and circularly polarized antennas (for base stations) are used in this project.

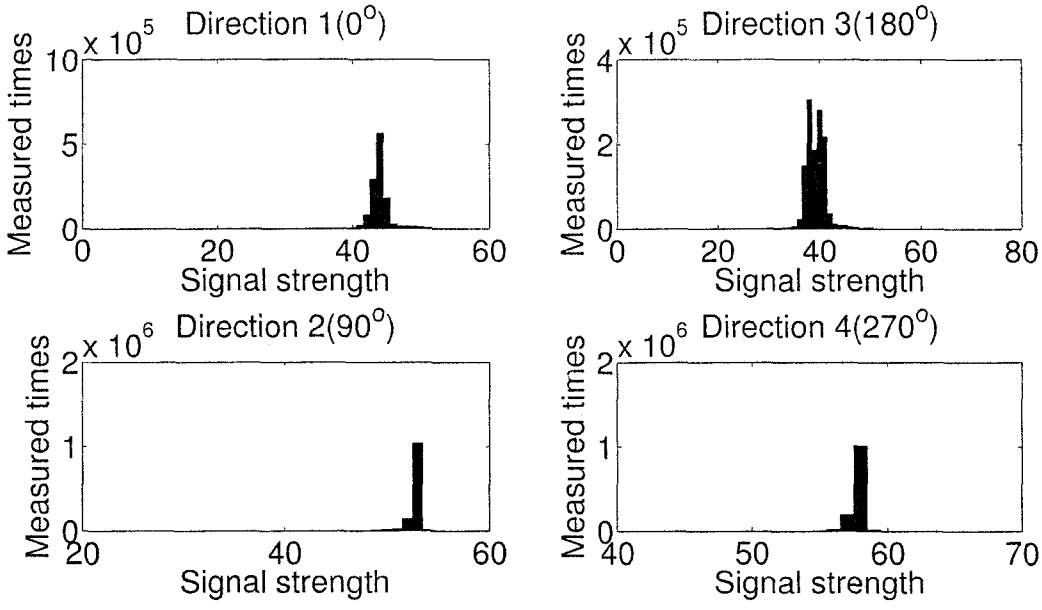

(a) Results with both linearly polarized antennas

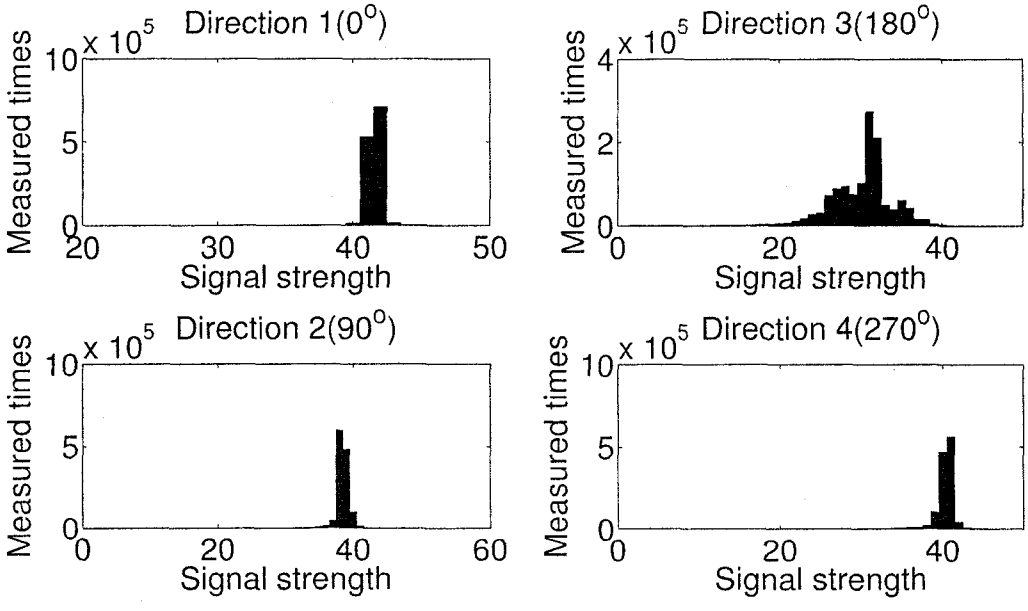

(b) Results with a linearly polarized antenna and a circularly polarized antenna

Figure 4.10 Effects of antenna polarization

Measurements have been performed to compare the performance between a combination of both linearly polarized antennas and a combination of a linearly polarized antenna and a circularly polarized antenna. During the measurements, the base station and the tag are placed in fixed locations. The base station uses the linearly polarized antenna as shown in figure 3.11. At first, the tag uses a same linearly polarized antenna. Then the tag uses a circularly polarized antenna as shown in figure 3.5. With four different antenna directions by changing the direction with 90 degree each time, four measurements have been made for both the linearly polarized antenna and the circularly polarized antenna. Figure 4.10 shows the measured RSS distribution. The mean values and standard deviations are shown in table 4.1 for comparison. It can be seen that there are big differences between the mean values when both linearly polarized antenna are used. The maximum difference is around 8dB. Even the minimum difference is around 5dB. But when a circularly polarized antenna is used, there is no big difference between them except the measurement with direction 2(90^o). As shown in table 4.1 and in figure 4.10(b), this measurement has a large standard deviation. And probably this is because of some errors in the measurement set up. Taking this measurement apart, the maximum difference between mean values is only around 3dB. Then undoubtedly a circularly polarized antenna and a linearly polarized antenna is a good combination to improve the positioning accuracy. Besides, it can be found here that for a fixed location, the mean value tends to become smaller when the standard deviation becomes larger. This might be useful to improve accuracy.

4.4 Positioning Algorithm

The positioning algorithm used is a kind of fingerprint method. It mainly consists of two steps. The first step is to build up an electronic map of the whole area that is required to cover by the system. This map is recorded in a database in the central server. The

Measurement	Linear polarization with Linear polarization		Linear polarization with Circular polarization	
	Mean	Standard deviation	Mean	Standard deviation
Direction 1(0^o)	44.0	1.9	41.5	0.6
Direction 2(90^o)	39.2	2.5	30.0	4.3
Direction 3(180^o)	52.7	1.0	38.4	1.1
Direction 4(270^o)	57.8	0.62	40.2	1.8

Table 4.1 Comparison between linear polarization and circular polarization

other step is for practical positioning application, where locations of tags are provided by the system. In this step, tags will first record RSS information from all available base stations and transmit this information to the base station with the strongest signal strength.

In order to build up the electronic map, the total area will be covered by a grid. The points in the grid are reference points. The grid size is determined by the required accuracy and the achievable accuracy in that environment. The grid size should be smaller than the required accuracy and larger than the achievable accuracy. In general indoor environment, a value ranging from 2 meters to 4 meters can be used as the grid size. And the grid size can be different in different locations to make the system more efficient. For example, if there is a wall between two points in the grid, then the distance between these two grids can be smaller than the standard size. If two points in the grid are in the same room and there is nothing between them or nearby, then the grid size for these two points can be larger. Then the RSS from all available base stations at all positions in the grid will be recorded for a certain period long enough to represent the RSS distribution for that point, such as 12 hours. Only the RSS distributions need be saved. In order to reduce the time it takes for real-time positioning process, all the points in the grid should be divided into groups according to the base stations from which they can receive signal.

After the electronic data base is built, the system is ready for use. When a person under

monitor falls down at a location p_{tag}, the tag will detect this fall and starts the positioning process. At first, the tag will search for all available base stations, BS^1_{found},....BS^n_{found}. Because there are only seven frequency bands for base stations and every base station must use one of these frequency bands, the tag can search these frequency bands one by one to check available base stations. It should be noted that there are only a maximum of seven base stations by which a location is covered. For each available base station found by the tag, BS^j_{found}, its RSS information, $RSS_{BS^j_{found}}$, will be recorded by the tag for a predefined period of time. The length of time is dependent on the accuracy requirement. Several minutes can be used in general indoor environment. After the RSS information of all available base stations is recorded, the tag will record all the RSS information, $RSS_{BS^1_{found}}$,$RSS_{BS^2_{found}}$,....$RSS_{BS^n_{found}}$. Then the tag will try to send this information to the available base station with the strongest RSS. This is because it is easier to successfully transmit the information to the base station with the strongest RSS than to a base station with smaller RSS. And hence reduce the energy consumption of the tag. The information will then be transmitted to the central server of the system by the base station via internet. The central server will compare this information with all the reference points in the grid, p^i_{map}, where RSS information are recorded in the electronic map built up before. If the whole area is very large, there will be a great number of reference locations in the grid. If the server compares the information with RSS information recorded at all these locations, it will take a lot of time. In order to reduce the cost of processing, the server will first find the identities of all the base stations whose RSS is recorded in this information. Then the server will find the matching group G_{match}, inside which all points, can reach all or most of the base stations, BS^1_{found},BS^2_{found},....BS^n_{found}. Then the server will only compare this information with the RSS information of these points.

The method used to find the point p^r_{map} in the grid that has the minimum distance from the real location of a tag p_{tag} is a distribution matching method. This point p^r_{map} is one of the point in the group G_{match} as mentioned above. Base on how much the RSS

distribution measured at p_{tag} is matched to that of these points, a weight is given to each of the points in the group G_{match}. The weight of a point p^i_{map} corresponding to the RSS distribution of the base station BS^j_{found} is represented by w^j_i. Let us suppose that the distribution function of the RSS from the base station BS^j_{found} for the point p^i_{map} in the group G_{match} stored in the database is $P^{i/j}_{map}(x)$, and the distribution function of the RSS from the base station BS^j_{found} measured in the location p_{tag} is $P^j_{tag}(x)$. The weight w^j_i is calculated by the following equation:

$$w^j_i = \int_{RSS} P^{i/j}_{map}(x) \times P^j_{tag}(x)dx \tag{4.5}$$

Let us suppose that the maximum of the RSS values from BS^j_{found} at the point p^i_{map} is $RSS^{i/j}_{max}$, the minimum of the RSS values from BS^j_{found} at the point p^i_{map} is $RSS^{i/j}_{min}$, the maximum of the RSS values from BS^j_{found} measured at the position of the tag is $RSS^{tag/j}_{max}$, the minimum of the RSS values from BS^j_{found} measured at the position of the tag is $RSS^{tag/j}_{min}$,. Then the upper limit of the integral interval in equation 4.5 can be defined as:

$$RSS_{upper} = Max(RSS^{i/j}_{max}, RSS^{tag/j}_{max}) \tag{4.6}$$

And the lower limit of the integral interval can be defined as:

$$RSS_{lower} = Min(RSS^{i/j}_{min}, RSS^{tag/j}_{min}) \tag{4.7}$$

Because we have:

$$\begin{aligned} P^{i/j}_{map}(x) &= 0 \quad \text{when} \quad x < RSS^{i/j}_{min} \quad \text{or} \quad x > RSS^{i/j}_{max} \\ P^j_{tag}(x) &= 0 \quad \text{when} \quad x < RSS^{tag/j}_{min} \quad \text{or} \quad x > RSS^{tag/j}_{max} \end{aligned} \tag{4.8}$$

The lower and upper limit of the integral interval in equation 4.5 can be changed to:

$$RSS_{lower} = Max(RSS_{min}^{i/j}, RSS_{min}^{tag/j})$$
$$RSS_{upper} = Min(RSS_{max}^{i/j}, RSS_{max}^{tag/j}) \tag{4.9}$$

The total weight of a reference location p_{map}^{i} in the group G_{match} can be calculated by the following equation:

$$W_i = \prod_{j=1}^{N} w_i^j \tag{4.10}$$

where N is the total number of base stations reachable by the tag. Then the reference point p_{map}^{r} can be found by its total weight:

$$W_r = Max(W_1, W_2, ...W_M) \tag{4.11}$$

where M is the total number of reference points in the group G_{match}. If more than one reference points have their weights very close to this maximum weight, the position of the tag can be represented by the average of all these reference points.

4.5 Performance

In order to evaluate the performance of the positioning algorithm, measurements and simulations were carried out. At first, RSS at a fixed location from several base stations is measured and saved. Based on the data from these measurements, Monte-Carlo method is used to show the performance.

The measurements have been made around our microwave laboratory in École Polytehcnique de Montréal, where there are many people walking around in the day time. A tag which is connected to a computer through RS-232 interface, is set to receive RSS infor-

mation from several base stations and transmits these information to the computer. RSS information from each base station has been recorded by the tag for around 12 hours, from 9:00am to around 9:00pm, with a sampling rate of 1000 values/second. The total RSS information from a base station is recorded in 24 files. Each file records the RSS information of 30 minutes. The distances between the tag and those base stations range from around 6 meters to 15 meters. The distances between those base stations range from 5 meters to 15 meters.

Then simulations are performed based on these data. Some assumptions are made in the simulation:

1. Assume all these base stations have the same distance R with the tag. And they are uniformly distributed in a circle with the location of the tag as its center and with a radius of R. This doesn't affect the simulation results because distances between the tag and base stations can only affect the performance in the way that the loss factor varies when distances change. But here the loss factor is not changed.

2. Assume the distribution of RSS from a certain base station that has been measured for 12 hours can represent the general distribution of RSS from that base station received the location of the tag, that is, the RSS distribution measured for 12 hours in day time doesn't change much from day to day.

3. The tag can only give the RSS with integers. Then assume the RSS has been rounded. For example, if the RSS is 10.2dBm, the read out value will be 10dBm.

4. The grid size used here is 1 meter. Then it is reasonable to assume that the distributions of RSS from a base station, measured at the location of the tag and at locations that are not more than 1 meter far away from the tag, are the same.

The simulation set up is shown in figure 4.11. Based on these assumption, simulations are performed as following:

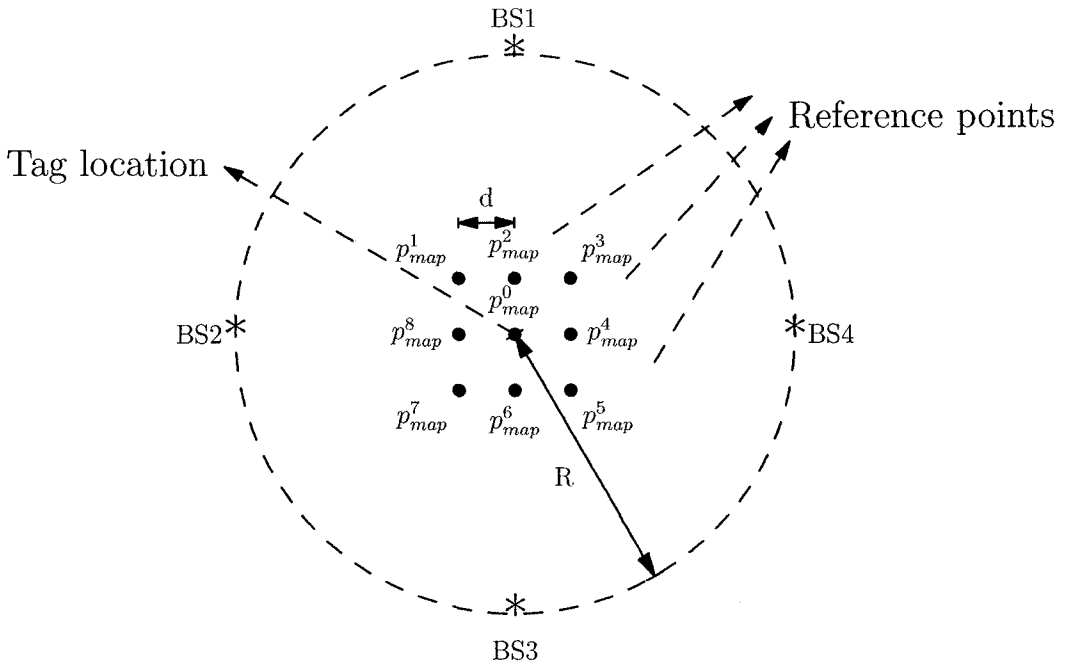

Figure 4.11 Simulation set up

1. with the recorded data, all distributions of RSS from all base stations, $P^{i/j}_{map}$ where $i = 0$ and $j = 1, 2....4$, are calculated. This is considered as the RSS fingerprint of the location of the tag in the electronic map. Because the location of the tag is also a point in the grid.

2. RSS distributions for reference points around the tag, $P^{i/j}_{map}(x)$ where $i = 1, 2....8$ and $j = 1, 2....4$, are calculated to create electronic map information for their locations.

3. RSS values as the real-time measurements by the tag from each station are randomly generated according to the measured RSS distribution. If not specified, the number of RSS values recorded for each base station corresponds to a time length of around 10 seconds.

4. Calculate the distribution of those RSS values mentioned in step 3, $P^{j}_{tag}(x)$ where $j = 1, 2....4$.

5. Then calculate the weight for all 9 reference points shown in figure 4.11 with equation 4.5.

6. The reference point with the largest weight will be assumed the location of the tag. If this point is not at reference point p^0_{map}, which is the real location of the tag, an error will be recorded.

7. Repeat step 3 to step 6 for many times. When finished, the error probability is the ratio of total error number to the total number of simulations.

The difference of RSS from a certain base station received at a reference point p^i_{map} and by the tag is calculated by:

$$\Delta RSS_i = \text{Loss factor } \times (10log_{10}(d_i) - 10log_{10}(R)) \tag{4.12}$$

where d_i is the distance between the reference point and the base station and R is the distance between the tag and the base station. And the $P^{i/j}_{map}(x)$ in step 2 is calculated by:

$$P^{i/j}_{map}(x) = P^{0/j}_{map}(x + \Delta RSS_i) \tag{4.13}$$

In order to compare the performance of this positioning algorithm, another positioning method based on the RSS Euclidean distances(Gezici, 2008)(Yeung and Ng, 2006)(Hatami et al., 2006)(Kaemarungsi and Krishnamurthy, 2004)(Bahl and Padmanabhan, 2000) other than distribution matching is also used for simulations. In that method, instead of equation 4.5, the following equation is used to calculate the weight of a point p^i_{map}:

$$w'^j_i = \frac{1}{(\overline{RSS^{i/j}_{map}} - \overline{RSS^{i/j}_{tag}})^2} \tag{4.14}$$

where $\overline{RSS^{i/j}_{map}}$ is the average of all RSS values from base station BS^j_{found} recorded at

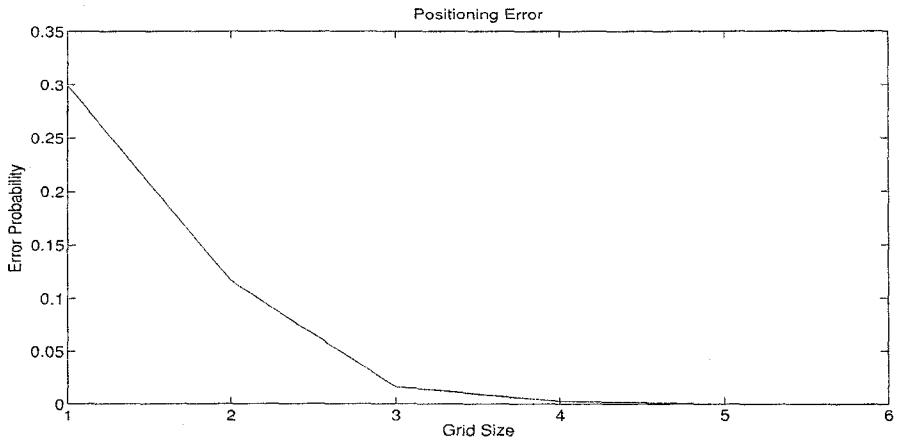

(a) Distribution matching method

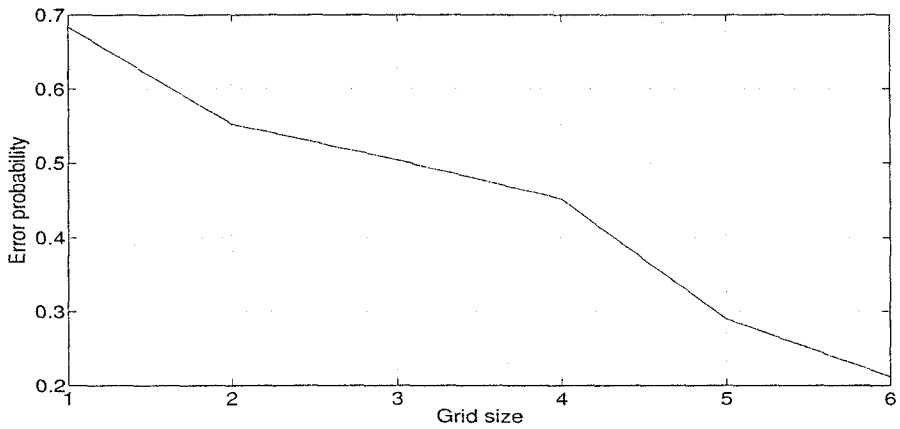

(b) Euclidean distance method

Figure 4.12 Positioning performance with different grid size

the reference point p^i_{map} and $\overline{RSS^{i/j}_{tag}}$ is the average of all real-time RSS values from the same base station recorded by the tag, which is generated in the third step of simulations as mentioned above. The total weight of the reference point in the group G_{match}, instead of using equation 4.10, is calculated by the following equation:

$$W'_i = \frac{1}{\sum_{j=1}^{N} \frac{1}{w'^j_i}} \tag{4.15}$$

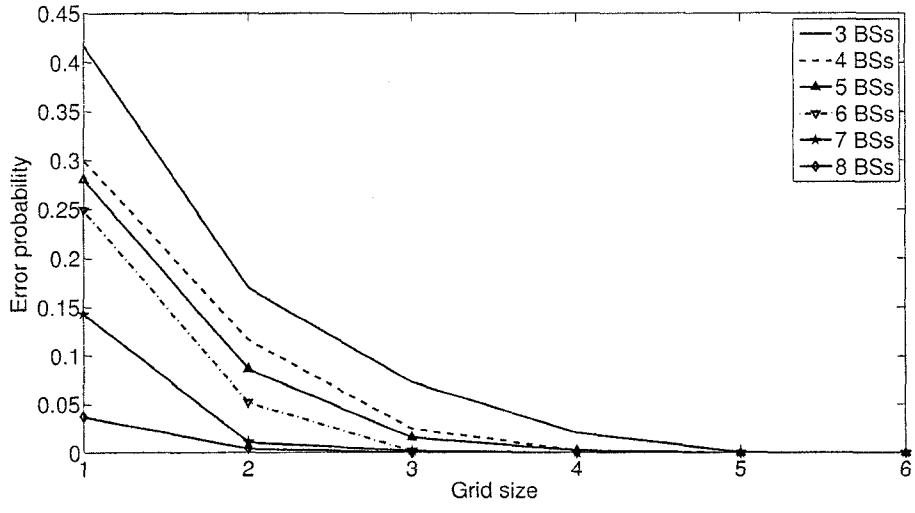

Figure 4.13 Positioning performance with different number of base stations

Figure 4.12 shows the system performance when different grid size is chosen. Because the location of the tag is also the position of a reference point, the absolute error distance in equation 4.1 is not used here. The error here means that a reference point other than the one that is closest to the location of the tag is determined to be the location of the tag by mistake. From figure 4.12(a), we can see that with the distribution matching method, with a probability of around 70%, the tag can be located in a position less than 1 meter from its real location. With a probability of around 88%, the tag can be located in a position less than 2 meters from its real location. With more than 95%, the tag can be located in a position less than 3 meters from its real location. Compared with figure 4.12(b), it is obvious that this method works very well. With the Euclidean distance method, there is only a probability of 30% that the tag is estimated within 1 meter of its real location and a probability of 80% that it is estimated within 6 meters of its real location.

Figure 4.13 shows the effects of the number of base stations. The system performance with 3 to 8 base stations has been simulated. As expected, with more base stations, higher accuracy can be obtained. As shown in this figure, with 8 base station, there is a

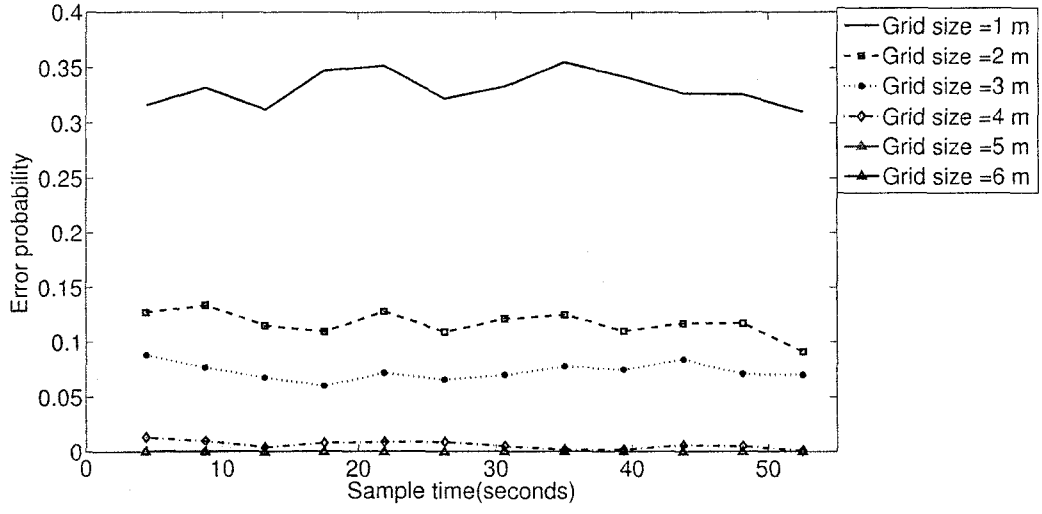

Figure 4.14 Positioning performance with different RSS sampling time

probability of more than 95% that the tag can be positioned to its closest reference grid point. However, more base stations means more cost. For the purpose of this project, 4 base stations can provide an location accuracy enough for positioning persons.

The effects of the length of RSS sampling time is shown in figure 4.14. Different time length ranging from around 4 seconds to 55 seconds has been used. This result show that the length of sampling time almost has no impact on the system performance using the distribution matching method. By comparing the result with a sampling time length of 4 seconds and the result with the length of 55 seconds, only little improvement is obseved. The performance may be improved with a time length much larger than those used here and a time length much less than those used here may degrade the performance very much. But clearly it shows that the a sampling time length of several seconds, instead of several minutes, can be used for positioning. Because the result is obtained with distribution matching method, it also shows that the RSS distribution at a certain place in an indoor environment usually doesn't change too much during a period in the order of senconds or several minutes. This makes sense, because usually people's activities, such as walking, are not very fast and can be measured in the order of seconds.

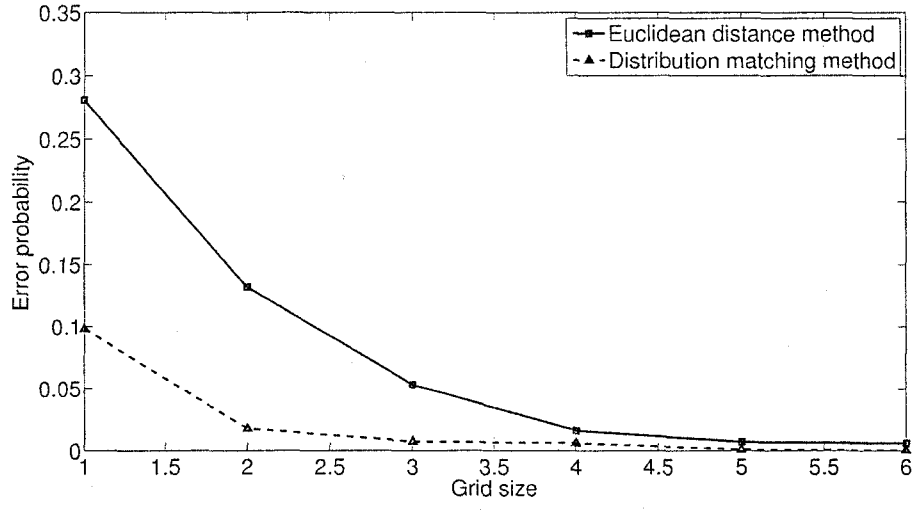

Figure 4.15 System performance with RSS database limited in an hour

All the above results are obtained by comparing the real-time sampled RSS information by a tag and the RSS information measured for around 12 hours, which is stored in the electronic map. Because people may have different activities at different time during a day, the RSS properties at a certain place may change a lot. For example, people inside a building may do not move too much in the morning and in the afternoon while they walk around and go for lunch at noon, then RSS may not vary too much in the morning and in the afternoon but changes very much at noon. As mentioned before, the RSS information is not only dependent on the location where it is measured but also dependent on the time when it is measured. The system performance can be further improved if this time information can be used. In other words, if the RSS information stored in the electronic map has its time information, the real-time measured RSS information by a tag can be processed with the RSS information in the database which is measured at a similar time during the measurement. For example, RSS information of each reference point in the electronic map can be divided into three parts: one part is meaured in morning and also used for positionings in morning, one measured at noon and used for positionings at noon and another measured in afternoon and used for positionings in afternoon.

A simulation that is the same as above presented simulations except that the database is composed of RSS information measured in reference points for only 1 hour instead of 12 hours, is performed to varify this point of view. The simulation result shown in figure 4.15 shows a marked improvement, which means that if the RSS distribution inside a certain hour is similiar for each day, improvement can be obtained by including time information in the electronic map. Instead of for the time length of one hour, assume the RSS distribution measured for a time length T_L is similiar for each day. T_L may be different for different environment. The RSS distribution function measured at the reference point p^i_{map} from the base station BS_j, $P^{i/j}_{map}(x)$, will become a function of RSS and time, $P^{i/j}_{map}(x,t)$, which is the RSS distribution function measured from the time $t - T_L/2$ to the time $t + T_L/2$. Then, when a person falls down at a time t_o, the RSS information measured by the tag on that person's body can be processed with the RSS distribution function $P^{i/j}_{map}(x,t_o)$ measured for T_L, other than a longer time, such as a day. And the performance can be improved.

CHAPTER 5

CONCLUSION AND FUTURE WORKS

5.1 Conclusion

In this thesis, a fall detection system based on energy expenditure calculation has been analyzed, designed and fabricated. A series of measurements have been made to analyze the performance of the proposed fall detection method. The whole system consists mainly of two parts: the triaxial acceleration sensor and the data processing unit. This can make the whole circuit small enough for people to wear on their bodies. Measurement results show that this system is able to distinguish falls with other daily activities.

To validate the proposed concept, wireless positioning based on RSS has been analyzed in an indoor environment. Some special considerations, such as the antenna polarization, have been presented. Several wireless units and several antennas of different polarization have been designed and fabricated with standard PCB technology. The influence of several factors has been studied and tested. Because wireless signal strength in an indoor environment fluctuates with time, it is difficult to obtain a good performance based on RSS. A novel position estimation method, the Probability Matching method, has been proposed to improve the system performance.

Many published works have taken the RSS distribution in an indoor environment as normal distribution. However, measurements show that this is not the general case. The RSS distribution is highly dependent on its environment and people's daily activities. Other than using normal distribution, the Monte-Carlo method using measured RSS distribution has been employed to evaluate the performance of the positioning system. The

results show that the distribution matching method can improve the performance significantly. With this method, it is feasible to realize an accuracy ranging from 1 meter to 3 meters in an indoor environment, which is enough for applications that need location information of people.

5.2 Future works

First, since the wireless unit for positioning is put on a targeted person, the effect of human body on the performance of the antenna should be studied. This effect can be taken into account by taking the human body and the antenna as a new antenna. When the model of human body is known, this effect can be investigated by simulating an antenna with a human body model using HFSS.

Second, the antennas used in this project are not small enough. In order to prevent the wearable positioning unit from bringing much uncomfort to targeted people, smaller antennas with acceptable performance should be investigated in future. Circularly polarized patch antennas are used for the wireless node in this project, which may be not very good for a large coverage. A specially designed circularly polarized antenna should be studied in order to provide a coverage as large as possible.

Moreover, when a person falls down, the direction of the antenna is uncontrollable. Even a circularly polarized antenna has been used, the unpredictable direction of the antenna will also degrade the performance. Some methods could be used to reduce the performance degradation of the system due to this effect, such as by putting more units on a person.

Besides, the measurements in this work have been made in a laboratory environment while this system is intended to work in other kinds of environment, such as a nursing

building. For several reasons, the result of measurements made in a nursing building could be different from that in a laboratory environment. For example, the number of people in a laboratory environment may be quite different at different time while that in a nursing building usually does not change much. Then, measurement should be made in a nursing building to further investigate the performance of the system.

REFERENCES

Analog Device (2007). Adf7021: High performance narrowband ism transceiver.

Bahl, P. and Padmanabhan, V. (2000). RADAR: an in-building RF-based user location and tracking system. In *INFOCOM 2000. Nineteenth Annual Joint Conference of the IEEE Computer and Communications Societies. Proceedings. IEEE*, volume 2.

Bart, J. and Rudi, D. (2006). Context aware inactivity recognition for visual fall detection. In *Proc. of 2006 Pervasive Health Conference and Workshops*, pages 1–4.

Caspersen, C., Powell, K., and Christenson, G. (1985a). Physical activity, exercise, and physical fitness: definitions and distinctions for health-related research. *Public Health Reports*, **100**(2), 126.

Caspersen, C., Powell, K., and Christenson, G. (1985b). Physical activity, exercise, and physical fitness: definitions and distinctions for health-related research. *Public Health Reports*, **100**(2), 126.

Chen, W., Wu, C., and Wong, K. (1998). Compact circularly polarised microstrip antenna with bent slots. *Electronics Letters*, **34**(13), 1278–1279.

Dedes, G. and Dempster, A. (2005). Indoor GPS positioning-challenges and opportunities. In *Vehicular Technology Conference, 2005. VTC-2005-Fall. 2005 IEEE 62nd*, volume 1.

Doukas, C., Maglogiannis, I., Tragas, P., Liapis, D., and Yovanof, G. (2007). Patient Fall Detection using Support Vector Machines. In *Artificial Intelligence and Innovations 2007 from Theory to Applications: Proceedings of the 4th IFIP International Conference on Artificial Intelligence Applications and Innovations (AIAI 2007)*. Springer.

Duthie, E. (1989). Falls. *Medical Clinics of North America*, **73**, 14.

Gezici, S. (2008). A Survey on Wireless Position Estimation. *Wireless Personal Communications*, **44**(3), 263–282.

Gurley, R. J. Lum, N. S. M. L. B. K. M. H. (1996). Persons found in their homes helpless or dead. *New England Journal of Medicine*, **334**, 1710.

Harter, A., Hopper, A., Steggles, P., Ward, A., and Webster, P. (2002). The Anatomy of a Context-Aware Application. *Wireless Networks*, **8**(2), 187–197.

Hatami, A., Pahlavan, K., Heidari, M., and Akgul, F. (2006). On RSS and TOA based indoor geolocation-a comparative performance evaluation. In *IEEE Wireless Communications and Networking Conference 2006.(WCNC*, volume 1, pages 3–6.

Hirasawa, K. and Haneishi, M. (1991). *Analysis, design, and measurement of small and low-profile antennas.* Artech House Boston.

JAMES, J. and HALL, P. (1989). Handbook of microstrip antennas. *IEE electromagnetic waves series.*

Kaemarungsi, K. and Krishnamurthy, P. (2004). Modeling of indoor positioning systems based on location fingerprinting. In *INFOCOM 2004. Twenty-third AnnualJoint Conference of the IEEE Computer and Communications Societies*, volume 2.

Lindemann, U., Hock, A., Stuber, M., Keck, W., and Becker, C. (2005). Evaluation of a fall detector based on accelerometers: A pilot study. *Medical and Biological Engineering and Computing*, **43**(5), 548–551.

Luo, S. and Hu, Q. (2004). A dynamic motion pattern analysis approach to fall detection. In *Biomedical Circuits and Systems, 2004 IEEE International Workshop on*, pages 1–5.

Malik, W.Q. Edwards, D. S. C. (2006). Frequency-dependent pathloss in the ultra-wideband indoor channel. In *Communications, 2006. ICC '06. IEEE International Conference on*, volume 12, pages 5546–5551.

Mathie, M., Basilakis, J., and Celler, B. (2001). A system for monitoring posture and physical activity using accelerometers. In *Engineering in Medicine and Biology Society, 2001. Proceedings of the 23rd Annual International Conference of the IEEE*, volume 4.

Mathie, M., Lovell, N., Coster, A., and Celler, B. (2002). Determining activity using a triaxial accelerometer. In *Proceedings of the second joint EMBS conference.*

Maxim Integrated Products (2005). 8-port, 5.5v constant-current led driver with led fault detection and watchdog.

Microchip datasheet (2003). PIC16F87X Data Sheet. *linked from www. microchip. com, Document DS30292C, Microchip Technology, Inc., 2355 West Chandler Blvd., Chandler, AZ 85224–6199, 2001.*

MMA7260Q 3D Accelerometer (2008). MMA7260Q 3D Accelerometer. *URL http://www. freescale. com.*

Nait-Charif, H. and McKenna, S. (2004). Activity summarisation and fall detection in a supportive home environment. In *Pattern Recognition, 2004. ICPR 2004. Proceedings of the 17th International Conference on*, volume 4.

Priyantha, N., Chakraborty, A., and Balakrishnan, H. (2000). The Cricket location-support system. In *Proceedings of the 6th annual international conference on Mobile computing and networking*, pages 32–43. ACM Press New York, NY, USA.

RF Technologies (2001). Pinpoint 3d-id(http://www.rft.com/solutions/pinpointrtls/).

Rougier, C. and Meunier, J. (2006). Demo: Fall Detection Using 3D Head Trajectory Extracted From a Single Camera Video Sequence. In *First International Workshop on Video Processing for Security (VP4S-06), June*, pages 7–9.

Rougier, C., Meunier, J., St-Arnaud, A., and Rousseau, J. (2006). Monocular 3D Head Tracking to Detect Falls of Elderly People. In *Engineering in Medicine and Biology Society, 2006. EMBS'06. 28th Annual International Conference of the IEEE.*

Shin, D. and Sung, T. (2002). Comparisons of error characteristics between TOA and TDOApositioning. *Aerospace and Electronic Systems, IEEE Transactions on*, **38**(1), 307–311.

Sixsmith, A. and Johnson, N. (2004). A Smart Sensor to Detect the Falls of the Elderly. *IEEE PERVASIVE COMPUTING*, pages 42–47.

Tideiksaar, R. (1997). *Falling in Old Age: Prevention and Management.* Springer Publishing Company, 2 edition.

Tinetti, M., Baker, D., Dutcher, J., Vincent, J., and Rozett, R. (1994). Reducing the risk of falls among older adults in the community. *Yale FICSIT.*

Toreyin, B., Dedeoglu, Y., and Cetin, A. (2005). HMM Based Falling Person Detection Using Both Audio and Video. *LECTURE NOTES IN COMPUTER SCIENCE*, **3766**, 211.

WANT, R., HOPPER, A., and GIBBONS, V. (1992). The Active Badge Location System. *ACM Transactions on Information Systems*, **10**(1), 91–102.

Williams, G., Doughty, K., Cameron, K., and Bradley, D. (1998). A smart fall and activity monitor for telecare applications. In *Engineering in Medicine and Biology Society, 1998. Proceedings of the 20th Annual International Conference of the IEEE*, volume 3.

Yeung, W. and Ng, J. (2006). An Enhanced Wireless LAN Positioning Algorithm based on the Fingerprint Approach. In *TENCON 2006. 2006 IEEE Region 10 Conference*, pages 1–4.

Zhang, T., Wang, J., Liu, P., and Hou, J. (2006a). Fall Detection by Embedding an Accelerometer in Cellphone and Using KFD Algorithm. *IJCSNS*, **6**(10), 277.

Zhang, T., Wang, J., Xu, L., and Liu, P. (2006b). Fall Detection by Wearable Sensor and One-Class SVM Algorithm. *LECTURE NOTES IN CONTROL AND INFORMATION SCIENCES*, **345**, 858.